AFFDL-TR-71-73

PARTICLE CONTAMINATION
IN
HYDRAULIC SYSTEMS

R. J. AKERS

B. SCARLETT

P. J. LLOYD

J. I. T. STENHOUSE

A. S. WARD

UNIVERSITY OF TECHNOLOGY
LOUGHBOROUGH
LOUGHBOROUGH, LEICESTERSHIRE
ENGLAND

D D C

MAY 11 1972

TECHNICAL REPORT AFFDL-TR-71-73

JUNE 1971

Approved for public release; distribution unlimited.

AIR FORCE FLIGHT DYNAMICS LABORATORY
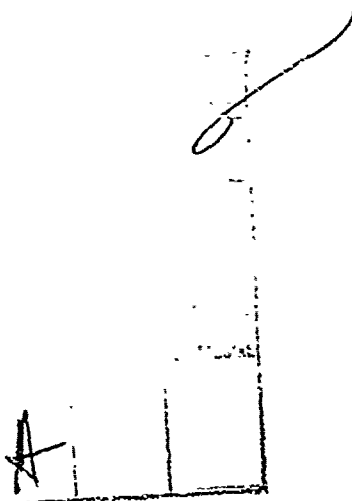AIR FORCE SYSTEMS COMMAND
WRIGHT-PATTERSON AIR FORCE BASE, OHIO 45433

NOTICE

When Government drawings, specifications, or other data are used for any purpose other than in connection with a definitely related Government procurement operation, the United States Government thereby incurs no responsibility nor any obligation whatsoever; and the fact that the government may have formulated, furnished, or in any way supplied the said drawings, specifications, or other data, is not to be regarded by implication or otherwise as in any manner licensing the holder or any other person or corporation, or conveying any rights or permission to manufacture, use, or sell any patented invention that may in any way be related thereto.

Approved for public release; distribution unlimited.

Copies of this report should not be returned unless return is required by security considerations, contractual obligations, or notice on a specific document.

DOCUMENT CONTROL DATA - R & D

(Security classification of title, body of abstract and indexing annotation must be entered when the overall report is classified)

1. ORIGINATING ACTIVITY (Corporate author)	2a. REPORT SECURITY CLASSIFICATION
Department of Chemical Engineering University of Technology, Loughborough Leicestershire, England	Unclassified
	2b. GROUP N/A

3. REPORT TITLE

Particle Contamination in Hydraulic Systems

4. DESCRIPTIVE NOTES (Type of report and inclusive dates)

Final Tech Report Jan 1970 - Dec 1970

5. AUTHOR(S) (First name, middle initial, last name)

Richard J. Akers   James I. T. Stenhouse
Brian Scarlett   Anthony S. Ward
Phil J. Lloyd

6. REPORT DATE	7a. TOTAL NO. OF PAGES	7b. NO. OF REFS
June 1971	viii + 213	32

8a. CONTRACT OR GRANT NO.	9a. ORIGINATOR'S REPORT NUMBER(S)
F61052-70-C-0007	
b. PROJECT NO. 8225	
c. Task No. 822510	9b. OTHER REPORT NO(S) (Any other numbers that may be assigned this report)
d.	AFFDL-TR-71-73

10. DISTRIBUTION STATEMENT

Approved for Public release; distribution unlimited.

11. SUPPLEMENTARY NOTES	12. SPONSORING MILITARY ACTIVITY
	Air Force Flight Dynamics Laboratory Air Force Systems Command Wright-Patterson Air Force Base, OH 45433

13. ABSTRACT

This report is part of a wide ranging survey of the effects of contamination on aeroplane flight control hydraulic subsystems. It analyses the current state of the problem and proposes a method by means of which long term research should be directed to obtain a general solution. It shows how the behaviour of particles in a complete hydraulic system may be represented in terms of a mathematical model based on matrix representations of both particle concentrations and characteristics of the system components. Also reported on are coincidence problems in stream scanning particle size analysis, particularly the Coulter Counter, ARF 598, automatic image analysis as applied to particle size analysis, the stereological representation of particles, the theoretical efficiency of non-isokinetic sampling devices, a new method for representing the efficiency of a filter and techniques for analysing the composition of particles in a fluid and for studying simultaneously the flow behaviour in a pipe of both liquid and particles.

KEY WORDS	LINK A		LINK B		LINK C	
	ROLE	WT	ROLE	WT	ROLE	WT
Hydraulic						
Flight control						
Contamination						
Particle						
Sample						
Filter						
Mathematical model						
Matrix						
Particle size						
Fluid flow						
Servo valve						

PARTICLE CONTAMINATION
IN
HYDRAULIC SYSTEMS

R. J. AKERS

B. SCARLETT

P. J. LLOYD

J. I. T. STENHOUSE

A. S. WARD

UNIVERSITY OF TECHNOLOGY

LOUGHBOROUGH

LOUGHBOROUGH, LEICESTERSHIRE

ENGLAND

Foreword

This report was prepared by the Chemical Engineering Department,
Loughborough University of Technology, England Under Air Force Contract
No. F61052-70-C-0007. The work was administered under the direction of
the Air Force Flight Dynamics Laboratory, (AFFDL/FGL), Project 8225,
Task 822510, Wright-Patterson Air Force Base, Ohio with Mr. V. R. Schmitt
as project engineer.

The report covers work done during the period January to December 1970.

The Principal Investigators were Dr. R. J. Akers and Mr. B. Scarlett.

This report has been reviewed and is approved.

George H Purcell
GEORGE H. PURCELL
Acting Chief
Control Systems Development Branch
Flight Control Division

ii

Abstract

The work carried out under this contract was part of a wide ranging investigation into the effects of particulate contamination on the performance of aerospace hydraulic control sub-systems. This phase of the work included the devising of techniques for studying this problem and the application of these techniques. Amongst the subjects studied were methods of particle size analysis, the theoretical prediction of the efficiency of sampling devices, the development of a mathematical modelling technique to simulate particle behaviour in complete systems, a discussion of the meaning of particle size and how this may be related to analytical techniques and a new method for characterising the efficiency of filters.

A brief analysis of the current situation with regard to particulate contamination of hydraulic systems and a proposed framework within which work should continue is also included.

Preceding page blank

List of Figures

List of Tables

List of Tables

List of Symbols

$\underline{a}$ Increase in particle concentration caused by erosion of pump valve plate $(wt.vol^{-1})$

A The projected area of a particle

$\underline{bu}$ Weight of particles retained in control valve per volume leaked

$\underline{b}$ Increase in particle concentration by release from pipe wall $(wt.vol^{-1})$. e.g. $\underline{b}$ release from pipe between pump and filter.

c Concentration of particles in sample removed

c Volume of fluid leaking through closed control valve

c_o Concentration of particles in main fluid stream

C Diagonal collection matrix, e.g. C_{pv} - collection in pressure relief valve

C_d Particle drag coefficient

$\underline{d}$ Increase in particle concentration caused by erosion of pump shoes and swash plate $(wt.vol^{-1})$.

d_a The diameter of a circular particle of equal projected area

d_p " " " " " " " " perimeter

d_f " " " " " " " " Feret diameter

ds An element of perimeter

D The orifice diameter of a Coulter Counter

D Particle size

$\overline{D}$ The mean length of a set of filaments

E Triangular erosion matrix, e.g. E_{pv} - erosion in pressure relief valve

f Fraction of feed passing unfiltered to filtrate

$\underline{f}$ Concentration of particles leaving filter $(wt.vol^{-1})$

F Matrix representing action of filter

$F(D)$ Fractional wt. less than D in solids passing filter

I A unit matrix

I	Current passing through Coulter Counter orifice
ΔI	Change in I due to presence of particle
$\underline{j}$	Concentration of particles leaving actuator
$\underline{k}$	Increase in actuator particle concentration due to external contamination $(wt.vol^{-1})$
k	The length of a void filament
K	Overall action of actuator on external contamination
$\bar{K}$	Ratio of particle orifice diameter in Coulter Counter
$\underline{\ell}$	Concentration of particles leaving valve $(wt.vol^{-1})$
ℓ	The length of a particle filament
1	The distance between particles in a stream scanning device
L	Radius of sampling tube
L	Overall leakage effect of valve. e.g. L_c - leakage effect when valve is closed
m	Relative mass of a particle
$\underline{m}$	Concentration of particles leaving reservoir $(wt.vol^{-1})$
n	The number of particles counted in a stream scanning device
$n(i)$	A number distribution with respect to the quantity i
$N(i)$	A cumulative distribution with respect to the quantity i
N_o	The number of particles in volume v of a stream scanning device
N	The true number of particles passing through a stream scanning device
N	The total number of chords for a particle
o	The volume of fluid leaking through a control valve when that valve is open
p	Pressure
P_f	Fluid density
$\underline{p}$	Concentration of particles leaving pump $(wt.vol^{-1})$
$P(i)$	The probability of a multiplet of i particles occurring in a stream scanning device

Q	Strength of point source
Q(D)	Fractional weight less than D in feed
r	Fraction of feed retained by all mechanisms other than retention at the medium
$\underline{r}$	Concentration of particles in reservoir (wt.vol^{-1})
r_p	Particle radius
R	Matrix representing overall effect of return line filter
R(D)	Fraction weight less than D in retained solids
R^1	Radius of concentric sphere of uniform field strength in the absence of a particle
R_e	Reynolds number
∂R	The resistance change when a particle passes through a Coulter Counter orifice
Stk	Stokes number
t	The time spent by a particle in the sensing volume of a stream scanning device
t	Time
Δt	The thickness of a chord or filament
u	A fluid velocity
U	Velocity resolute in x direction
U_o	Main stream velocity
v	The sensing volume of a stream scanning device
V	Velocity resolute in y direction
v_i	The volume of element i in a hydraulic system, e.g. v_z - volume of line between pressure relief valve in reservoir
$\underline{v}$	Concentration of particles leaving valve at pressure port
V_R	$\dfrac{\text{fluid velocity in sampling device}}{\text{fluid velocity in main stream}}$
x_i	Collection point i of particles in control valve

x   A distance of separation

$\underline{z}$ Concentration of particles leaving pressure relief valve $(wt.vol^{-1})$

Z   Overall action of pressure relief valve

ϵ The probability of finding one particle in volume v of a stream scanning device

$\eta(D)$ Overall point retention efficiency of a filter

$\eta_r(D)$ Point retention efficiency due to action of medium

η The efficiency of a sampling device

ϕ The proportion of particles retained at a point in a four way valve

μ Fluid viscosity

μ The reciprocal mean separation of particles in a stream scanning device

ρ Density difference between particle and fluid

ρ^0 Resistivity of electrolyte

$\bar{\tau}$ The mean 'time distance' between particles in a stream scanning device

Σ The voids ratio in a packed bed

ϕ)
ψ)   The proportion of particles retained at a point in a four way valve

Chapter 1

Introduction

PART I

CHAPTER 1

Introduction

1.1   Layout of Report

This report is an account of an investigation of some of the techniques used to study the concentration and behaviour of particulate contamination in hydraulic flight control sub-systems and a basic investigation of some of the phenomena associated with the presence of these contaminants. The introductory chapter will contain a brief resume of the situation as it is seen to exist at present followed by an account of the approach the investigators have taken to the problem.

The following sections of the report are then devoted to particular topics, these sections often being the work of one particular investigator or group of investigators. The final section of the report is an account of some of the techniques which have either been developed in the course of this work or are considered of utility in a study of the subject.

The personnel involved in this work were Principal Investigators – Dr. R. J. Akers and Mr. B. Scarlett, Associate Investigators – Mr. P. J. Lloyd, Mr. J. I. T. Stenhouse and Mr. A. S. Ward, with the invaluable assistance of Dr. P. Allen, C. R. G. Treasure, Miss C. Forsling, Mr. I. Sinclair, Mr. C. A. Troakes, Mr. J. Walker, Mr. R. Buxton, Miss C. Bostock, Mrs. M. Warren, Mr. L. Moore and Mr. A. Saffell, all of the Chemical Engineering Department, Loughborough University of Technology, England.

The appropriate references are given at the end of each section.

1.2. Historical Background

When hydraulic systems were first introduced into aircraft it was to aid the performance of utility functions such as undercarriage retraction, bomb door opening and flap deployment. The earliest systems were simple hydrostatic circuits consisting of a force transmitting piston and a linear actuator. With the increased use of hydraulic power in aircraft the hydrostatic systems were superseded by multi-purpose systems consisting of main distribution and return manifolds pressurised by a motor driven pump and having selector valves to control the flow of fluid to linear and rotary actuators. As a general rule the actuators were only required to be in one of two positions, i.e., fully extended or retracted, hence the selector valves needed only to be of the on-off type. If more than two positions were needed, as in flap operation, a double actuator was used. As such systems were only operated intermittantly and because considerable force, applied either manually or electromagnetically was available to operate the selector valves, catastrophic failures were relatively few and wear rates, except in the case of continuously operated pumps, low.

The development of powered flight control systems has meant the need for continuously operating hydraulic systems with a very high degree of reliability and being capable of moving control surfaces with precision in response to electrical or mechanical analogue signals. In order to achieve this, servo valves of very great mechanical sophistication are employed and it is these servo valves in particular, and the general reduction of available forces and mechanical clearances that have made hydraulic systems less tolerant to particulate contamination.

3.

1.3   The Present Situation

Discussions on the effects of particulate contamination in hydraulic systems have been held with hydraulic component and air frame manufacturers and with U.S.A.F. in their roles as aircraft users and originators of specifications (see 1-5). The picture that emerged showed much confusion. The airframe manufacturers considered hydraulic contamination to be a serious problem if only in what it cost both in terms of precautions during manufacture and elaboration of the hydraulic system. The attitude was very much a 'play safe' one and it was felt that more precise information on system tolerances would be of considerable value. It is well recognised that some vehicles are more prone to contamination problems than others, although the difficulties inherent in reliable sampling and analysis of fluids from actual systems makes it difficult to draw firm conclusions as to the best choice of components for a given system and the specification of its operating cleanliness conditions.

Among hydraulic component manufacturers, particularly servo valve manufacturers, three attitudes were discernable.

These were:

    (i)   No serious problem existed.

    (ii)   That the effects of contamination could be 'designed out.'

    (iii)   That a serious problem did exist.

It was felt however that these attitudes were themselves open to considerable interpretation. At one servo valve manufacturer belonging to the 'no serious problem' school photographs were shown of servo valve first stage filters and metering orifices blocked with fibrous and particulate contaminant. This was construed as an occasional but inevitable result of operation of the system rather than a serious problem in system design or specification. Several members of the "design it out" school were of the opinion that there was an optimal level of dirt in a system and that if 'cleaner operation' was insisted upon, valve leakage rates would increase. The reliance on a degree of contamination to reduce leakage implies that the build up of silt within the valve with its effects on both valve wear and performance degradation. No studies have yet been made on the effects of 'silt' on the forces necessary to 'break out' a spool, but whatever their magnitude they would add something to the hysteresis of the valve. With respect to valve second stage

leakage, no direct experimental information was available as to the separate contributions of port overlap or underlap and leakage through the annular spool/sleeve clearance. A recent study (AFFDL-TR-69-136) has shown the effect of particulate contamination on both second stage port dimensions, wear of the flapper plate (fig. 1.1), and causing respectively an increase in port overlap and jet/flapper clearance.

The increasing stringency of fluid cleanliness standards will impose now demands on filter manufacturers. It is probable that woven wire filters are getting near the economic and technical limit in the production of fine woven wire cloth and that the change towards filters of the depth type using non-woven porous media will continue. The loading/pressure and maximum dirt holding characteristics of these filters might also be considered more attractive.
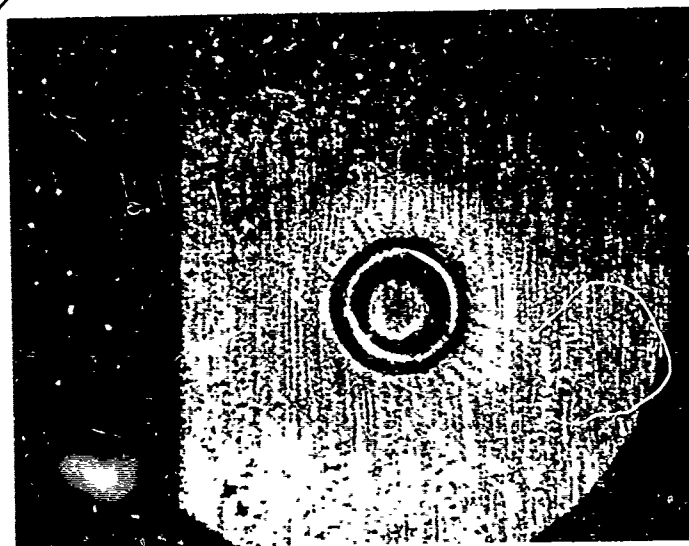
FIGURE 1   EROSION OF FLAPPER PLATE

6.

1.4. Problem of Specifying Cleanliness Standards

In specifying minimum fluid cleanliness standards for a given system by any means other than arbitrary selection it will be necessary to start from the contamination characteristics of those components whose design is dictated by the operational requirements of the system, and then select other components such as filters to meet their cleanliness specification. To do this much information is needed about the contamination characteristics of a wide range of hydraulic components. Included in this would need to be a study of the rates of deposition and removal of particles from the interior surfaces of pipelines, hydraulic accumulators and other components and the effects of vibration and accelerating forces on those processes.

The operators of aircraft would like a simple go/no go test of hydraulic cleanliness but until the order of seriousness of the factors involved, e.g., particle size and size distribution, particle hardness, etc., any such test would be based upon very unsure foundations. In particular, with the reduction of radial clearances in servo valves to 50 micro inches (i.e., ~2 μm) considerable attention must be given to studying the effects of particles finer than those counted by existing techniques. Unfortunately there are few particle size analysis techniques available for particles < 1 μm and those that there are tend to be laborious.

1.5. General Effects of Particulate Contamination

These may be classified as:

1.5.1. Wear

If a component in which sliding contact occurs, e.g., an actuator, is dismantled after service, longitudinal scratches will be seen on the sliding surfaces, these being due to particles trapped between the mobile and stationary members. Although wear of this type is general it is of particular significance in hydraulic piston pumps, where it mainly occurs between the valve plate the cylinder block and between the slippers and swash plate. Less extensive wear will also occur in the pistons and cylinder bores. The overall effect of this wear is to reduce the efficiency of the pump by increasing leakage and also, more importantly from the point of view of particle contamination of the whole system, generating large numbers of fine particles. Several studies of the effect of artificially contaminated oils on pumps have shown them to be very effective grinding machines with the pump output containing size reduced contaminant particles and metal from the pump originating in wear caused by contaminant passing through the pump. Wear of this type between sliding surfaces is also observed in actuators where it is not a major problem except in those cases where an actuator is dithered for long periods of time about one position, and in the spools and sleeves of servo valves where it leads to increase leakage and degradation of the valves performance in terms of such parameters as flow again and hysteresis.

1.5.2 Blockage of Orifices

This is a possible although uncommon mode of failure. The finest orifices found in conventional flight control systems are the metering orifices in the first and second stages of servo valves. However these orifices are almost invariably protected by filters built into the valve. It is well known that contamination by fibres is very important in leading up to the blockage of an orifice by a bed of particles each of which individually is smaller than the orifice and this type of blockage cannot be discounted even in filter protected situations.

8.

1.5.3 Silting

Tests of electro-hydraulic servo valves operating with contaminated oil shows silting to be one of the major effects produced. Silting manifests itself as mechanical binding between two surfaces, e.g., spools and sleeve; leading to reduced flow gain and increased hysteresis. The mechanism of silting is not very well understood. If it is due to particles entering the annular space between the spool and sleeve the particles concerned must be smaller (in their smallest dimension) than the diametrical clearance. When a granular material flows it has to rearrange its packing in order to allow the particles to move freely over one another. This brings about a reduction in density, i.e., the volumetric "dilation" of Osborne Reynolds. In the spool/sleeve situation this dilation cannot occur due to the constrained geometry. Very little is known of particle flow under these conditions of fixed volume.

Alternate explanation of silting is an off axis tilting of the spool and subsequent binding due to particles jammed under one side, although calculations of the maximum angular deflection possible in a modern valve make this unlikely, or alternatively the build up of a "fillet" of particles between the faces of the spool and the sleeve wall which would tend to become jammed in the annulus when the spool moves. This latter mechanism is more likely and would probably occur along with particle build up in the annular space.

1.5.4 Filter Blinding

Because it is necessary to control the number of particles circulating in a hydraulic circuit, filters are introduced into the system. As a consequence of their action filters gradually become 'blinded' with particles and have to be replaced or cleaned. The design of a filter is an attempt to optimise the performance in terms of the fineness of particle retained with the longest time between services.

9.

1.6. Aims & Methods of the Investigation

The object of this programme is to study the effects of particulate contamination on hydraulic flight control sub-systems and if possible define design criteria and contamination levels to enhance the life and reliability of such systems. From previous studies it is known that the reliability of systems varies widely from one design of vehicle to another and also between different examples of the same vehicle. These studies have tended to be empirical in that they have attempted to correlate the probability of the various modes of failure with the contamination level present at one or several points in the hydraulic system.

This project is an attempt to apply analytical techniques to this problem. This has been done by constructing a mathematical model of the system (Chapter 3) in terms of the characteristics of the individual components and the particle fluxes present. This approach is illustrated in fig. 2 , where it is seen that the ultimate test of the model is direct comparison with a real, if simplified, hydraulic system.

In order to use this model it is necessary to characterise the individual components of the system. By characterise we mean the number and size of particles leaving the component as a function of the number and size of particles entering, the flow rate and any other relevant operating parameters, e.g., dirt loading present on a filter. The modelling of the individual components may be either by experimental study, theoretical analysis or a combination of the two.

Whichever of these two approaches is followed it is necessary to be able to describe particles in a way that can be used subsequently in an analytical description of their behaviour. Traditionally the size of a particle is expressed in terms of a sphere equivalent in a property such as area (e.g., permeability) volume (e.g., "Coulter" Counter) projected area (e.g., Hiac' Counter) or sedimentation velocity. Alternatively a statistical diameter is used. Well known examples are those of Martin and Feret, and of particular interest in hydraulic engineering is the maximum projected linear dimension used in ARP 598 and similar methods. These various diameters are functions of the particle shape and are only equal for spheres. However, because so much information is lost when an irregular particle is defined in terms of one parameter, alternative descriptions are needed if properties of assemblies of particles are to be deduced. Such a method is
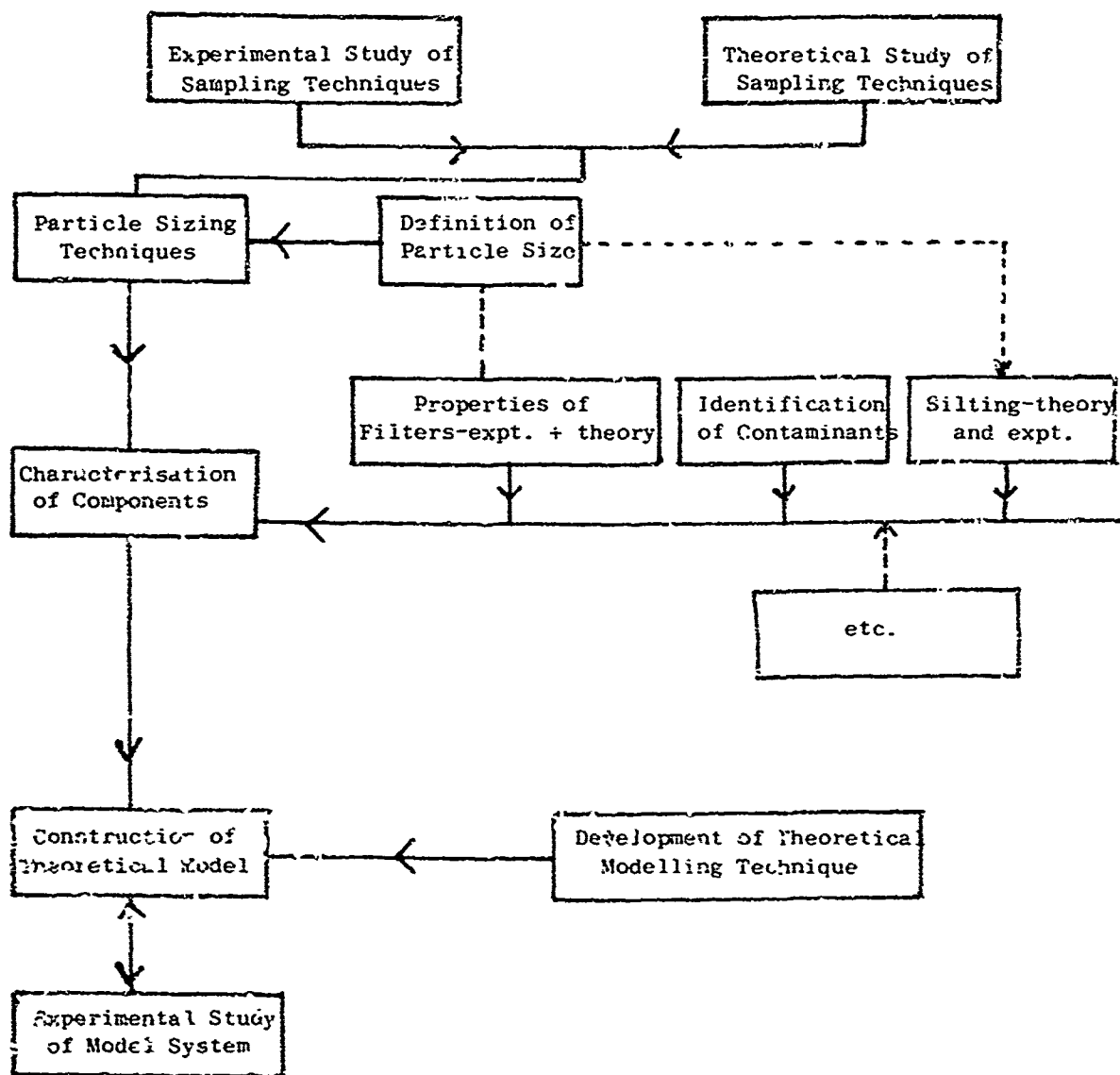
FIGURE 2   Flowsheet of Progress

11.

proposed in Chapter 4 and an application of it is shown in Chapter 6. To exploit this technique as a practical method further dev lopments are required in particle size analysis and these are described in Chapter 5. One of the consequences of such a method is that from the description of the particle system so obtained the particle size distribution in terms of any of the more familiar techniques of characterisation should be available. These relationships are being investigated.

Fig. 2 shows how the definition of particle size is related to the characterisation of components through both theoretical and experimental techniques and does in fact provide a link between them.

In order to carry out meaningful particle size analyses, whether during the characterisation of individual components or in the study of complete systems, it is necessary to be able to take a representative sample from the system or some point in the system. This is discussed in Chapter 2 which describes mainly theoretical studies of the flow of suspensions through sampling devices. Experimental work to check these predictions is in progress.

1.7. Sources of Information

In the course of preparing this report discussions were held with representatives of the following organisations. This opportunity is taken of acknowledging their assistance.

U.S.A.F.   Wright-Patterson Air Force Base, Ohio
    Air Force Flight Dynamics Laboratory
    Air Force Materials Laboratory
    Air Force Logistics Command

31st Air Reconnaissance Wing, R.A.F. Alconbury, England

Aircraft Porous Media, Inc., Glen Cove, L.I.N.Y.

Bendix Corporation, Detroit Mi.

Douglas Aircraft, Long Beach, Ca.

Dowty (Bolton-Paul) Wolverhampton, England

Fairey Hydraulics Ltd., Heston, England.

High Accuracy Products Corp., Claremont, Ca.

Hydraulics Research & Manufacturing, Rye Canyon, Ca.

Hydraulics Research & Manufacturing (Filters Division) Pacoima, Ca.

Lockheed Corp., Rye Canyon, Ca.

LTV, Arlington, Tx.

McDonnel Corp., St. Louis, Mo.

Michigan Dynamics, Detroit, Mi.

Pall (U.K.) Ltd., England.

Vickers Inc. Troy, Mi.

Weston Hydraulics, Van Nuys, Ca.

General Electric Co. Johnson City, N.Y.

Chapter   2

Sampling of Hydraulic Fluids

2.1 Introduction

In order to study the effect of particles on the behaviour of hydraulic systems or to establish the degree of contamination in operating systems it is necessary to be able to remove representative samples of fluid from the system, or, alternatively, to insert a contamination measuring device into the system. The latter will not be considered here.

Any sampling device has to satisfy several requirements. These are:

(a) That the sample should be removed from the system at such a point that it indicates the state of fluid arriving at a contamination sensitive element in the system or the state of the fluid leaving an element known to give rise to significant amounts of contamination. As examples of these are servo valves and pumps respectively. This condition is complicated by the fact that some system components are known to accumulate particles and then release them in a short period of time. An example of this type of device is a hydraulic accumulator.

In any hydraulic system the rate of fluid flow at any given point varies widely and undergoes very rapid accelerations. As a simplification the flow rate may be considered as being comprised of leakage with pulses superimposed on it. An ideal sampling device would integrate the contamination over a period of time. This could be done by withdrawing a representative sample over a considerable period of time, although this would be unacceptable in flight control systems on account of the volume of fluid withdrawn, particularly in military aircraft or missile systems with their small reservoir capacities. An alternative to this would be the installation of an on stream monitor. Only one particle counting device capable of being installed in an operating system is currently available, the Hiac Counter, and this has the disadvantage of being sensitive to flow rate (see 5.3). Alternatively a sample could be withdrawn from the system at a particular point and from a knowledge of the system as a whole its significance interpreted in terms of the probability of performance degradation or catastrophic failure. To do this requires a mathematical representation of the system as described in Chapter 3.

15.

(b)   That the sample presented to the sampling device be representative of the fluid flowing in that particular line. It is known that when a dilute suspension of non deformable particles flows along a cylindrical tube at flow rates corresponding to Reynolds Numbers in the laminar flow region, a radial concentration gradient is set up with the particles migrating towards the tube wall. Conversely deformable particles (e.g. water droplets) will migrate towards the axis (Goldsmith, H.L. and Mason, S.G. in Rheology, Vol. 4, Ed. Eirich, Academic Press 1967).

To satisfy this requirement either the flow velocity must be great enough to cause sufficient turbulence to ensure efficient mixing or turbulence must be artificially induced just upstream of the sampling point. By normal design criteria the Reynolds Number in a hydraulic pipe-line has a maximum value of approximately 7000, with minimum values corresponding to leakage flows for servo valves being in the range 200-800. As the high flow rates can only be maintained (in systems containing 'linear actuators) for short periods of time a realistic sampling device must sample from a system flowing at the minimum rate hence requiring the artificial induction of turbulence. This may be done by either changing the shape of the flow channel, as in the Prosser Industries sampling valve or by placing structures within the existing cylindrical pipe. Whatever the design of turbulence inducer it must create the maximum turbulence with minimum pressure drop. Also the possibilities of erosion within the device due to turbulence must be considered.

(c)   That the sampling device is capable of removing from the system the representative fluid as presented to it (section 2.2.).

(d)   That the sampling device does not generate or retain contaminant. Generation is most likely to happen in the valve portion where sliding surfaces may be present. It is desirable that valves be designed to prevent this kind of motion occurring, e.g. the sampling valve manufactured by Fairey Hydraulics, U.K.

(e)   That the sampling device does not impair the safety or reliability of the system.

16.

2.2 Theory of Sampling Devices

In any sampling system the fluid flow is not planar. Under non planar conditions the solid particles due to their inertia will cross the fluid stream-lines such that any fluid withdrawn will not be representative of the fluid as a whole. The errors due to this mechanism can be estimated theoretically. The procedure employed is to calculate the trajectories of particles of different inertia levels in the flow field pertaining under the particular sampling conditions. A pre-requisite of such a theory is an adequate description of the fluid flow field.

Variations on two basic geometries have been used in sampling valves. These are:

(i) An open aperture in the side wall of a tube (fig. 3) or in the case of the Prosser Industries valve (fig. 4) within a chamber containing turbulent flow.

(ii) A probe, usually central, within the tube carrying the flow. Various shapes of probe have been used, e.g. pointing upstream (fig. 5), perpendicular to the stream (fig. 6) perpendicular to the stream and cut obliquely (fig. 7)

From the point of view of their flow fields these latter two designs probably incorporate characteristics of both (i) and (ii) above.

Most of the flow situations encountered in sampling valves are not readily amenable to analytical description so the flow field in such components must be determined using flow visualisation techniques and described empirically. A flow visualisation technique has been developed and is currently being used to investigate the flow fields under a range of conditions. This technique is described in 2.3.1.

The theoretical technique has been developed using an ideal model of the flow field in a simple sampling valve. This technique and the results which have been achieved using it are described in 2.2.1 below.

Since the particle is moving in the linear Stokes regime equation (?) may be replaced by the more familiar trajectory equations:

$$\left(\frac{m}{6\pi\eta r_p}\right) \frac{d^2x}{dt^2} + \frac{dx}{dt} = u$$
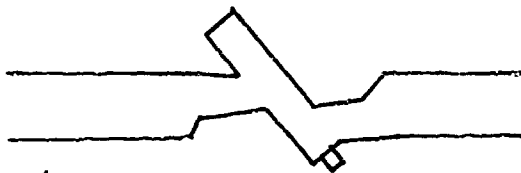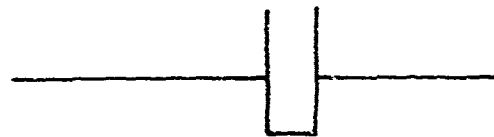
FIGURE 3 - 7   Sampling valve configurations

23.

$$\left(\frac{m}{6\pi\mu r_p}\right) \frac{d^2y}{d\tau^2} + \frac{dy}{d\tau} = v$$

where u and v are the x and y resolutes of the fluid velocity.

Equations (2.3) may be reduced to a dimensionless form by using the conversions in table 1.

TABLE I   Notation

Parameter	Symbol	Derivation
Velocity	U V	u/Uo v/Uo
Co-ordinate	X Y	x/l y/l
Time	τ	Uo τ/l
Stokes Number	Stk.	$r_p^2 \rho\, Uo/9\mu l$

The Stokes number is the ratio of the distance a particle with initial velocity, Uo, will travel before coming to rest, to some dimension l, of the system.   In the case of a tube withdrawing a sample from a stream in planar flow, as in fig. 3 ,l is the radius of the sampling tube.   Hence equation (2.3) becomes:

$$2\,Stk\ \frac{d^2X}{d\tau^2} + \frac{dX}{d\tau} = U \qquad\qquad 2.4a$$

$$2\,Stk\ \frac{d^2Y}{d\tau^2} + \frac{dY}{d\tau} = V \qquad\qquad 2.4b$$

Expressions for U and V in terms of X and Y are normally complex necessitating a computer solution for equation (2.4).   For this purpose the equations are expressed in finite difference form ignoring terms higher than those of a second order in a Taylor expansion.   Expressions 5 thus derived, are used in a step by step calculation of particle trajectories:

$$X_2 = \frac{1}{(4Stk + \tau)}\ \left[2U\tau^2 + Stk\, X_2 + (4Stk-\tau)\, Xo\right] \qquad 2.5a$$

$$Y_2 = \frac{1}{(4Stk + \tau)}\ \left[2V\tau^2 + Stk\, Y_1 + (4Stk-\tau)\, Yo\right] \qquad 2.5b$$

19.

2.2.1 Theoretical Estimation of Sampling Efficiency of a Tube Probe

The sampling valve under consideration is shown diagramatically in fig. 8.
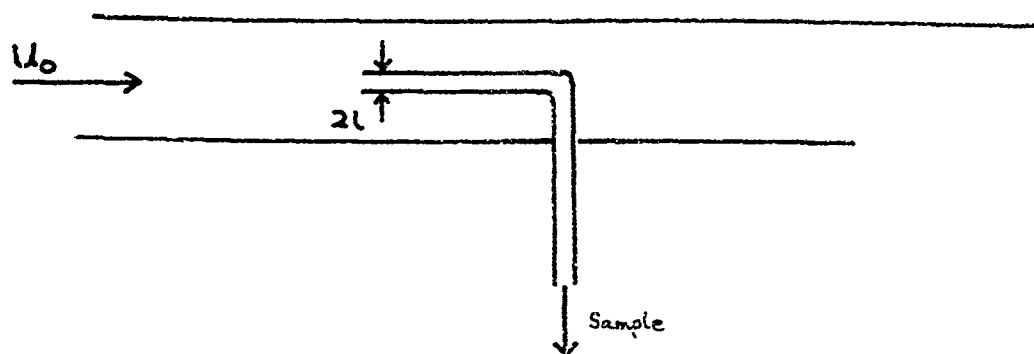
FIGURE 8

Central Probe Sampling Valve

It consists of a sampling probe which is inserted in the main pipe in which the fluid is flowing with a velocity U_o. In this system sampling will be perfect if the sampling velocity is identical to the main stream velocity. However, if the sampling is anisokinetic then the flow will not be planar and sampling errors will arise due to inertial forces acting on the particles.

2.2.1.a Description of Flow Field

The flow field may be approximated to a point source in a planar flow. The field will be valid for small values of l and high Reynolds Numbers. The cartesian velocity resolutes are given by:-

$$\frac{u}{U_o} = 1 + \frac{Qx}{4\pi U_c} \left(x^2 + y^2\right)^{-3/2} \qquad 2.1a$$

$$\frac{v}{U_o} = \frac{Qy}{4\pi U_o} \left(x^2 + y^2\right)^{-3/2} \qquad 2.1b$$

20.

Q represents the strength of the point source. Obviously for isokinetic sampling conditions it is zero. The relationship between Q and the relative sampling velocity, V_R, is given by:

$$V_R = 1 + \frac{Q}{2\pi l^2}.$$

V_R is the ratio of the mean velocity in the sampling probe to the main stream velocity.

2.2.1.b Calculation of Particle Trajectories

The particle is considered as a point mass, which does not effect the flow field in the proximity of the sampling probe. The critical trajectory, for which the particle just touches the edge of the probe is computed.

A force balance on a particle in a fluid results in the following vector equation:-

$$m \frac{du}{dr} = C_D \pi r_p^2 \rho f \left(\frac{U - u}{2} \right)^2 \qquad 2.2$$

2.2.1.c Trajectory Calculation

It is assumed that a particle approaches in the x direction with the main stream velocity to a point 12 upstream from the probe. Equations 25 are then used to calculate the path taken by the particle until it is level with the mouth of the probe. New starting points on the Y axis are taken for the trajectory until the critical trajectory is found. The distance upstream of the starting point and the step length in the calculation have been chosen in such a way that the calculation errors resulting from the use of a finite difference technique are not significant. The calculation was performed using a 1905 ICT digital computer.

2.2.1.d Results and Discussion

The efficiency of sampling can conveniently be defined by

$$\eta = \frac{c}{c_o} = \frac{\text{concentration of contaminant in sample}}{\text{concentration of contaminant in main stream}}$$

The calculated efficiency is shown as a function of V_R, the relative velocity, and Stk, the particle Stokes No. in fig. 9   It is obvious that as the Stokes No. tends to zero, $\frac{c}{co}$ must tend to 1.0. Again as Stk $\longrightarrow \infty$, then

$$\frac{c}{co} \longrightarrow \frac{1}{V_R}$$

Agreement with these limiting values is shown in fig. 2.7 which shows that the transition range of Stokes Nos. for this kind of sampler is 0.1 - 10.0.

On applying the data in fig. 9 to conditions in a hydraulic system with fluid viscosity 20cS flowing through a $\frac{1}{2}$" bore pipe at flow rates corresponding to Re = 200 (0.6 g.p.m.) and Re = 6,000 (18.2 g.p.m.), a sampling orifice 1/8" dia. containing spherical aluminium, copper and tungsten carbide particles of 10 µm, 50 µm and 200 µm the following sampling efficiencies are found for V_R = 2.0 and V_R = 0.5 (Table II).

22.

FIGURE 9   Efficiency of conical probe sampling valve

$V_r = 1.0$

$V_r = 0.75$

$V_r = 1.25$

$V_r = 1.5$

$V_r = 1.75$

$V_r = 2.0$

$V_r = 2.5$

$V_r = 0.50$

$V_r = 0.25$

Stk

ξ_p

23.
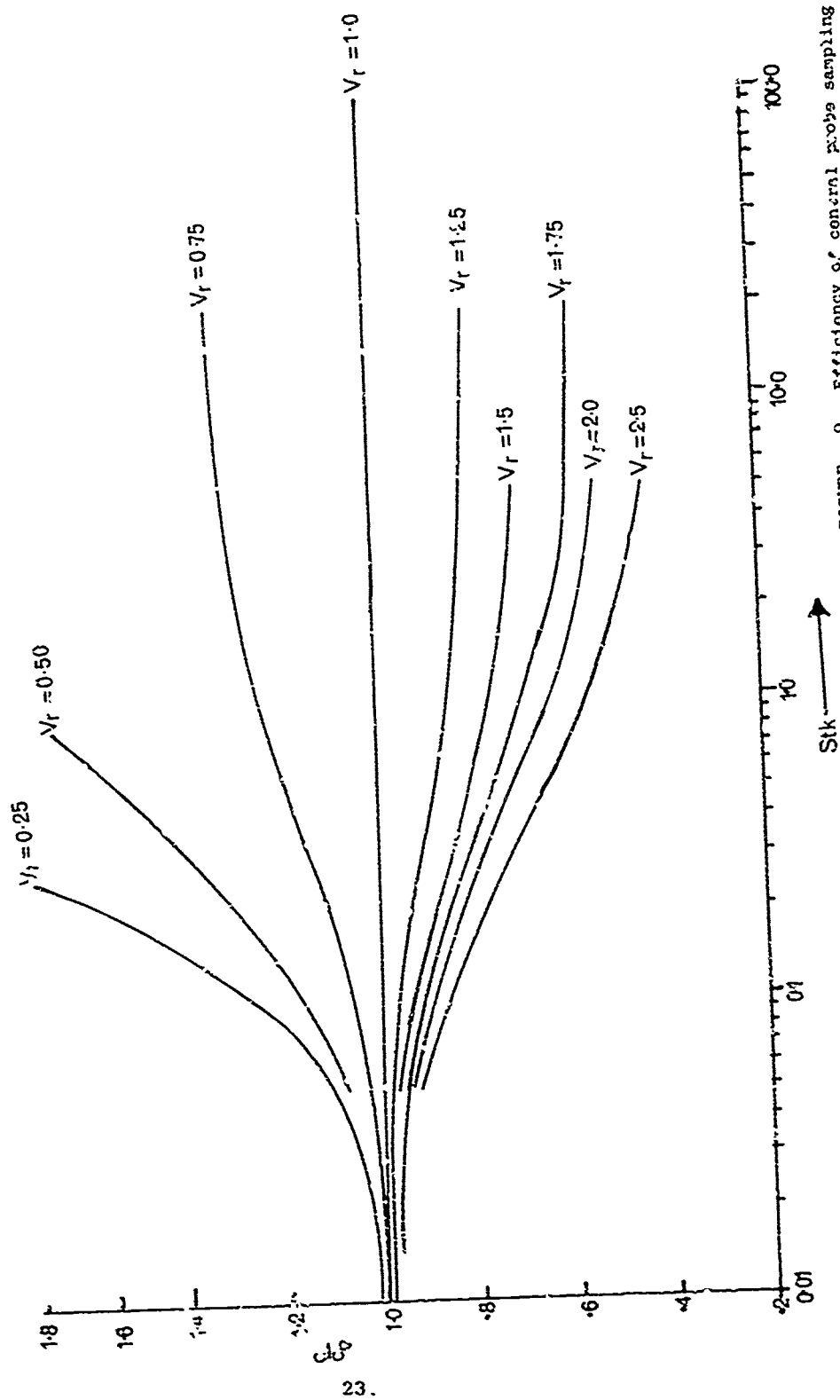
TABLE II   Calculated efficiency of central probe sampler

	D_n (µm)	V_R =	Re = 200		Re = 6,000	
			2.0	0.5	2.0	0.5
Al	10		$0.98 < E < 1.00$	$1.02 > E > 1.00$	$0.98 < E < 1.00$	$1.02 > E > 1.00$
	50		$0.98 < E < 1.00$	$1.02 > E > 1.00$	$0.95 < E < 1.00$	$1.05 > E > 1.00$
	200	$C/C_0 = E$	$0.95 < E < 1.00$	$1.05 > E > 1.00$	0.72	1.55
Cu	10		$0.98 < E < 1.00$	$1.02 > E > 1.00$	$0.98 < E < 1.00$	$1.02 > E > 1.00$
	50		$0.98 < E < 1.00$	$1.02 > E > 1.00$	0.85	1.28
	200		0.90	1.17	0.58	2.0
WC	10		$0.98 \; E \; 1.00$	$1.02 > E > 1.00$	$0.98 < E < 1.00$	$1.02 > E > 1.00$
	50		$0.98 \; E \; 1.00$	1	0.80	1.34
	200		0.87	1.21	0.54	2.0

These results show that sampling in the range $0.5 < V_R < 2.00$ from a system at leakage flow rates would be satisfactory for particles $\leq 100 \; \mu$ whatever their composition and hence density.   Hence one possible approach to sampling would be to have a turbulent flow valve throttled for approximately isokinetic operation (i.e. $0.5 < V_R < 2.0$) at leakage flow just upstream of the sensitive component.

2.3   Experimental Study of Sampling Systems - Determination of Flow Field

Flow visualisation techniques are used to determine the flow fields in models of sampling valves, the fields in which are not amenable to analytical description.   The technique used is that of streak photography of neutral density particles.

Figure 10 shows a diagram of the apparatus.   Light from an iodide-quartz lamp is collimated into a two-dimensional (1/8" thick) beam to illuminate a plane within the sampling valve.   The valves are transparent models of the sampling valves encountered in practice.   To avoid problems of parallax in observing the flow inside the valves the model is enclosed in a box which contains liquid which has the same refractive index as the valve.   In this way a flat smooth surface is presented for photography.

The liquid (water) being used contains a very low concentration of small neutral density particles (polystyrene) which will follow the path lines of the fluid.   Streak photographs taken at an angle of 120° to the light beam show the path of these particles clearly enabling the complete flow field to be determined.   The conditions which are being studied are dynamically similar to those which are used in sampling aircraft hydraulic systems.   This technique is now being used to study flow fields in a number of sampling valves under a range of conditions and the full results will be reported at a later date.

One of the first photographs taken whilst making a feasibility study of the system is included in this report as fig. 11.   This is a photograph of the flow in a simple T valve.   The path lines of the fluid are clearly shown by the faint streaks.   In this particular test 100 micron classified particles of aluminium dust were added to the fluid.   These are shown by the more intense streaks. It can be seen that these particles which have high inertia cut across the fluid streamlines.   When this occurs in practice, the sample obtained will not be representative.

25.

Quartz iodine
light

Mirror

Glass model of sampling valve

Collimator

Box containing liquid of same refractive
index as glass

120°

Camera

Collimated beam of light
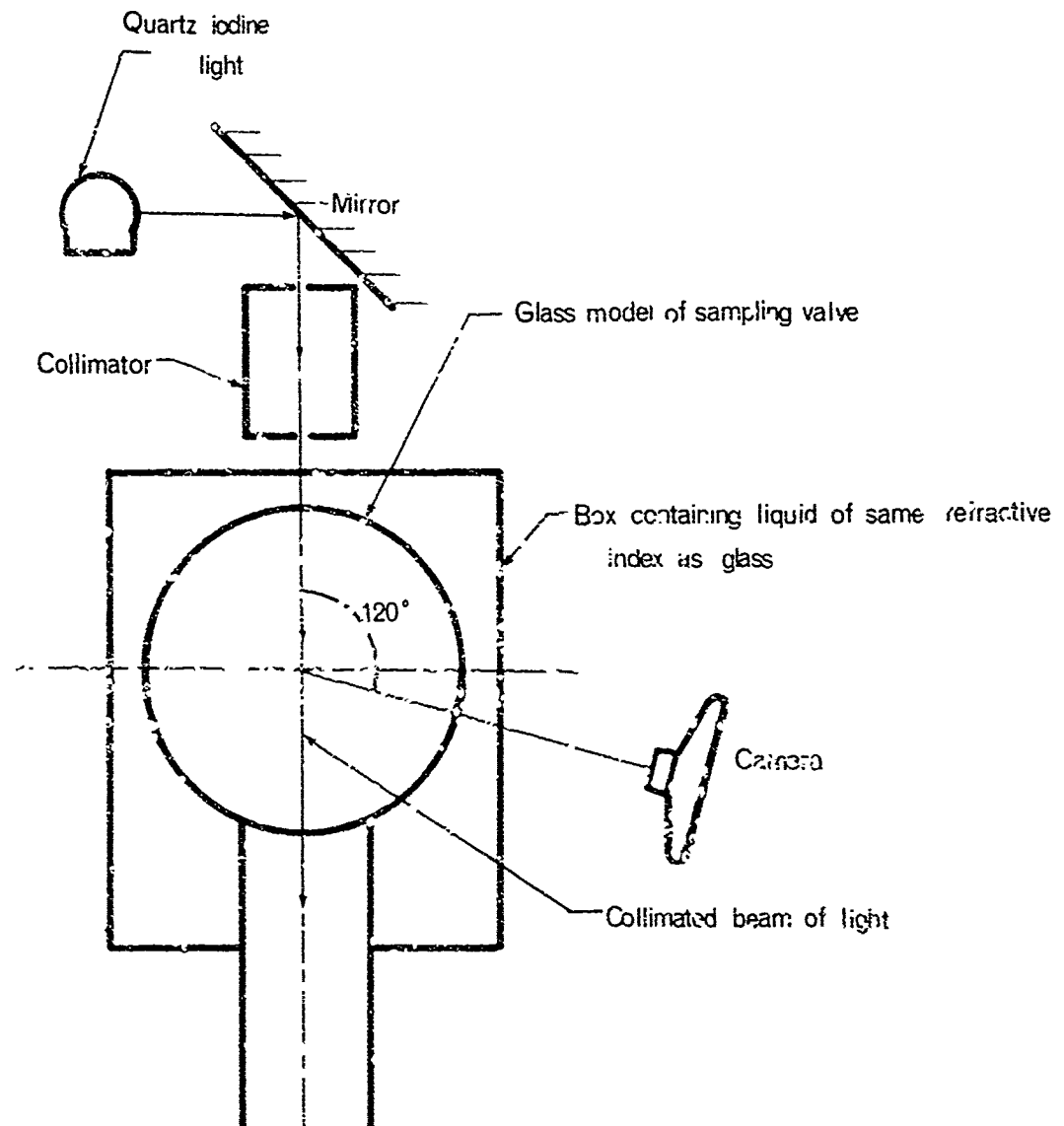
FIGURE 10   Apparatus for flow visualisation

26.
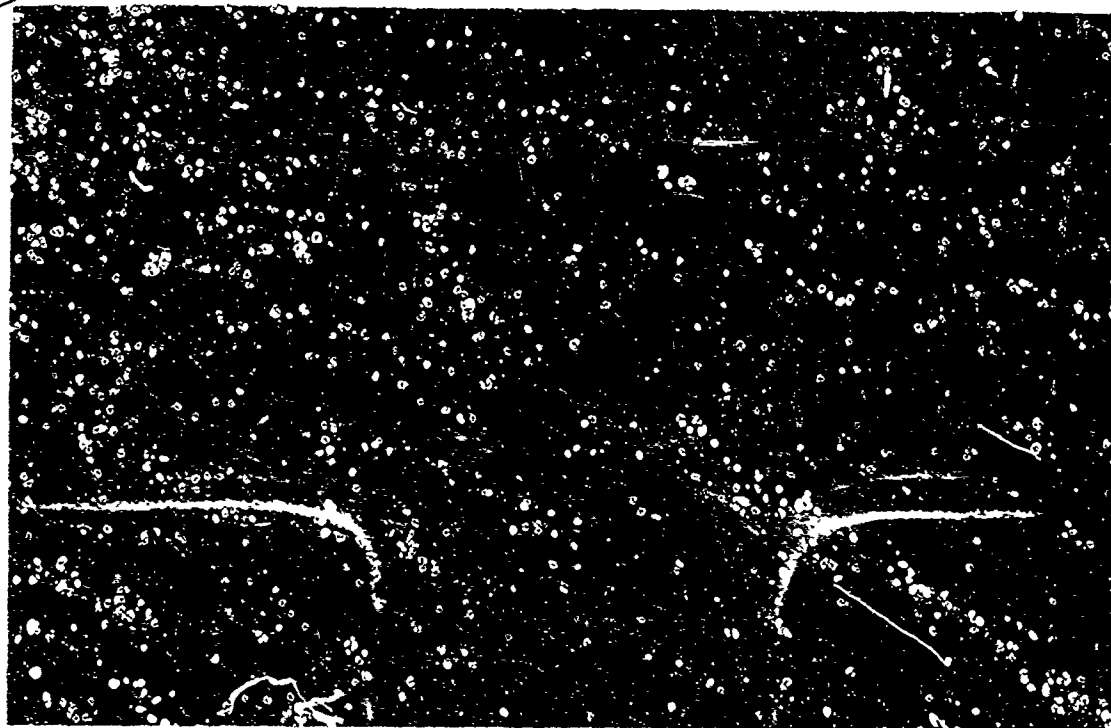
FIGURE 11

Fluid and particle flow in a 'T' piece

47.

Chapter 3

Mathematical Modelling of

a Hydraulic System

28.

3.1. Introduction

This section describes an attempt to model a simplified aircraft hydraulic actuating system, so that given sufficient information the model might be used to calculate the probability of a failure occurring within the system. This simplified model system is not normally found in practice but however it does illustrate how the mathematical techniques could be employed to describe any real system. No actual calculations have been carried out on the model, because at present sufficient information about the parameters involved is not available. Methods of obtaining this information is of course the major function of this contract. The model used is based upon the representation of particle concentrations by vectors and the system by matrix operations upon these vectors. The model will be complex and is therefore most useful if it is in a form suitable for computer solution. This fact was considered throughout the report and the final form of the model is a computer flow sheet.

3.2. Aircraft Hydraulic Systems

3.2.1. A hydraulic system is a means of transmitting power which makes use of pressurised fluid. The system must consist of at least 3 parts, a pressure source, a transmission line, and an actuator.

3.2.2. In aircraft systems the pressure source is a mechanical pump taking its power from either the main aircraft engines or from auxiliary power supplies. The most usual type of pump is a constant pressure, variable delivery pump. However the system modelled in this report makes use of a constant delivery pump.

3.2.3. The motor transforms the work available in the moving fluid back into mechanical power. The simplest and most usual form of motor is a piston actuator, which provides oscillatory motion only. If rotating motion is required, then a motor similar in design to the pump is employed.

3.2.4. A hydraulic fluid must meet many requirements amongst which are reasonable viscosity over the desired temperature range, resistance to mechanical and chemical breakdown, good lubricity characteristics, compatibility with constructional metals and elastomer components, low specific gravity and reasonable price.

3.2.5. The basic system considered in this report is shown in Figure 12

3.2.6. The reservoir is necessary to accommodate changes in the volume of fluid within the circuit and to provide a reservoir of fluid to replace that lost by leakage.

3.2.7. A filter is included in the pressure line from the pump. In real circuits there are several filters, but almost invariably one in the pump pressure line.

3.2.8. The system illustrated has a pressure relief valve in conjunction with a constant delivery pump. It would not be difficult to alter the model to accommodate a constant pressure variable delivery pump with the relief valve only being used to relieve excess pressures in the pumping circuit.

3.2.9. The system is equipped with a 4-way valve enabling an actuator to be operated in both directions.

3.2.10. In Figure 12 arrows show the direction of flow of the fluid. In the system illustrated the flow is unidirectional in all components before the 4-way valve, but beyond the valve is in either direction depending upon the valve position.
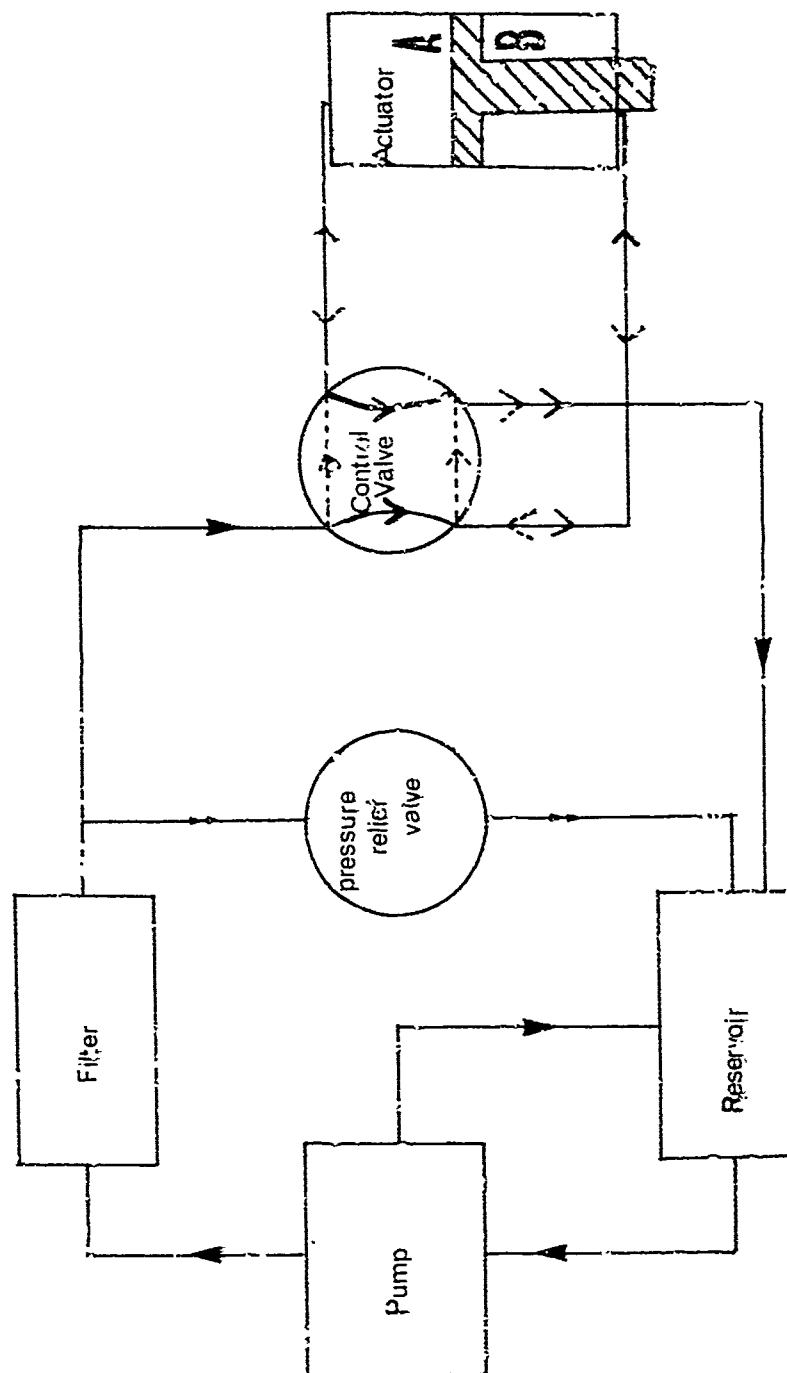
FIGURE 12   Model hydraulic system

31.

The part of the system before the valve in which the fluid flows in one direction only is called power circuit.

The operation of the system shown in Figure 12 may be understood by studying the diagram. It will be seen that the control valve has 3 positions. In the position illustrated pressure is applied to the underside of the power piston and the fluid from above the power piston flows through the valve and back to the reservoir. When the valve position is changed, as shown by the dotted lines, fluid is forced by the pump into the actuator above the piston and fluid below the piston passes through the valve and back to the reservoir. In this way it is possible to obtain a power stroke in either direction using the combination of 4-way valve and double acting actuator.

32.

3.3 The Use of Matrices for Modelling Particulate Systems

3.3.1 In order to construct a mathematical model for a system in which individual components may alter the concentration of particles it is necessary to be able to describe efficiently the particle size distribution and the way in which this is changed by the system. One convenient technique is to represent particle size distributions as column vectors, and operators which change them by square matrices. This has the advantage that any calculation requires only the use of matrix algebra.

3.3.2 The simplest method of representing a particle size distribution as a vector is to equate the elements of the vector with the columns of a frequency/size histogram for the distribution. Thus the histogram:
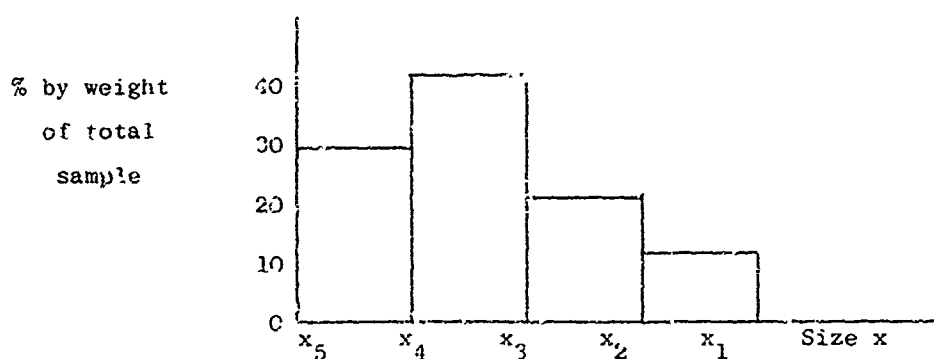
would be represented by the vector:

$$s = \begin{bmatrix} s_1 \\ s_2 \\ s_3 \\ s_4 \end{bmatrix} = \begin{matrix} = \\ = \\ = \\ = \end{matrix} \begin{bmatrix} 10 \\ 20 \\ 40 \\ 30 \end{bmatrix}$$

where s_1 is the percentage by weight in the size range x_1 to x_2, s_2 is the percentage by weight in the size range x_2 to x_3, and so on. Using this technique it is

33.

possible to represent the particle size distribution in terms of any convenient parameter, e.g., weight, number, volume or any of the other parameters used in particle size analysis.

3.3.3   An alternative method is to let s_1, s_2, etc., be actual weights in each size fraction. The sum of the elements of the vector is then equal to the total weight of particles in the system. Thus for example, a particle sample with the following sieve analysis:-

TABLE III

Sieve Analysis

Size range	Weight retained gm.
300 μm	0.03
300-200 μm	0.28
200-100 μm	0.47
100 μm	0.41
Total	1.19

could be represented in vector form by:-

$$\underline{s} = \begin{bmatrix} 0.03 \\ 0.28 \\ 0.47 \\ 0.41 \end{bmatrix}$$

3.3.4.   The use of actual weights rather than percentages by weight has one important advantage when matrix techniques are used to represent particulate systems. For example, the perfect mixing of two particle size distributions $\underline{r}$ and $\underline{s}$ is represented by addition of the vectors, provided that both size distribution vectors are in terms of actual weights,

$$\therefore \quad \begin{bmatrix} r_1 \\ r_2 \\ r_3 \\ r_4 \end{bmatrix} + \begin{bmatrix} s_1 \\ s_2 \\ s_3 \\ s_4 \end{bmatrix} = \begin{bmatrix} r_1 + s_1 \\ r_2 + s_2 \\ r_3 + s_3 \\ r_4 + s_4 \end{bmatrix}$$

Size distribution vector for mixed material.

If, however, the size distribution vectors are expressed in terms of percentage by weight, then they must be multiplied by the sample weight ρ and ρ before addition can be performed.

i.e.,

$$\rho \begin{bmatrix} r_1 \\ r_2 \\ r_3 \\ r_4 \end{bmatrix} + \sigma \begin{bmatrix} s_1 \\ s_2 \\ s_3 \\ s_4 \end{bmatrix} = (\rho + \sigma) \begin{bmatrix} \dfrac{\rho r_1 + \sigma s_1}{\rho + \sigma} \\ \dfrac{\rho r_2 + \sigma s_2}{\rho + \sigma} \\ \dfrac{\rho r_3 + \sigma s_3}{\rho + \sigma} \\ \dfrac{\rho r_4 + \sigma s_4}{\rho + \sigma} \end{bmatrix}$$

For this reason it is more useful to express particle size distribution vectors in terms of weights rather than percentages by weight, and the former method of representation is used in the following chapters of this report.

Where it is more appropriate, weight concentrations in the fluid, or weight feed-rates, i.e.. weight passed per unit time, are used instead of actual weights.

3.3.5.   Operations, other than perfect mixing, which affect particle size distributions may be represented by square matrices. Matrix models for classifying and steady state grinding operations have already been developed to a considerable extent, ref.3.1, and matrix modelling work in other types of particle processing should prove equally fruitful.

In general, if a size distribution $\underline{r}$ is changed to a size distribution $\underline{s}$ by a process, then the process may be represented by a matrix A such that:

$$\underline{s} = A \underline{r}$$

Thus, if $\underline{r} = \begin{bmatrix} r_1 \\ r_2 \\ r_3 \\ r_4 \end{bmatrix}$, $\underline{s} = \begin{bmatrix} s_1 \\ s_2 \\ s_3 \\ s_4 \end{bmatrix}$ and $A = \begin{bmatrix} a_{11} & a_{12} & a_{13} & a_{14} \\ a_{21} & a_{22} & a_{23} & a_{24} \\ a_{31} & a_{32} & a_{33} & a_{34} \\ a_{41} & a_{42} & a_{43} & a_{44} \end{bmatrix}$

multiplying $\underline{s} \leftarrow A \underline{r}$ gives:

$$s_1 = a_{11}r_1 + a_{12}r_2 + a_{13}r_3 + a_{14}r_4$$

$$s_2 = a_{21}r_1 + a_{22}r_2 + a_{23}r_3 + a_{24}r_4$$

$$s_3 = a_{31}r_1 \quad a_{32}r_2 \quad a_{33}r_3 \quad a_{34}r_4$$

$$s_4 = a_{41}r_1 \quad a_{42}r_2 \quad a_{43}r_3 \quad a_{44}r_4$$

The coefficients a_{ij} of A represent the fraction of particles of size j which are changed to size i.

3.3.6.   In many cases, several of the coefficients of A are zero. For example a classifier is usually considered not to cause changes in particle sizes. The only non zero elements a_{ij} are thus those where i = j. A typical classifier matrix C, has the form:

$$C = \begin{bmatrix} c_{11} & 0 & 0 & 0 \\ 0 & c_{22} & 0 & 0 \\ 0 & C & c_{33} & 0 \\ 0 & 0 & 0 & c_{44} \end{bmatrix}$$

For a perfect classifier the coefficients c_{ii} are either unity or zero, depending upon whether a size range is greater or smaller than the classifier size. For a real classifer, however, the coefficients represent the classifier efficiencies for the size ranges concerned.

3.3.7. In a grinding machine it is reasonable to assume that no size enlargement takes place, therefore a matrix representing grinding would contain zero coefficients for all those terms representing enlargement. The final matrix would be lower triangular in form:

$$
M = \begin{bmatrix}
m_{11} & 0 & 0 & 0 \\
m_{21} & m_{22} & 0 & 0 \\
m_{31} & m_{32} & m_{33} & 0 \\
m_{41} & m_{42} & m_{43} & m_{44}
\end{bmatrix}
$$

Since there is no generation or loss of solids in the mill then the sum of all m_{ij} for any constant j is unity, i.e., the sum of all fractions of particles from a given size range is equal to the weight of particles in that size range.

Thus:

$$r_1 = m_{11}r_1 + m_{21}r_1 + m_{31}r_1 + m_{41}r_1$$

$$r_2 = m_{22}r_2 + m_{32} + m_{42}r_2$$

$$r_3 = m_{33}r_3 + m_{43}r_3$$

$$r_4 = m_{44}r_4$$

This property, of the sums of the elements in each column being equal to unity, is common to all operator matrices which change only the particle size distribution, and not the total weight of the particles.

3.3.8. A size enlargement device may also be represented by a matrix. In this case no particle is decreased in size, so the matrix reduces to an upper triangular matrix:

$$
E = \begin{bmatrix}
e_{11} & e_{12} & e_{13} & e_{14} \\
0 & e_{22} & e_{23} & e_{24} \\
0 & 0 & e_{33} & e_{34} \\
0 & 0 & 0 & e_{44}
\end{bmatrix}
$$

37.

3.3.9. All operations involving particles may be considered to be a combination of the three basic operations above, classification, size reduction and size enlargement. A matrix representing any operation can thus be built up from the three basic processes by analysis of the operation in terms of these three basic processes. For example, filtration is a form of classification; erosion is a form of grinding although the generation of particles results in the sums of the matrix columns being greater than unity.

3.3.10. The values of the matrix coefficients are best determined experimentally, e.g., the coefficients of a classifier matrix are the classifying efficiencies for each size range. Much work is being done, however, towards theoretical determination of matrix coefficients, especially in the matrices associated with grinding operations.

References

3.1   R. Braithwaite, Loughborough University Ph.D. Thesis 1968.

3.4 Characterisation of Individual Components in a Hydraulic System

3.4.1 In order to set up a mathematical model for the complete system it is necessary to find a matrix description of each component in the circuit. The main items considered are the pump, filter, pressure relief valve, reservoir, the 4-way valve, and the actuator. The volumes of fluid retained in the connecting pipework must also be considered. Details of models used for each item in the circuit together with the assumptions made in order to devise each model are given in paragraphs 3.4.3 to 3.4.8 below. Paragraph 3.4.2 summarises the nomenclature used in this and subsequent chapters. Fig. 16 shows the particle concentrations and fig. 17 the volume elements in the model system.

3.4.2 Consistant units must be employed for the particle size distribution vectors at all points in the system. Unless otherwise stated, all particle size distribution vectors, in this and succeeding chapters, have the units (weight of particles) (unit volume of fluid). The coefficients of all matrices are dimensionless. The notation used throughout is:

(1) Upper case letters - all matrices

(2) Lower case letters, underlined - all particle size distribution vectors.

(3) Lower case letters, not underlined and greek symbols - scalars, usually velocities or volumes.

e.g. $\underbrace{(x - z)}_{\text{Scalars}}$ $\underbrace{A.B.}_{\text{Matrices}}$ $\underbrace{(\underline{c} - \underline{d})}_{\text{Vectors}}$

A list of all the symbols used, in alphabetical order, is given on pages xiii-xvi

3.4.3 The Pump

The pump considered in the circuit is a constant displacement swash plate piston pump of the type used in aircraft systems. The major points of wear and hence sources of particles will be considered as the valve plate and the piston shoes. There is comparatively little erosion of the pistons and cylinder barrel and this may be ignored as a first approximation. Also the simplifying assumption is made that the rate of wear of the valve plate and piston shoes is independent of the concentration of particles in the fluid, but depends upon the speed of rotation of the pump and to some extent upon the age of the pump. It is also assumed that there is no leakage of particles in the case drain fluid

39.

(1)   The eroded particles may because of the constructional materials of the pump , be very hard and might be expected to cause further erosion of the pipework and other items in the circuit. Assuming again that the pump is operated at constant speed, the rate of erosion will be constant, the fluid flow rate will be constant and hence the concentration of particles in the fluid, as the result of pump erosion, will be constant. Now $\underline{m}$ is the particle concentration in the fluid leaving the reservoir and $\underline{b}_m$ is the increase in concentration as a result of breakdown of the line between the reservoir and the pump.

$\therefore$ the concentration at the pump inlet $= \underline{m} + \underline{b}_m$.

Let the concentration at the pump outlet be $\underline{p}$.

Let the increase in concentration as a result of erosion of the valve plate be $\underline{a}$.

If it is assumed that:

(1)   there is no accumulation of particles inside the pump,

(2)   there is no loss of particles as a result of leakage into the case,

then a particle mass balance over the pump gives:

$$\underline{p} = \underline{m} + \underline{b}_m + \underline{a}.$$

Let the particle concentration of eroded material from the piston shoes be $\underline{d}$. If it is assumed that there is no accumulation of particles inside the case, then the particle concentration of the fluid leaving the case drain valve is $\underline{d}$.

3.4.4.   The Filter

The filter acts as a classifier on the particles. The particle concentration at the filter inlet, including particles in the fluid as a result of breakdown of the pipework is $(\underline{p} + \underline{b}_p)$.

Let the output concentration be $\underline{f}$.

Then $\underline{f} = F. (\underline{p} + \underline{b}_p)$

where F is a diagonal matrix of the form:

$$F = \begin{bmatrix} f_{11} & 0 & 0 & 0 \\ 0 & f_{22} & 0 & 0 \\ 0 & 0 & f_{33} & 0 \\ 0 & 0 & 0 & f_{44} \end{bmatrix}$$

The matrix coefficients may be represented by the filter efficiencies for each size range. These, however, are not constant but depend upon the fluid velocity and acceleration, particle loading, and cake thickness.

3.4.5   The Pressure Relief Valve

In the pressure relief valve, erosion of the valve seat by the hard particles occurs first, followed by collection of particles inside the valve. Since many of the particles are hard, and there are considerable difficulties in the practical differentiation between hard and soft particles, we have assumed, for the purposes of the model, that all the particles are hard. It may even be possible to incorporate this difference in the coefficients of the erosion matrix, although this is beyond the scope of this report.

The particle concentration at the pressure relief valve inlet including pipework breakdown is $(\underline{f} + \underline{b}_f + \underline{b}_g)$. After erosion this is changed to $E_{pv} (\underline{f} + \underline{b}_f + \underline{b}_g)$ where E_{pv} is a lower triangular matrix similar to that used to represent a grinding machine. E.g.:

$$E_{pv} = \begin{bmatrix} e_{11} & 0 & 0 & 0 \\ e_{21} & e_{22} & 0 & 0 \\ e_{31} & e_{32} & e_{33} & 0 \\ e_{41} & e_{42} & e_{43} & e_{44} \end{bmatrix}$$

This concentration is changed, by the collection of particles inside the valve, to $C_{pv} E_{pv} (\underline{f} + \underline{b}_f + \underline{b}_g)$ where C_{pv} is a diagonal matrix.
This concentration is equal to the outlet concentration $\underline{z}$

$$\therefore \quad \underline{z} = z (\underline{f} + \underline{b}_f + \underline{b}_g).$$

3.4.6   The Reservoir

The reservoir is assumed to be a perfect mixer. Since it is assumed that there is no leakage, and there is no generation or settling of particles in the reservoir, then the reservoir composition is easily calculated by a mass balance across the reservoir. The method used to determine this mass balance depends entirely upon the model used for the circuit. The methods used for our final model are described in detail in 3.7.

The reservoir outlet contains a filter. If the particle concentration inside the reservoir is $\underline{r}$, and the outlet concentration is $\underline{m}$, then: $\underline{m} = R\underline{r}$ where R is a diagonal matrix representing the filter, e.g.:

$$R = \begin{bmatrix} r_{11} & 0 & 0 & 0 \\ 0 & r_{22} & 0 & 0 \\ 0 & 0 & r_{33} & 0 \\ 0 & 0 & 0 & r_{44} \end{bmatrix}$$

3.4.7 The 4-way Valve

The directional control valve is a 4-way servo valve, but in order to simplify the model, is only considered as having 3 operating conditions, the neutral position and the hard over position in either direction. As an example of a valve for this circuit one could consider a manually operated valve similar to the second stage of an electro-hydraulic spool and sleeve valve. This valve is illustrated in figs. 13-15.

It will be assumed that particle build up, i.e.silting occurs in those positions within the valve where high pressure fluid is leaking to the return, and these positions will be called x_1, x_2 and x_3. The close fit between the valve spool and spool cylinder will cause the leakage points to act as filters, collecting particles at points x_1, and x_2 and x3. The particles remaining in the leaking fluid then cause erosion of the spool and cylinder wall.

The inlet particle concentration for the valve, including breakdown of pipework is
$$(\underline{f} + \underline{b}_f + \underline{b}_h)$$
Let the outlet concentration of the valve be $\underline{\ell}$

$$\therefore \quad \underline{\dot{\ell}} = E_{vc} \cdot C_{vc} \, (\underline{f} + \underline{b}_f + \underline{b}h \,)$$

where E_{vc} is a triangular matrix representing erosion, and C_{vc} is a diagonal matrix representing particle collection. E_{vc} and C_{vc} can be multiplied to give a triangular matrix L_c, representing the overall leakage effect when the valve is closed. This gives:
$$\underline{\ell} = L_c \, (\underline{f} + \underline{b}_f + \underline{b}_h \,)$$
Since the valve is of symmetrical design it is reasonable to assume that the action of the valve on the particles is exactly the same when the actuator is being raised as it is when the actuator is being lowered. When the actuator is being raised, (fig. 15), the only action of the valve itself is erosion by the particles in the fluid. This is quite small and has been ignored. However, the concentration of particles leaving the valve is affected by the particles collected at x_3, x_4 and x_5 during leakage.

Total weight of particles captured $=\sum\limits_{1}^{c} (1-C_{vc}) \, (\underline{f} + \underline{b}_f + \underline{b}_h)$
where C is the total volume of fluid which has leaked.

However, only a fraction, ϕ, of this weight collects at point x_3.

Further, accumulation of particles at point x_3 will probably result in compacting of the particles. Thus when the valve is open some particles will probably adhere

42.
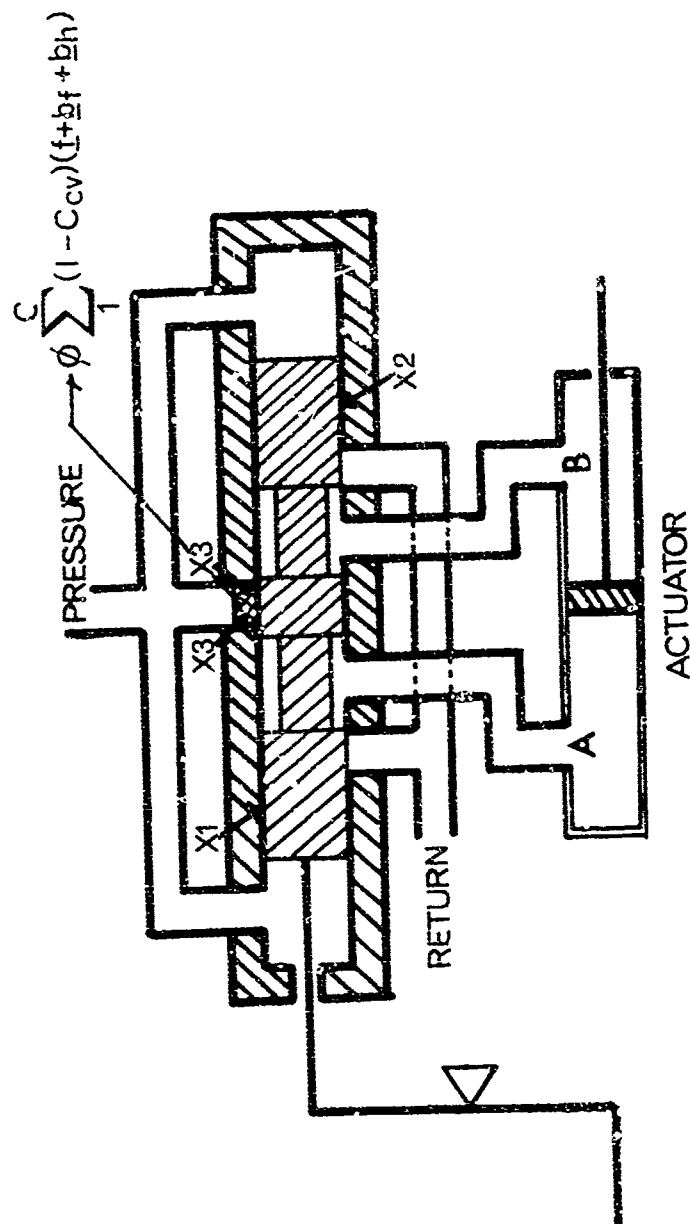
FIG.13 VALVE ACTUATOR STATIONARY

$$\phi \sum_1^C (1-C_{cv})(f+\underline{b}_f+\underline{b}_h)$$

PRESSURE

X3

X3

X1

X2

RETURN

A

B

ACTUATOR

43.
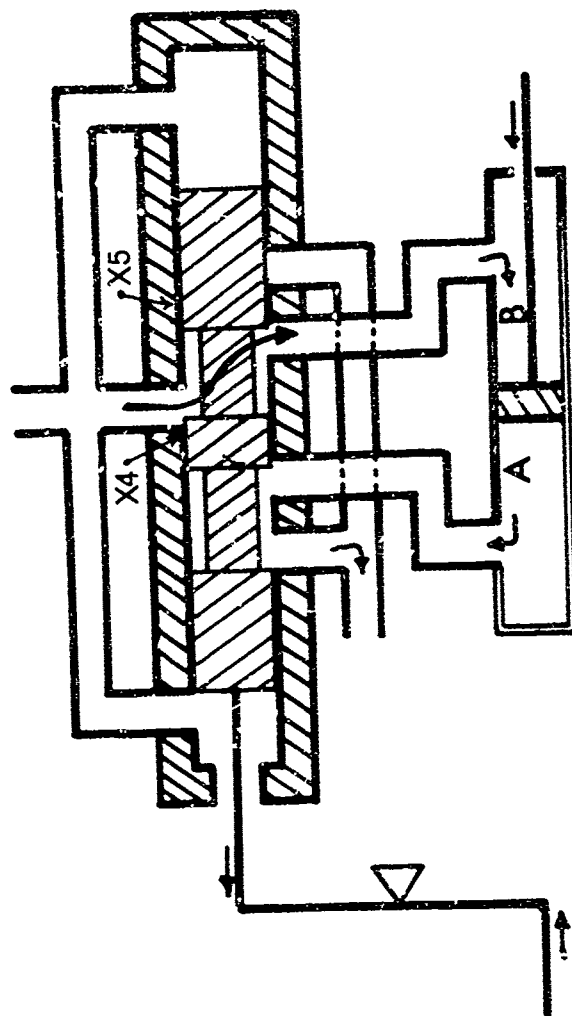
FIG 14 VALVE ACTUATOR MOVING TO LEFT

X5

X4

B

A
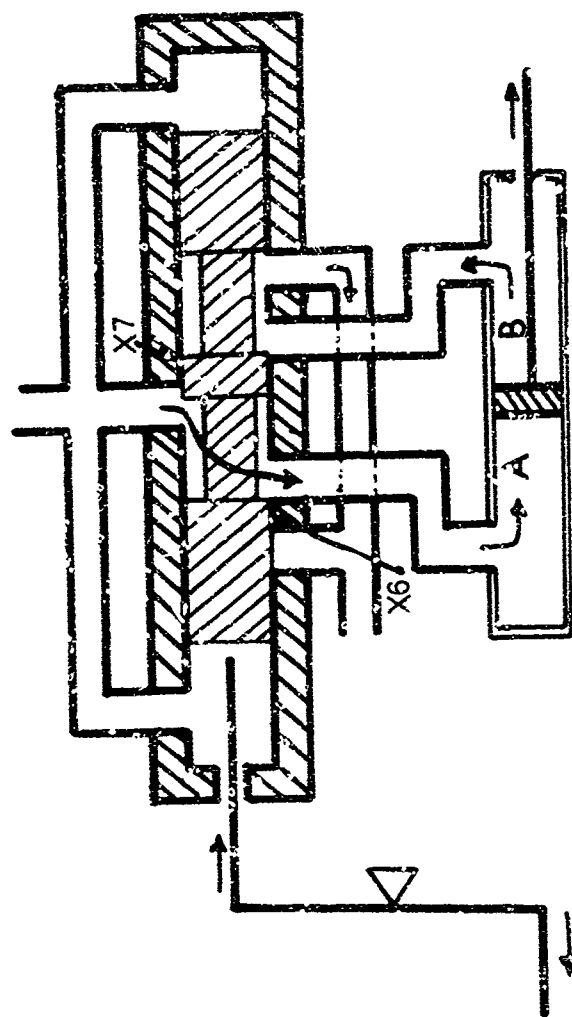
FIG 15 VALVE ACTUATOR MOVING TO RIGHT
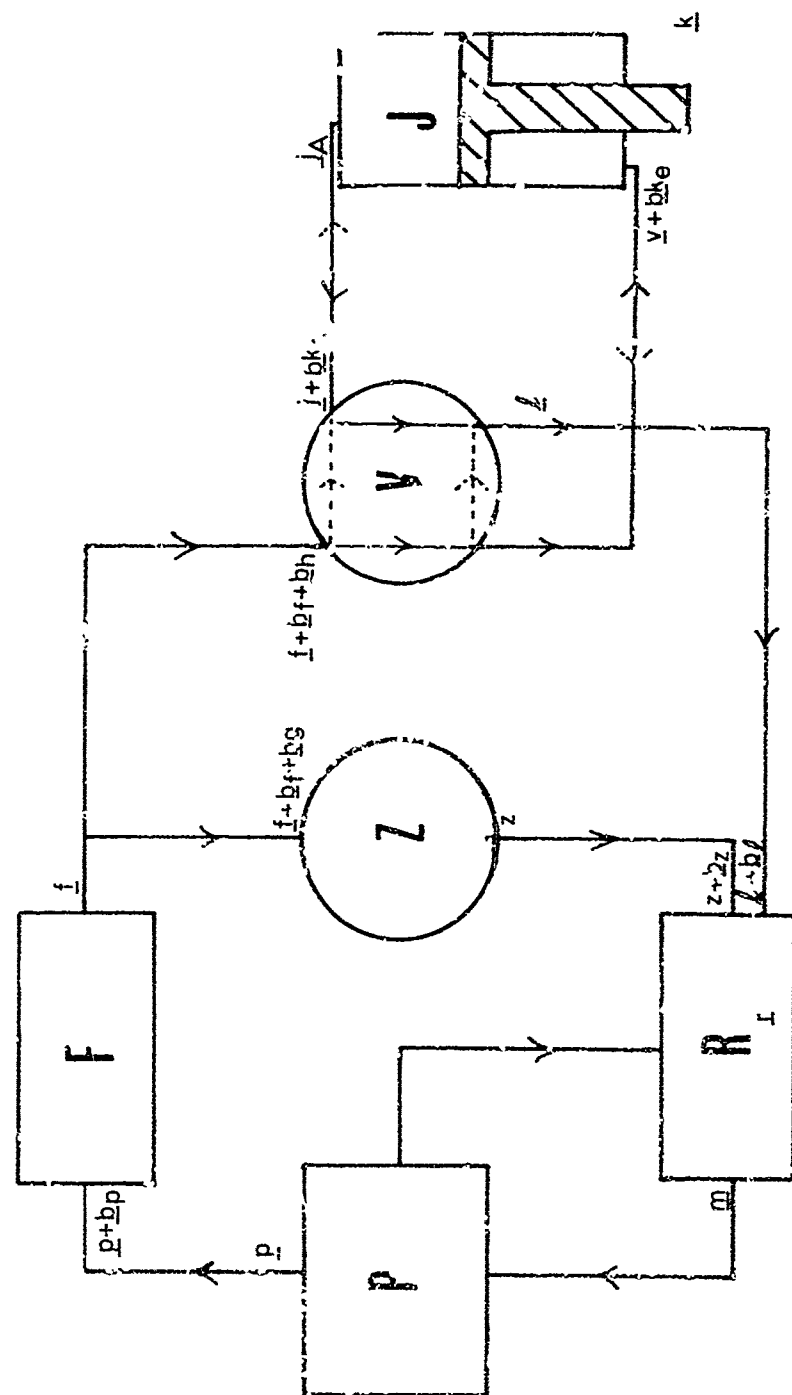
FIGURE 16   Particle concentrations in model hydraulic system

46.
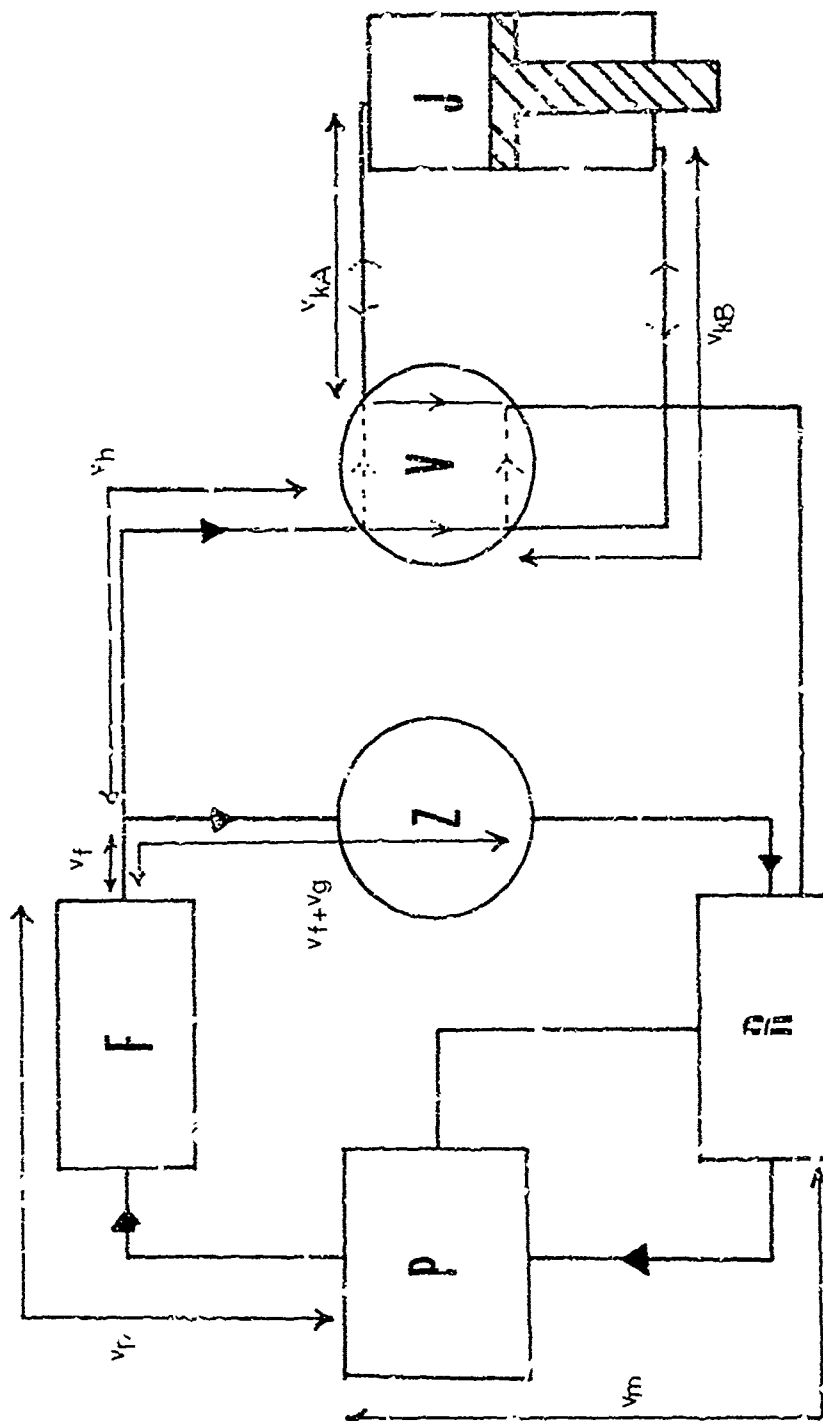
FIGURE 17   Volume elements in model hydraulic system

47.

to the orifice walls. If the fraction of particles which does not adhere is θ, then the weight of particles which enters the fluid being pumped into the actuator is given by:

Weight of particles released form $x_3 = \theta \phi \sum_1 (I-C_{vc}) (\underline{f} + \underline{b}_f + \underline{b}_h)$.

Whilst the actuator is being raised, further leakage occurs at points x_2, x_4 and x_5. The mechanism of this leakage is exactly the same as for leakage when the valve is closed, the only difference being that the leakage points, and hence the matrix coefficients, are different. The equation for the leakage effect when the valve is open is thus:

$$\underline{\ell} = L_o (\underline{f} + \underline{b}_f + \underline{b}_h)$$

where $L_o = E_{vc} \cdot C_{vo}$ (the matrices being similar in structure to L_c, E_{vc} and C_{vc} above).

The total weight of particles captured as a result of this leakage is thus:

$$\sum_1^o (I-C_{vo}) (\underline{f} + \underline{b}_f + \underline{b}_h)$$

where o is the total volume of fluid which has leaked.

Since the high pressure fluid is in motion it is reasonable to assume that all particles captured as points x_4 and x_5 are carried into the actuator by the motion of the fluid. Thus if the fraction of the total particles captured which are captured at points x_4 and x_5 is Ψ then the weight of particles being pumped to the actuator is:

$$\Psi \sum_1^o (I-C_{vo}) (\underline{f} + \underline{b}_f + \underline{b}_h)$$

If the concentration of particles in the fluid as it leaves the valve before entering the actuator is $\underline{v}$, then:

$$\underline{v} = (\underline{f} + \underline{b}_f + \underline{b}_h) + \frac{1}{V_{jB}} \left[\theta \phi \sum_j^c (I-C_{vc}) (\underline{f} + \underline{b}_f + \underline{b}_h) \right.$$

$$\left. + \Psi \sum_1^o (I-C_{vo}) (\underline{f} + \underline{b}_f + \underline{b}_h) \right]$$

where V_{jB} is the total volume of fluid pumped into the actuator.

The effect of the valve on low pressure fluid returning from the actuator is erosion. Since this is only slight it may be ignored. Thus, if the

concentration at the valve inlet, including pipework breakdown, is $(\underline{j}_A + \underline{b}_{kA})$, then the outlet concentration $\underline{\ell}$ is given by:

$$\underline{\ell} = (\underline{j}_A + \underline{b}_{kA}).$$

The valve action when the actuator is lowered is similar to that above, the equations being:

$$\underline{v} = (\underline{f} + \underline{b}_f + \underline{b}_h) + \frac{1}{V_{jA}} \left[\theta\phi \sum_1^c (I-C_{vc}) \; (\underline{f} + \underline{b}_f + \underline{b}_h) \right.$$

$$\left. + \Psi \sum_1^o (I-C_{vo}) \; (\underline{f} + \underline{b}_f + \underline{b}_h) \right]$$

$$\underline{\ell} = (\underline{j}_B + \underline{b}_{kB})$$

The values of the total leakage volumes, c and o, are not necessarily the same as for those when the jack is being raised.

3.4.8 The Actuator

The action of the actuator is basically particle capture, at the inlet nozzle, on the piston rings and on the piston gland (side B only). On side B there is an additional effect due to ingress of fresh particles from the surface of the piston rod.

Consider side B, after it has been filled n times.

Total weight of solids in actuator = (contents of line 5) + (make-up from line 3) + (ingress from piston rod).

The volume of line 5 is V_{kB} and the particle concentration is $\underline{j}_{Bn}-1$.

If the collection effect as fluid enters the actuator is $\cup_{jB1}$, then the total weight of particles which enters the actuator from line 5 including pipework breakdown is:

$$V_{kB} \; C_{jB1} \; (\underline{j}_{Bn}-1 + \underline{b}_{kB})$$

The volume of fluid from line 3 which is required to make up the actuator volume is $(V_{jB}-V_{kB})$, assuming that the actuator volume is larger than the volume of line 5. The concentration of fluid entering the actuator from line 3 is $(\underline{v} + \underline{b}_{kB})$. Thus the total weight of particles from line 3, including pipework breakdown, which enters the actuator is:

$$C_{jB1} \; \sum_1^{(V_{jB}-V_{kB})} (\underline{v} + \underline{b}_{kB})$$

49

The reason for a sum is that $\underline{v}$ is not constant but varies with each step change.

The weight of particles which enters the actuator as external contamination on the piston rod is assumed to be constant and equal to $\underline{k}'$.
Let the total weight of solids inside the actuator be $\underline{s}_{BN}$

$$\dot{\underline{s}}_{BN} = v_{kB} \ C_{jB1} \ (\underline{\dot{j}}_{Bn-1} + \underline{b}_{kB}) + C_{jB1} \ \overset{(v_{jB} - v_{kB})}{\underset{1}{\sum}} (\underline{v} + \underline{b}_{kB}) + \underline{k}'.$$

$\therefore$ The particle concentration inside the actuator is $\dfrac{1}{v_{jB}} \ \underline{\dot{j}}_{Bn}$.

As side B empties, particles are collected on the piston rings, outlet nozzle, and piston rod gland. If these effects are represented by the matrices C_{jB2}, C_{jB3} and C_{jG} respectively, then the actuator outlet composition $\underline{\dot{j}}_{Bn}$ is given by:

$$\underline{\dot{j}}_{Bn} = \frac{1}{v_{jB}} \left[(C_{jB2} + C_{jB3} + C_{jG}) \ \underline{s}_{Bn} \right]$$

$$\underline{\dot{j}}_{Bn} = \frac{1}{v_{jB}} \left[C_{jB} \left(v_{kB} \left(\underline{\dot{j}}_{B,n-1} + \underline{b}_{kB} \right) + \overset{(v_{jB} - v_{kB})}{\underset{1}{\sum}} (\underline{v} + \underline{b}_{kB}) \right) + K.\underline{k} \right]$$

where $C_{jB} = (C_{jB2} + C_{jB3} + C_{jG}) \ C_{jB1}$

$K = (C_{jB2} + C_{jB3} + C_{jG})$

If the increase in particle concentration in the actuator as a result of external contamination is $\underline{k}'$, then:

$$\underline{k}' = v_{jB} \cdot \underline{k}.$$

Rearranging the equation for $\underline{\dot{j}}_{Bn}$ gives:

$$\underline{\dot{j}}_{Bn} = \frac{1}{v_{jB}} \left[C_{jB} \left[v_{kB} \cdot \underline{\dot{j}}_{Bn-1} + \overset{(v_{jB} - v_{kB})}{\underset{1}{\sum}} \underline{v} \right] + C_{jB} \ \underline{b}_{kB} + K.\underline{k}' \right]$$

By a similar process the concentration of particles leaving side A of the actuator after it has been filled n times is given by:

$$\underline{\dot{j}}_{An} = \frac{1}{v_{jA}} \left[C_{jA} \left[v_{kA} \ \underline{\dot{j}}_{An-1} + \overset{(v_{jA} - v_{kA})}{\underset{1}{\sum}} \underline{v} \right] + C_{jA} \ \underline{b}_{kA} \right]$$

where $C_{jA} = (C_{jA2} + C_{jA3}) \ C_{jA1}$

Note: Since there is no piston rod on side A, $\underline{k}$ and C_{jG} are both zero.

3.4.9   Erosion of Pipework

The erosion of pipework has been represented in the sections above as addition of particles rather than as matrices. Although pipework erosion is to some extent dependent upon particle concentration it is both a very complex phenomenon and also occurs on a very small scale, hence it will be ignored from now on.

51.

3.5   Modes of Failure Caused by Particle Contamination

3.5.1   Sources of Fluid Contamination

(1) Built-in contamination, i.e. dirt that is already in the components when the system is assembled. When hydraulic components are manufactured they undergo a rigorous ultrasonic cleaning process followed by flushing with clean fluids. However it has been found that when assembling the most critical systems that the act of tightening a screw thread will release a considerable number of particles into the system.

(Reference 3.5.1) These systems are now being designed so that no screw threads are in contact with the fluid circuit.

(2) Contaminant in new hydraulic fluid added to the system.

(3) Airborne dust infiltrating the system, e.g. dust brought in on the piston shaft and through reservoir breather valves if these exist.

(4) Contaminant generated within the system by pump wear, packing wear, etc.

(5) Contamination from hand tools etc., introduced when a system is opened for maintenance reasons.

(6) Contamination introduced by interchange of fluid with that of ground maintenance equipment.

2, 4, 5 and 6 may be largely controlled by effective maintenance of ground equipment and 3 by efficient seal design.

3.5.2   Types of Failure

Contamination induced failures of hydraulic systems and their components may be divided into three categories. (Ref 3.5.2)

(1) Malfunction due to single large particles, or a few large particles arriving simultaneously, interfering with the motion of moving parts, e.g. reseating of valves.

(2) Loss of performance and eventual failure due to wear.

(3) Loss of performance when frictional forces become significant with respect to driving forces, or when heavy contamination affects the driving forces, e.g. silting in servo control valves.

3.5.3   A particle large enough to plug an orifice, prevent a valve from seating, etc., is large enough to be easily seen and would be trapped by the coarsest filter. Its presence is indicative of carelessness on the part of

52.

manufacturing, overhaul, or maintenance personnel. Failure to deburr a drilled passage at the time of manufacture, for example, may eventually result in the burr being dislodged into the system. Good maintenance and the installation of coarse filters at critical points will prevent this type of failure.

Another failure of this type is possible. This is the probability of the simultaneous arrival of a number of particles at an orifice, etc., whose combined effect is the same as that described above for a large particle. (Ref. 3.5.3)

3.5.4   Failure due to a large particle blocking an orifice will be dependent upon the sizes of the orifice and the particle. If the particle is above a certain size it will cause block me, but this is very unlikely.

Failure due to a number of particles causing blockage can be calculated on a probability basis, the important criteria being the orifice size and the particle size distribution, i.e. two particles of one size range could cause blockage, whilst four of a small size range might be needed, or a combination of particles of different size ranges.

3.5.5   All moving parts are subject to wear at points of contact. The principal exceptions are hydraulic pumps, and continuous duty hydraulic motors. Infiltration of the precision fits on equipment by fluid borne particles results in wear, scoring and increased clearances. This sometimes causes sudden failure but more often results in a gradual loss of efficiency: planned maintenance can prevent this becoming critical.

3.5.6   Failure of items due to wear can be calculated on a total weight of solids lost basis, e.g. if the pump loses more than a certain weight of particles, it will fail.

3.5.7   Control valves, in particular electrohydraulic servo valves, may have limited forces available to drive the valve spool. Frictional forces may become great enough to cause degradation of performance although little or no wear has occurred.

Servo valves, also called transfer valves or hydraulic amplifiers, are usually designed to produce hydraulic flow output proportio   to an electric current. It is the performance of these units, more than any other factor, which has focussed attention on hydraulic fluid contamination in the last few years.

The valve design used in this project is similar to the second stage of a typical electrohydraulic servo valve.

In a spool valve, fig. 13 , particles tend to collect behind the spool at points x_1, x_2 and x_3 due to leakage effects. These particles increase resistance to motion of the spool, and may delay or even stop the motion, causing either complete failure, or a loss in efficiency which may be critical if the valve is part of a flight control loop.

References

Ref. 3.5.1.   Akers R.J. Personal communication from Hydraulic Research and Manufacturing Corp., Van Nuys, California.

Ref. 3.5.2   WADC Technical Report 50-29 part 6, April 1955.

Ref. 3.5.3   Schmitt V.R. Aerospace Fluid Power and Control Technologies, SAE A-3 Committee, Phoenix, Ariz., October 1967.

3.6. Models of Complete Systems

3.6.1.   The requirements of a model of an hydraulic system designed to predict failure of components due to particle action are:-

(1)   it must be able to calculate continuously changing particle concentrations,

(2)   it must be able to handle continuously operating and intermittently operating circuits,

(3)   it must be able to predict failure,

(4)   it must be able to handle changes in matrix coefficients, where they are dependent upon particle concentrations, or where they are changed by routine replacement of equipment represented by the matrices,

(5)   it must be capable of modification to simulate other hydraulic systems,

(6)   it must be in form suitable for solution by computer.

3.6.2.   There are two distinct types of model which fulfil these requirements:

(1)   Continuous,

(2)   Step wide based on either:

(1)   volume increments of fluid, or

(2)   time increments.

3.6.3.   A continuous model, which calculates particle concentrations as continuous functions of time. or possibly volume of fluid pumped theory.   However, matrix models are unsuited to continuous solution, particularly when the matrix coefficients themselves vary with time.

3.6.4.   The basis of the step-wise approach is to assume that a variable function is constant for a small increment of a fixed parameter, and then changes for the next increment.

The simplest parameters to consider are increments of volume and time.   The values of the particle concentrations in any increment depend upon the values in the previous increment and upon the size of the increment.   Each time these values are calculated, since they depend upon particle concentrations.

55.

If volume increments are used, and the particle concentrations are multiplied by the fluid velocity to give particle fluxes, the model will handle acceleration. This is discussed below as the step-wise flux model.

3.6.5. With the step-wise volume model. Size distributions can be very easily represented, all the requirements of 3.6.1 are met. However acceleration of the fluid cannot easily be dealt with by this model.

A step-wise time model again satisfies all the initial requirements, but once again acceleration cannot be handled. Particle size distributions must also be expressed in terms of volume and velocity which makes this model less attractive than a volume model.

A step-wise velocity or flux model is the only model which can handle accelerating fluid. It is also the best model for representing the continuous circuit. Difficulties, however, arise when the intermittent circuit (the actuator) is brought into action.

3.6.6. For the first model it was decided to represent the continuous circuit by a flux model, and the intermittent circuit by a volume model. The development of this model into the final model adopted is described below in 3.7.

3.7. The Final Mathematical Model of a Simple Hydraulic System

3.7.1. The first model was based on a division of the basic hydraulic system shown in Fig.   , into two distinct parts, a continuously operating circuit and an intermittent circuit. The continuously operating circuit consists of flow from the reservoir, through the pump, the filter and the pressure relief valve, and back to the reservoir, except when leakage occurs. During leakage, flow is from the reservoir, through the pump, the filter, leakage in the Control Valve, and back to the reservoir. The intermittent circuit comes into operation when the actuator is moved. It has been previously described in paragraph 3.4.8.

The continuous circuit was modelled by means of a mass balance on the reservoir, based upon fluid velocities and particle concentrations. This enabled the particle flux leaving the reservoir to be calculated. The main advantage of this model was that it could handle simultaneous flow through the pressure relief valve and the Control Valve. (Models based upon volume or time can only handle this by alternating the flow from one circuit to the other for successive volume or time increments).

In order to calculate particle concentrations, it was assumed that the concentration leaving the reservoir remained constant until particles travelling at the mean fluid velocity had made one complete circuit. Matrices were then adjusted and the process was repeated.

The intermittent circuit was based on an actuator volume, assuming that there was only one step change in particle concentration for each actuator stroke.

The model for the continuous circuit is the best available type since it can easily handle fluid acceleration. However, it was found to be extremely difficult to combine both circuits into a single model without drastically modifying one or other of the models.

3.7.2. A second model was then developed from the first by substituting a step-wise volume for the flux model. Again it was assumed that only one change in concentration was made per circuit.

Acceleration was handled by considering it to be infinite. This resulted in step changes in velocity which were accounted for by step changes in the operating matrices.
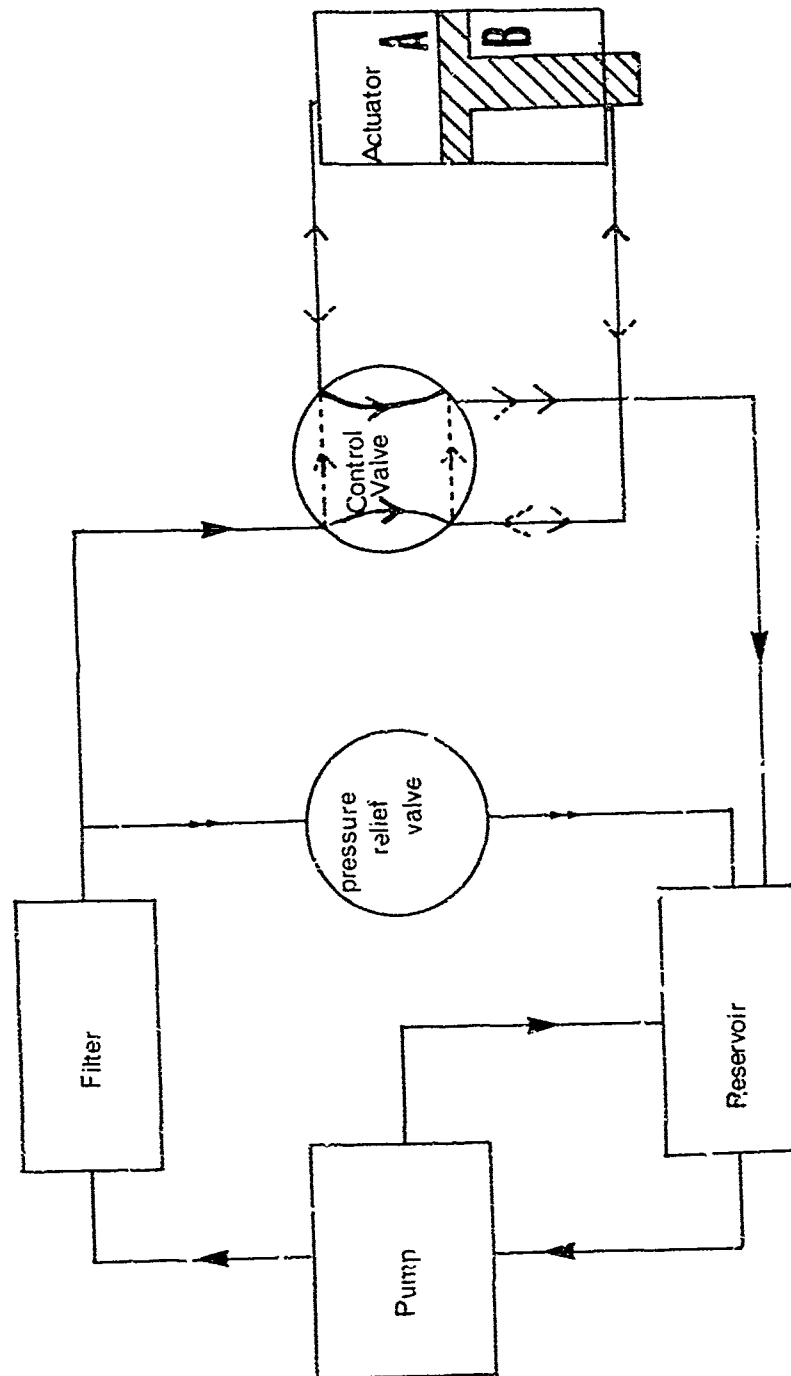
FIGURE 18   Model hydraulic system

Actuator

A

B

Control Valve

pressure relief valve

Filter

Reservoir

Pump

58.

This model inherited most of the disadvantages of the first model, the two most important being:

(1)   Difficulties arose in combining the models for the continuous and intermittent circuits.

(2)   Although the volume increment was small, the step change in particle concentration was quite large, since one volume increment was assumed to represent the whole system volume.

3.7.3.   A third model was then developed from the second model whereby the fluid was completely divided into unit volumes, and a step change in particle concentration was assumed to occur every time a unit volume left the reservoir. Each line volume and the actuator and reservoir volumes were assumed to be a whole number of unit volumes. Plug flow was assumed in all pipework and equipment except the actuator and the reservoir. Changes in particle concentration due to the action of equipment were assumed to be instantaneous, i.e., they took place between adjacent unit volumes. Since plug flow is assumed, there is no interchange of particles between adjacent volumes. In order to calculate the particle concentrations in the actuator and reservoir, both items are assumed to contain perfectly mixed fluid.

Step changes in matrices were brought about by considering the particle concentration of each unit volume entering the item of equipment concerned.

This model eliminated the two major difficulties of the previous models, and also handled changes in the actuator and reservoir volumes, but difficulties in programming led to a slight modification, and a fourth model was finally developed.

3.7.4.   In this model, unit volumes of the pipework and equipment were considered instead of unit volumes of fluid. The assumptions of plug flow in pipework, etc., and the perfect mixing in the actuator and reservoir still held. A step change in every volume was made each time the fluid had completely passed from one unit volume to the next. The unit volumes referred to are shown in Fig. 20   and are referred to in the text as line 1, etc.

A description of this model is given below:-

3.7.5.   Assumptions:

(1)   Changes in particle concentration, between two successive volume increments, are small. This justifies the use of a step-wise model.

59.

(2) The volume   e particles is small compared with the system
volume, and may be neglected.

(3) The high fluid viscosity and small particle size eliminates particle
settling from all points in the system.

(4) The flow regime in all pipework and equipment is plug flow, except
for the actuator body and reservoir, in which perfect mixing occurs.

(5) No fluid leaves the system as a result of leakage.

(6) Volume flow rates are constant for each of the three valve
positions.

(7) Acceleration of the fluid changing from one operating state to
another is infinite, i.e., the change of state involves a step
change in velocity.

3.7.6.   The action of equipment is exactly as described in 3.4 using the same
nomenclature as in Fig.   13   A summary of the equations used is given below.
where i is the number of unit volumes which have left the reservoir.

Outflow from reservoir:

$$\underline{m}_i = \underline{R}_i \, \underline{r}_i$$

Eq. 3.7.1

Pump action:

$$\underline{P}_i = \underline{m}_i + \underline{b}_m + \underline{a}$$

Eq. 3.7.2

Filter action:

$$\underline{f}_i = \underline{F}_i \, (\underline{p}_i + b_p)$$

Eq. 3.7.3

Pressure relief valve:

$$\underline{z}_i = z_i \, (\underline{f}_i + \underline{b}_f + \underline{b}_g)$$

Eq. 3.7.4

Control valve action:

(1) leakage when closed:
$$\underline{\ell}_i = L_{ci} (\underline{f}_i + \underline{b}_f + \underline{b}_h)$$

Eq. 3.7.5

(2) leakage when open:
$$\underline{\ell}_i = L_{ci} (\underline{f}_i + \underline{b}_f + \underline{b}_h)$$

Eq. 3.7.6

(3) flow of high pressure fluid:

$$\underline{v}_i = (\underline{f}_i + \underline{b}_f + \underline{b}_h) + \frac{i}{v_J} \left[\theta \phi \sum_{1}^{c} (1-C_{vc})(\underline{f} + \underline{b}_f + \underline{b}_h) + \psi \sum_{2}^{0} (1-C_{vo})(\underline{f} + \underline{b}_f + \underline{b}_h) \right]$$

Eq. 3.7.7

60.

(4) flow of low pressure fluid:

$$\underline{\ell}_i = \underline{j} + \underline{b}_k \qquad\qquad \text{Eq. 3.7.8}$$

The actuator compositions after the nth time it is filled are:

Side A:

$$\underline{j}_{An} = \left[\frac{1}{v_{jA}} \; C_{jA}(K_{kA} \; \underline{j}_{An}-1 + \begin{matrix} v_{jA}-v_{kA} \\ 1 \end{matrix} \; \underline{v}) \right] + C_{jA} \cdot \underline{b}_{kA} \cdot \qquad \text{Eq. 3.7.9}$$

Side B:

$$\underline{j}_{Bn} = \frac{1}{v_{jB}} \left[C_{jB} \; (V_{kB} \; \underline{j}_{Bn}-1 + \begin{matrix} v_{jB}-vkB \\ 1 \end{matrix} \; \underline{v}) \right] + C_{jB}\underline{b}_{kB} + \underline{k}k$$

$$\text{Eq. 3.7.10}$$

Derivations of all the above equations are given in 3.4.

The basic mass balance for the reservoir is:

$$\underline{r}_i = \frac{\rho-1}{\rho} \; \underline{r}_i \; \ell + \frac{\ell}{\rho} \cdot \text{(Input)} \qquad\qquad \text{Eq. 3.7.11}$$

where ρ is the reservoir volume.

The value of the input depends upon the state of the system.

There are two possible values:

(1)   When flow is through the pressure relief valve:

$$\text{Input} = (\underline{z} + \underline{b}_z + \underline{d}) \qquad\qquad \text{Eq. 3.7.12}$$

(2)   when flow is through the control valve:

$$\text{Input} = (\underline{l} + \underline{b}_t + \underline{d}) \qquad\qquad \text{Eq. 3.7.13}$$

The value of $\underline{l}$ depends upon the valve position, i.e., whether or not the actuator is being moved.

However, when the actuator is operated, there is a change in reservoir volume. This is because the two actuator sides have been different volumes, due to the piston rod in side A. Thus when side B is filling, the reservoir volume increases, when side A is filling the reservoir volume decreases. This effect may be allowed for by the method of paragraph 3.7.7 below.

61.

3.7.7. Whon the side B is filling, the increase in reservoir volume is accommodated by increasing the input at regular intervals, proportional to the ratio of the actuator volumes. Thus if the ratio of the actuator volumes is 5/4 then every fourth input is increased to $(2\underline{l} + 2\underline{b}_1 + \underline{d})$.

However $\underline{d}$ is not doubled since it depends upon the flow rate of the reservoir outlet.

The reservoir volume ρ is then increased by one unit before calculation of the next step.

When side A of the actuator is filling, the decrease in reservoir volume is accommodated by reducing every fifth input to $\underline{d}$ only, and decreasing the reservoir volume, ρ , by one unit before calculation of the next input.

3.7.8. It is assumed that failure of the system will only occur in the valve, and the methods of 3.5 are used to calculate this. The weights of particles collected in the valve are·

(1)   behind the spool (points x_1 and x_2):

$$\Sigma \, \underline{bu}_a \; = \; (1-\phi)\Sigma(1-C_{vc})(\underline{f} + \underline{b}_f + \underline{b}_h) \qquad \text{Eq. 3.7.14}$$

(2)   at the inlet (point x_3):

$$\Sigma \, \underline{bu}_c \; = \Sigma(1-\theta)\phi \; (1-C_{vc}) \; (\underline{f} + \underline{b}_f + \underline{b}_h) \qquad \text{Eq. 3.7.15}$$

(3)   inside the spool chamber (points x_4 and x_5, or x_6 and x_7):

$$\underline{bu}_f \; = \psi \; (1-C_{vo}) \; (\underline{f} + \underline{b}_f + \underline{b}_h) \qquad \text{Eq. 3.7.16}$$

Failure in other equipment can be handled using similar techniques to those described above.

3.7.9. The line filter and the reservoir filter pick up particles as a result of their action. This build up of particle can effect the filter efficiency and must be calculated. The build up of particle after n unit volumes of fluid have passed through is equal to:

$$\sum_{o}^{n} (\text{output} - \text{input}) \qquad \text{Eq. 3.7.17}$$

3.8.   The Computer Flow Sheet for the Final Model

3.8.1.   The hydraulic system is divided into six lines as shown in Fig. 18

     The computer flow sheet for predicting failure of a control valve due to particle contamination is outlined in Fig. 19 to Fig. 27

3.8.2.   The input statement consists of the values of the following:

$$
\left.\begin{array}{l}
v_{n} \\
v_{F} \\
v_{f} \\
v_{g} \\
v_{h} \\
v_{z} \\
v_{e} \\
v_{kA} \\
v_{kB} \\
v_{jA} \\
v_{jB}
\end{array}\right\}
$$
These are system volumes.

$$
\left.\begin{array}{l}
n \\
F \\
R \\
z \\
L_{c} \\
L_{o} \\
C_{jA} \\
C_{jB} \\
K
\end{array}\right\}
$$
These are all matrices which describe the action of the elements in the system on the particles.

$$\left.\begin{array}{l} \underline{k} \\ \underline{b}_p \\ \underline{b}_\dagger \\ \underline{b}_{g\,\pi} \\ \underline{b}_h \\ \underline{b}_z \\ \underline{b}_\ell \\ \underline{b}_{kA} \\ \underline{b}_{kB} \end{array}\right\}$$

These are vectors describing particle concentrations; $\underline{k}$ refers to the piston rod, while the $\underline{b}$'s refer to line breakage.

$$\left.\begin{array}{l} \text{SBUA} \\ \text{SBUC} \\ \text{SUF} \end{array}\right\}$$

These are vectors referring to build up in the value, their initial value is zero.

I

This is the number of increments which have left the reservoir, initial value is zero.

$$\left.\begin{array}{l} S \\ T \end{array}\right\}$$

These are parameters used in calculating reservoir volume, initial value is zero.

Another input statement is the value of the particle concentration of each unit volume in the system. If the system is to be modelled from start-up, we can assume that each unit volume has the same particle concentration $\underline{r}_o$, where $\underline{r}_o$ is the particle concentration of the clean fluid.

line 4

line 3

line 6

line 2
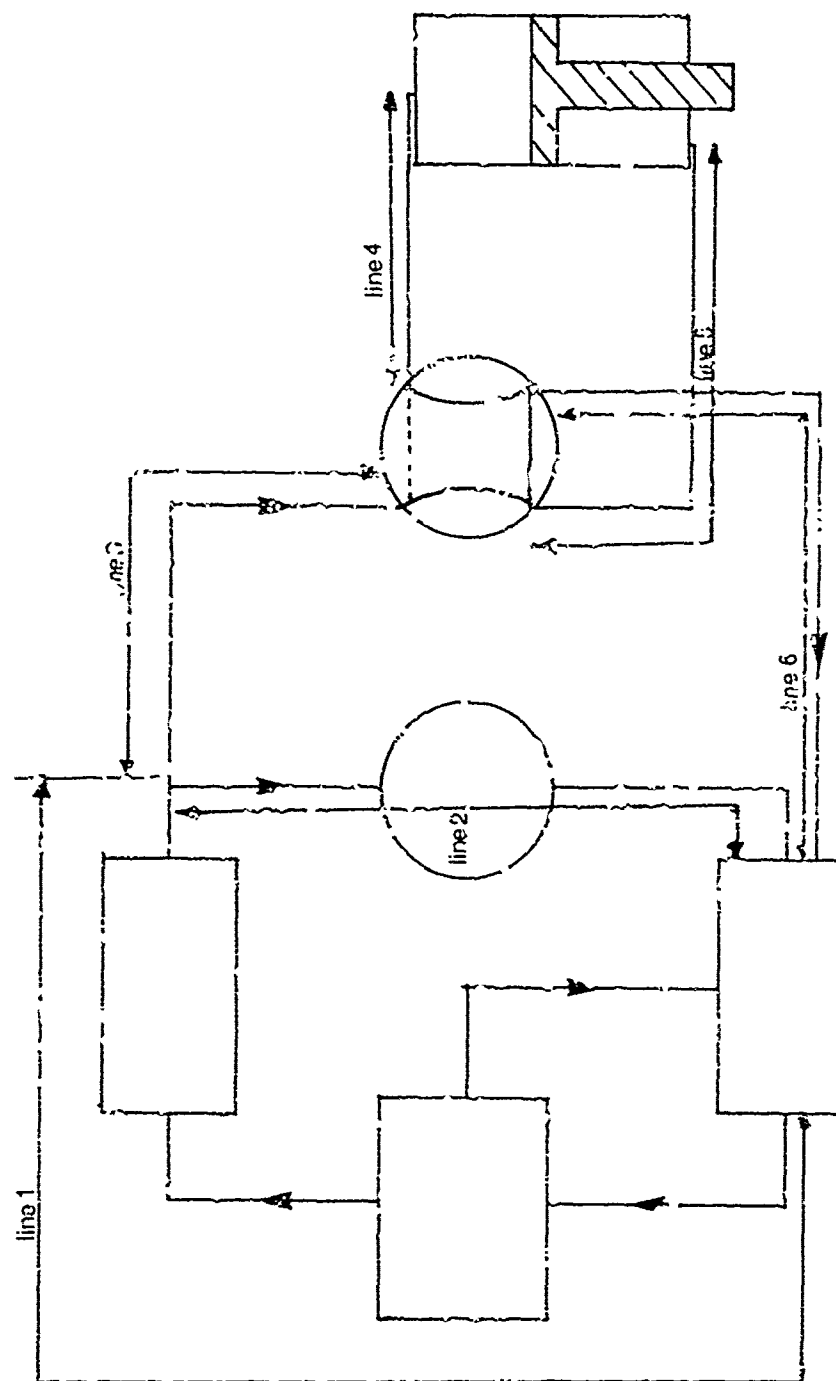
line 1

FIGURE 13 Assignment of volume elements in model hydraulic system.

2.3.2. The first step in the calculation is to calculate the particle concentration of one unit volume in line 1 after the fluid has moved one unit forward, (Fig. 20). The new particle concentration of the first volume is then calculated (Eq. 3.7.1). Other unit volumes are calculated by making the particle concentration of that unit volume equal to the particle concentration of the preceding unit volume, except when the fluid has to pass through a piece of equipment. The particle concentration of the $v_m + g$ unit volume, i.e., the first unit volume after the pump, is made equal to the action of the pump on the particle concentration of the v_m unit volume (Eq. 3.7.2.)

The process is then continuous until unit volume $v_p + v_m + 1$ is reached the particle concentration of this unit volume is made equal to the filter action on the particle concentration of the $v_p + v_m$ unit volume. The normal step process is then continued until all the particle concentrations of the unit volumes in line are known.

The particle build-up in the line filter and reservoir filter is then calculated (Eq. 3.7.10). This is done as the efficiency of the filter, and thus the value of the matrix coefficients is dependent on the build-up in the filter

2.3.3. Depending on the value of I the programme can now go five ways. (The five if statements (Fig. 20) are really one but are shown as five for clarity). These values of I can be adjusted to simulate any operating conditions The five paths are:

(1)   Flow through the pressure relief valve in the continuous circuit.

(2)   Flow due to leakage through the control valve in the continuous circuit.

(3)   Flow due to the actuator being raised, i.e., the intermittent circuit.

(4)   Flow due to leakage through the control valve during actuator operation.

(5)   Flow due to the actuator being lowered.

Statements 20 and 30 deal with the continuous circuit while statements 40, 50 and 60 refer to the intermittent circuit.

INPUT

10

Calculate Conc.
in line

Calculate Biuld-up in
filter & reservoir
filter

20

70

value of
I

value of
I

value of
I

50

30

60
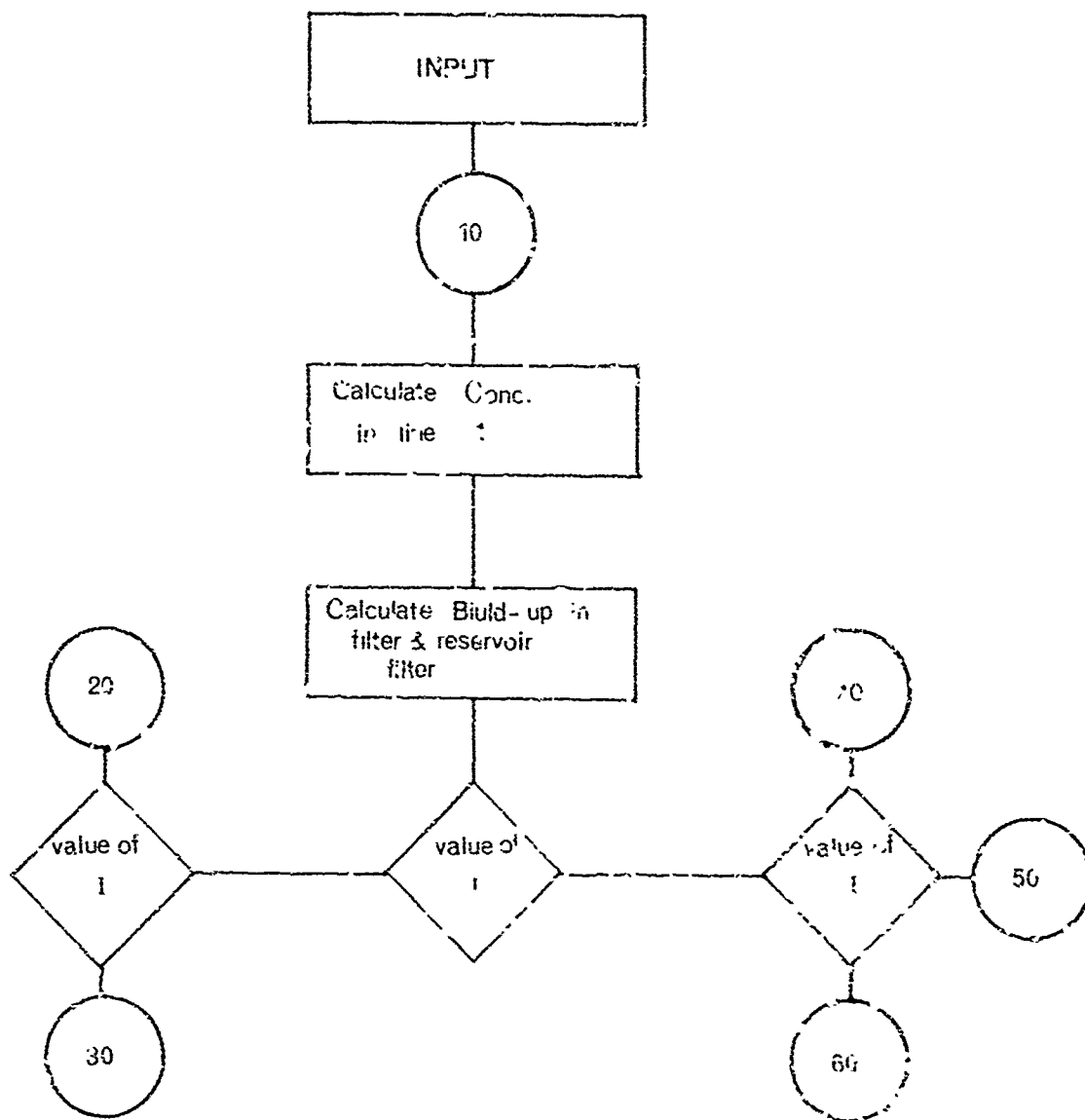
FIGURE 20   Computer programme flowchart - input

3.8.4.   Statement 20 (Fig. 21)   accounts for flow through the pressure relief valve. The first step is to calculate the particle concentration of the unit volumes in line 2. This is done by continuing the normal step process until unit volume $v_m + v_p + v_f + v_g + \ell$ is reached. This is made equal to the action of the pressure relief valve on the particle concentration of unit volume $v_m + v_p + v_1 + v_g + \ell$ (Eq. 3.7.4). The new value of $\underline{r}$ is then calculated (Eq. 3.7.12), I is increased by ℓ and the process repeated.

```
        ( 20 )
          |
  +-----------------+
  | Calculate Conc. of line |
  |          2              |
  +-----------------+
          |
  +-----------------+
  | Calculate      I |
  +-----------------+
          |
  +-----------------+
  |   I  =  i  +  j  |
  +-----------------+
          |
       ( GO
         to
         10 )
```
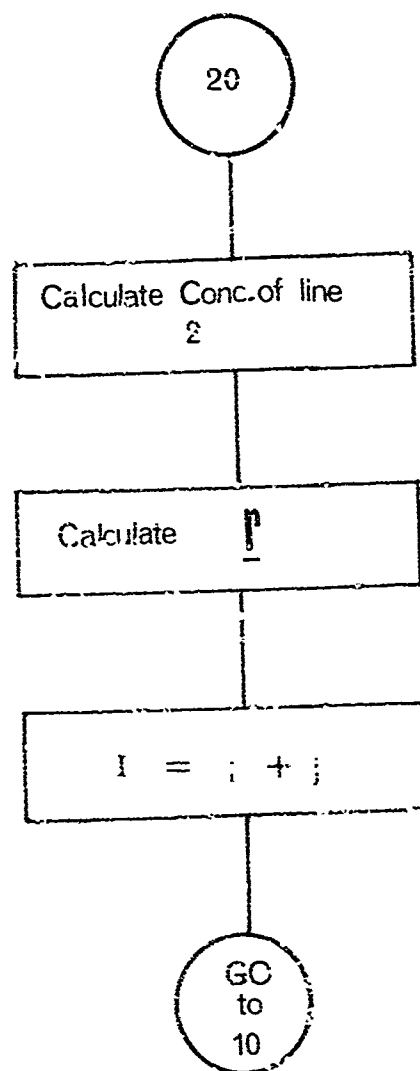
FIGURE 21.   Computer program flowsheet - Statement 20

89.

3.8.5.   Statement 30 (Fig. 22)   deals with leakage through the control valve when the actuator is not moving.

The first operation is to calculate the particle concentration of the unit volumes in line 3, and also the particle concentration of the first unit volume in line 6. This must be done as the fluid in line 6 can be obtained from either line 3, 1, or 5. The values in line 3 are calculated by the normal step process.

The particle concentration of the first unit volume in line 6 is equal, in this case, to the action of the valve in the particle concentration of the $v_m + v_p + v_f + v_h$ unit volume in line 3, (Eq. 3.7.5). Now the particle concentration of the $v_m + v_p + v_f + v_h$ unit volume can cause blockage of the valve as described in (3.5) so an IF statement is introduced and if blockage occurs a print out is obtained.

If no blockage occurs. build up in the valve in positions x_1, x_2 and x_3 as shown in Fig. 11   is then calculated. SBUA refers to the total build up in position x_1 and x_2 which will prevent the spool moving. SBUC refers to the build up in position x_3 and may cause blockage of the orifice. Expression for calculating whether these are critical have been discussed in   3.5.2. The test for SBUA is placed before the test for SBUC as the spool has to move before fluid can flow.
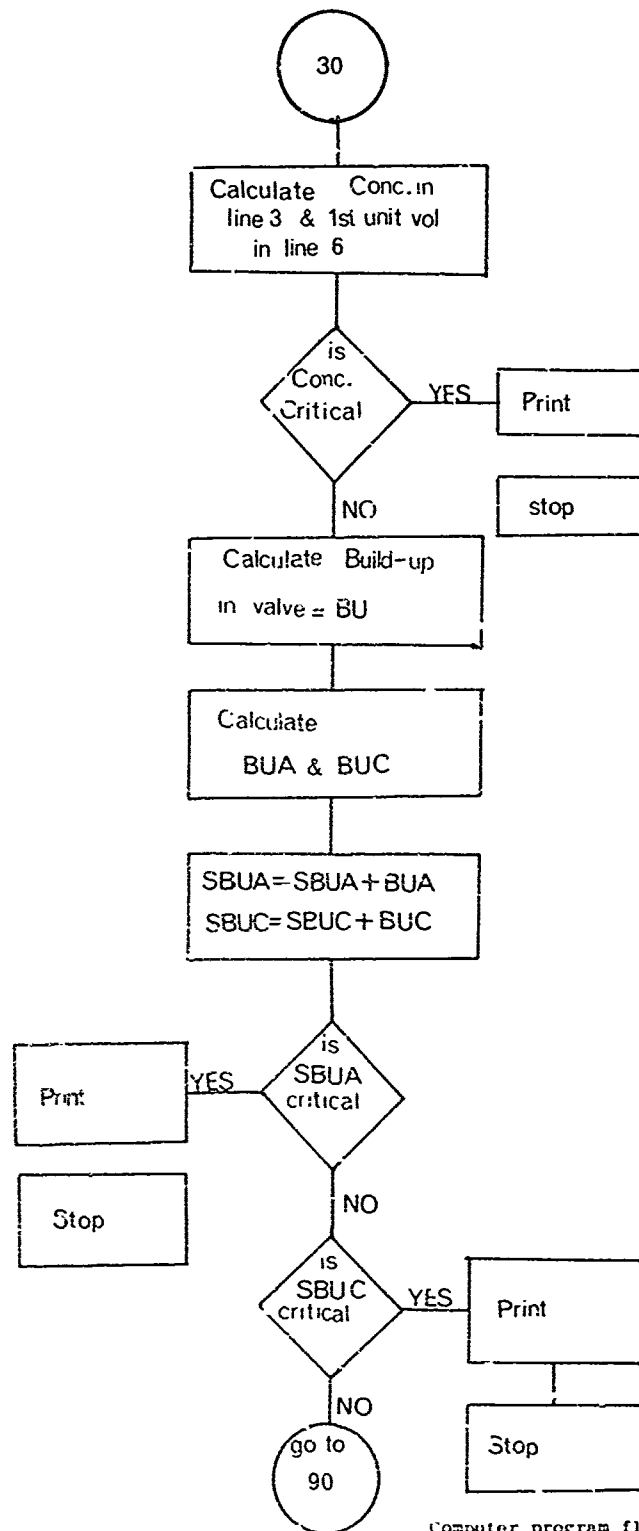
FIGURE 22

Computer program flowsheet – Statement 30

71.

If neither is critical the next stage, i.e., the 90 statement (Fig. 23), is to calculate the particle concentration of the unit volume in line 6. This can be done completely on the step basis as there are no components in this line.

The final stage is to calculate $\underline{r}$ (Eq. 3.7.13) and move the process on one stage.
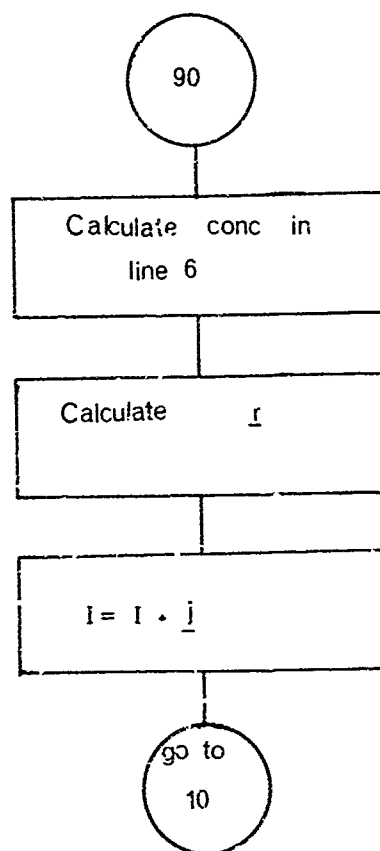
FIGURE 23   Computer program flowsheet – Statement 90

73.

3.8.6. Statement 40 (Fig. 24) describes raising of the actuator, i.e., filling of Side B. The first step is the calculation of the unit volume of line 3 and the first unit volume of line 4. Line 3 is calculated as above. The particle concentration of the first unit volume is equal to the valve action on the particle concentration of the $v_m + v_p + v_f + v_h$ unit volume (Eq. 3.7.7.) Again the next stage is to ensure that this particle concentration can flow through the valve without causing blockage. If it can pass through we move on to the next stage.

The first unit volume of fluid through the valve will take most of the build up in position x_3, i.e., SBUC, with it, and no other unit volume will take any part of this build up. Thus the first unit volume will take the left hard part of this build up. Thus the first unit volume will take the left hand path after the second IF statement. Here the first step is to calculate the particle concentrations of the unit volumes in line 4. The first unit volume in line 4 will be given by the valve action on the particle concentration given by the addition of the particle concentration of unit volume $v_m + v_p + v_f + v_h$ to (SBUC $- \dfrac{\text{SBUC}}{W}$), where $\dfrac{\text{SBUC}}{W}$ is the particle concentration of the particles left in position x_2. The program now moves on to calculate the new value of $\underline{JL}$ (Eq. 3.7.10). After the first volume of fluid has passed through the valve, the other volumes take the right hand path. Whilst the actuator is being moved leakage still occurs causing build up of particles in the spool chamber at points x_4 and x_5. (Fig. 15). This is known as BUF and is the particle concentration of the build up due to leakage of one unit volume. The first unit volume through the valve after a unit volume has leaked is assumed to carry the whole of BUF with it into the actuator line. This is then taken into account when calculating the particle concentration of the unit volumes in line 4 (Eq. 3.7.6). BUF is then set equal to zero since there is no collected solid left at points x_4 and x_5 until after another unit volume has leaked. BUF is calculated in Statement 50.

The next stage is to calculate the particle concentration of the unit volumes in line 5, the first new unit volume is calculated as the actuator action on the particle concentration of actuator side A, i.e., (Eq. 3.7.9). The particle concentration of the first unit volume of line 6 is then calculated as previously described (Eq. 3.7.7).

The particle concentration is then tested to see if it is critical for valve blockage, if the answer is negative the program moves on.

74.
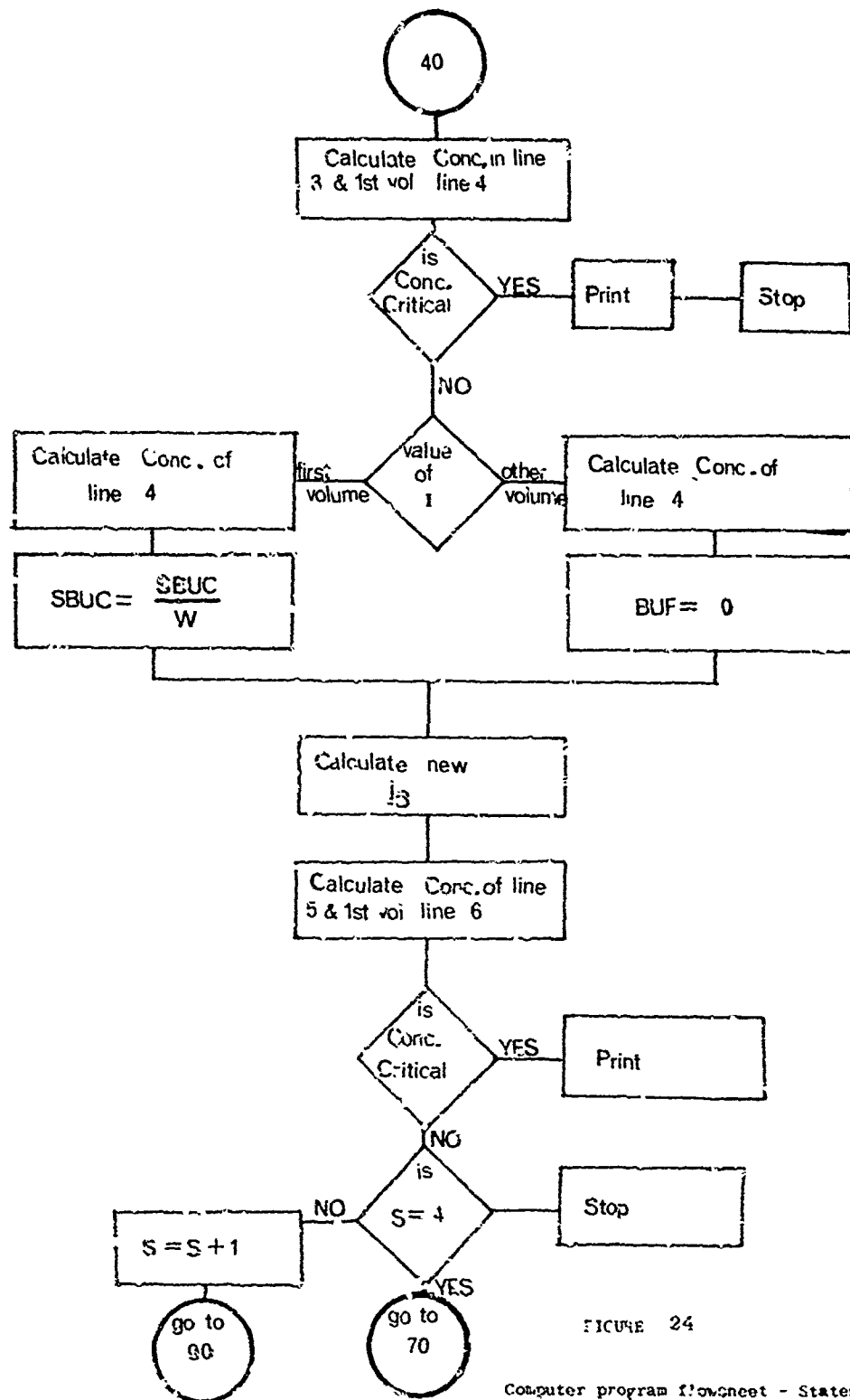
FIGURE 24

Computer program flowsheet - Statement 40

75

Another IF statement now follows to account for changes in the reservoir volume as described in Eq. 3.7.11. In this program the ratio of the actuator volumes $\frac{v_jA}{v_jB}$ is taken as $5/4$. If parameter S is a multiple of four, two unit volumes are added to the reservoir while only one unit volume leaves and Statement 70 deals with this. If S is not a multiple of four there is no difference in the reservoir volume input and output.

In Statement 70 (Fig. 25)   the first step is to calculate the particle concentration of the unit volumes in line 6. This can be done on a step basis as the particle concentration of the first unit volume of line 6 is already known. The particle concentration of the final unit volume is then set equal to the particle concentration of a dummy volume Y.

Since at $S = 4$ two unit volumes leave the actuator for only one leaving the reservoir, the fluid in lines 5 and 6 is moved on two unit volumes so the particle concentration of the unit volume in line 5 and the first unit volume in line 6 is then recalculated. The test for critical valve concentration then takes place and if the answer is negative the particle concentration of the unit volume in line 6 is then calculated as previously described.

The reservoir composition is then calculated remembering that the input to the reservoir is the unit volume Y and the final unit volume of line 6, the particle concentration of these volumes has already been calculated (Eq. 3.7.11). The new reservoir volume is then calculated by adding one unit volume to the old reservoir volume. The program is then moved on one stage and returned to 10.
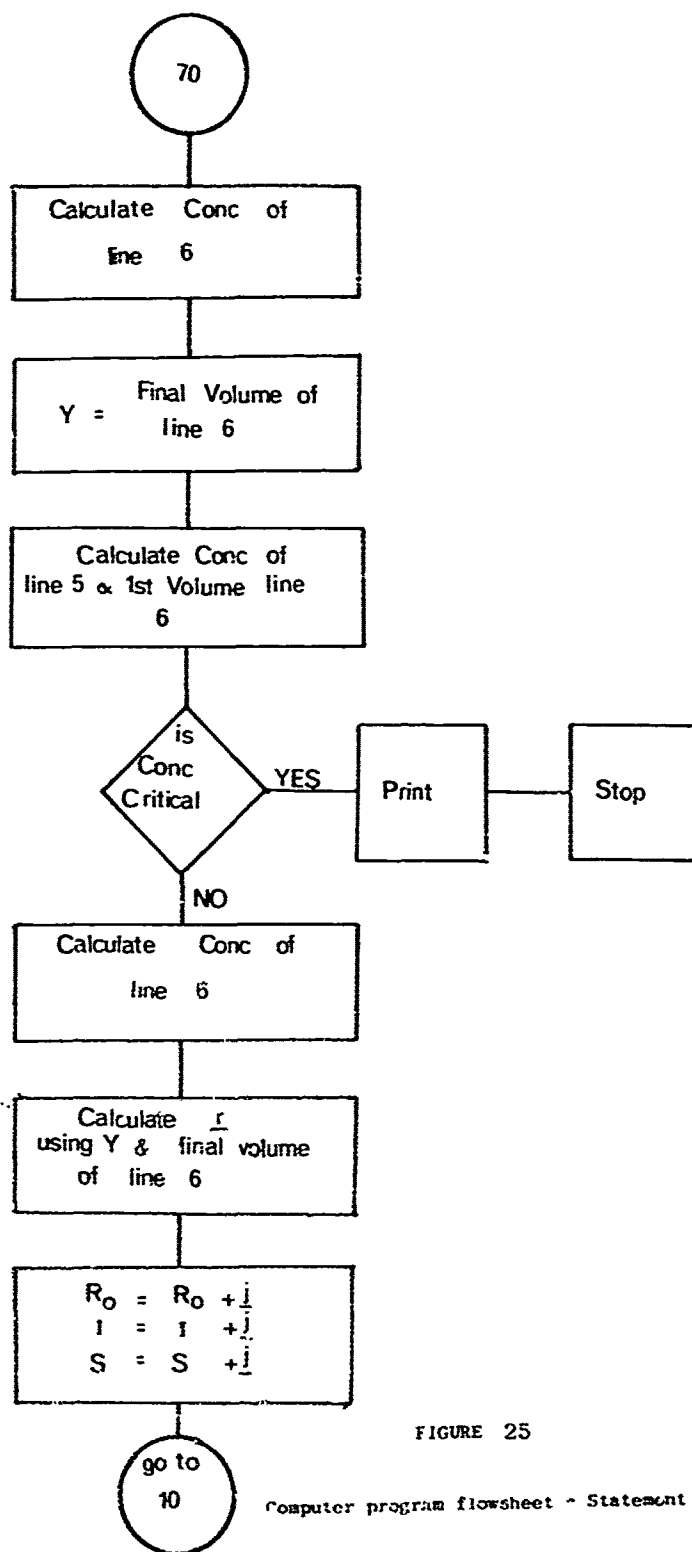
FIGURE 25

Computer program flowsheet - Statement 70

77.

3.8.7. Statement 50, (Fig. 26) deals with leakage through the valve while there is fluid flow through the valve, i.e., actuator operation. Leakage is assumed to occur at a certain value of I. The first calculation is of the particle concentration of the unit volumes in line 3 as described before, and the particle concentration of the 1st unit volume in line 6 (Eq. 3.7.6). Again a test for critical valve concentration takes place on the inflow to the valve. The next calculation is of the valve build up RUA and BUF as described in 3.4.4. SBUA is then calculated and tested to see if it will stop the spool moving, if a negative answer is obtained the program moves on to statement 90.
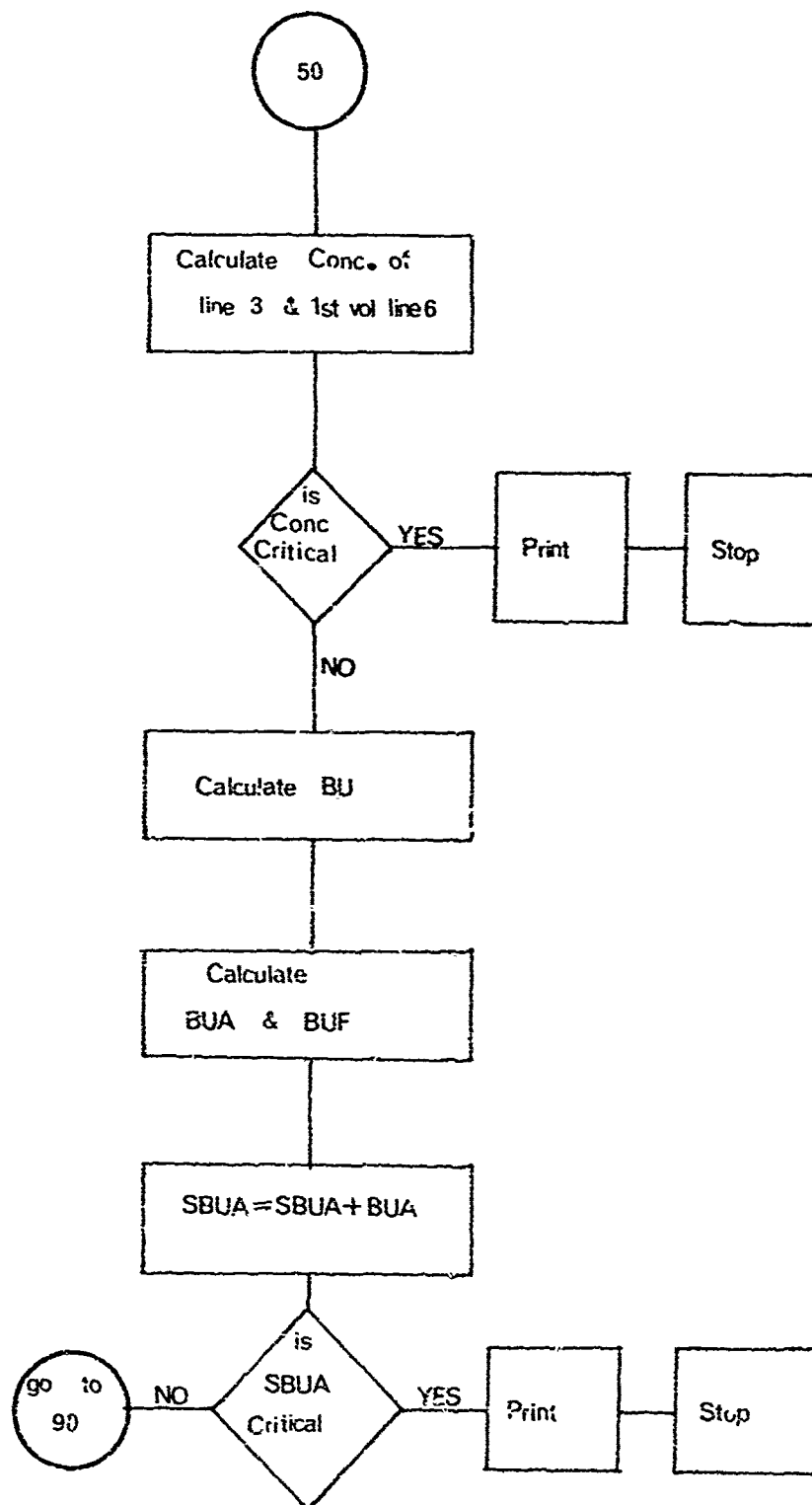
FIGURE 26   Computer Program Flowsheet – Statement 5G

79.

3.8.8. Statement 60 (Fig. 27) deals with fluid flow due to lowering of the actuator. When the jack is lowered side A is filled and thus there is a decrease in the volume of the reservoir. The first calculation is to calculate the particle concentration of the unit volume in line 3, as previously described, and the first volume of line 5, in a similar manner to the way the particle concentration of the first unit volume in line 4 was calculated in statement 40 (Eq. 3.7.7).

The test for critical value concentration then takes place if the answer is negative the program moves on to another IF statement. This IF statement is included to handle particle build up in the valve, and is of a similar form to that in statement 40. The next calculation of the particle concentration in actuator side A, i.e., (Eq. 3.7.9).

The next set of statement is designed to handle the change in reservoir volumes. As we assumed that the ratio of the actuator volume is $^5/4$, we look at the value of parameter T. If T is not a multiple of 4 we calculate the particle concentration of the unit volume in line 4, and the first unit volume in line 6 in a similar manner to the calculation used in statement 40.
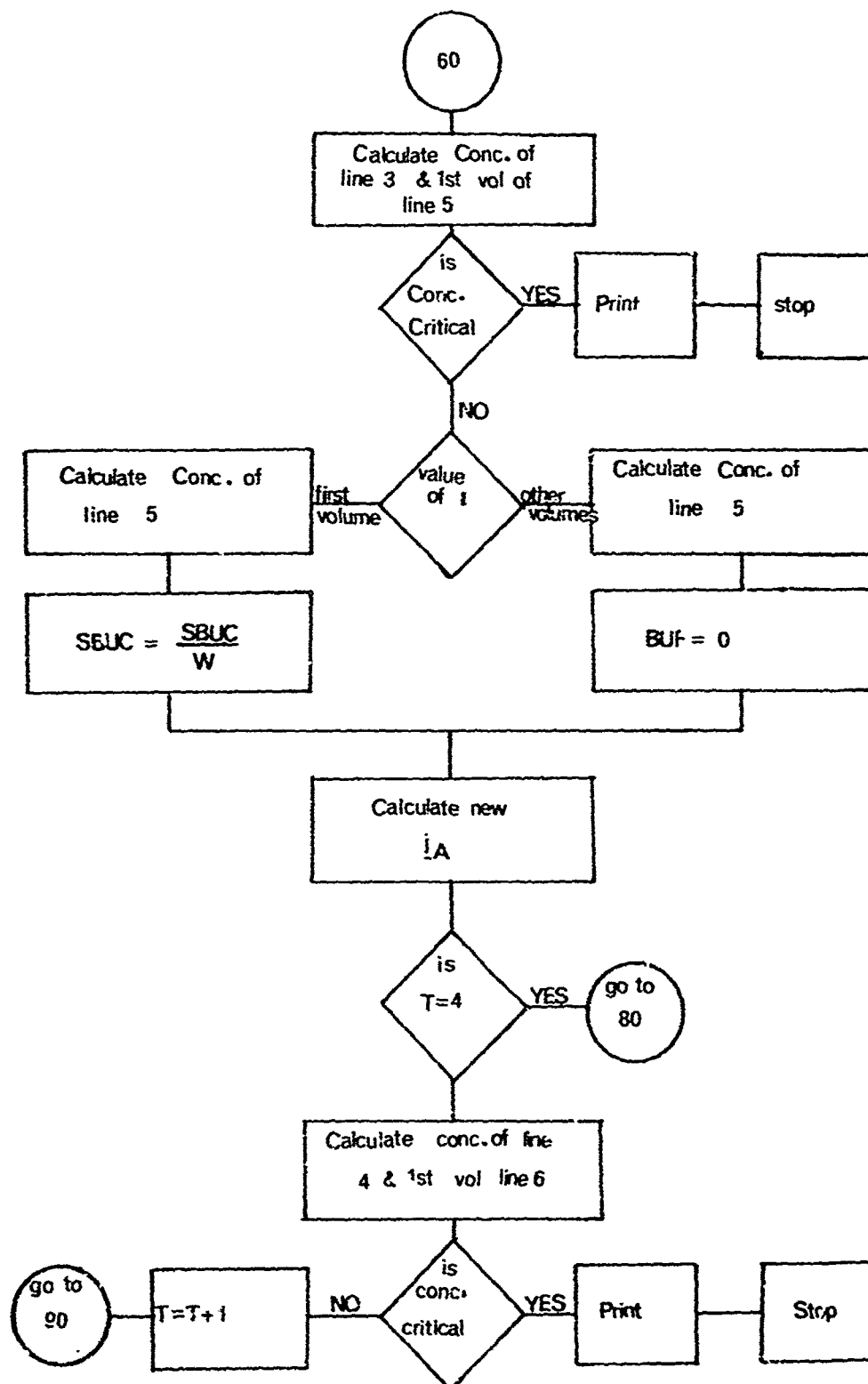
FIGURE 27   Computer Program Flowsheet - Statement 60

81.

If T is a multiple of four, we move to statement 80 (Fig. 28). This calculates the new reservoir composition (Eq. 3.7.11), decreases the reservoir volume by one unit volume, advances T and I by one and goes back to 10.

3.8.9. The above program will run until one of the critical tests is positive. It will then print out why failure was caused, the value of I, the number of times the actuator circuit is used, the reservoir concentration and both filter build-ups.

Calculate $\underline{r}$

$$r = r + \frac{\dot{a}}{c}$$

$$M = M + 1$$
$$R_o = R_o - 1$$
$$I = I + 1$$

go to 10
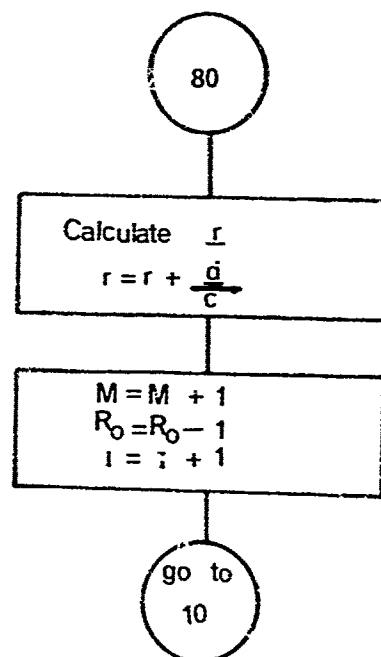
FIGURE 28   Computer program flowsheet - Statement 80

83.

3.9.   Conclusions and Suggestions for Further Work

3.9.1.   The mathematical model for the hydraulic system is presented in the report in computer flowsheet form. A computer program based on the flowsheet would be able to predict failure in the control valve. It could easily be modified to account for additional equipment in the circuit, and routine replacement of worn equipment by new equipment. It could also be used to predict failure in other items of equipment.

There are, however, several difficulties in writing the program and these are tabulated below. Most of them are essentially lack of available information for the input data.

The types of information required are:

Details of the volumes of components within a system, the initial particle concentrations, the frequencies of actuator operation and the number of operations, information on modes of equipment failure and above all experimental studies to determine the matrix coefficients for individual components. To do this would require detailed studies of the input and output of particles through given components under controlled conditions. Probably the most useful means of obtaining this information is to construct a test circuit and make experimental observations. This procedure must be used to obtain the initial values of the matrix coefficients since no theoretical work (to our knowledge) has been done towards calculation of these coefficients from the system parameters. This in itself would provide a heavy program of further work.

The complexity of the computer flow sheet would suggest that some work towards determining the comparative magnitude of the effects in each part of the system. If this information was available, the flow sheet could probably be simplified to a large extent, reducing considerably the amount of computer storage required to run the program.

84.

Chapter 4

The Characterisation

of Particles

85.

4.1.   Introduction

The behaviour of a particulate system depends on the properties of the individual particles which go to make up that system and also on their spatial arrangements with respect to each other. It is often said that particulate systems are particularly complicated because of the large number of variables involved. However, the variables are usually not independent and the basic properties of a particulate system are very few in number.

The easiest way to characterise a powder is to measure some macroscopic property of the powder and to predict its behaviour from that measurement. If the powder cannot be changed then, for engineering purposes, this kind of measurement may be sufficient. If, however, it is desired to change the macroscopic properties in a controlled manner or, alternatively, to find the best possible system, then this must be done by relating the macroscopic properties of the powder back to its primary properties. However, rarely does the behaviour of a powder have a unique relationship with its primary properties since the same powder can exist in different states. Unless the particles are so well dispersed that they behave as individual particles, the spatial arrangement of the particles must also be considered.

Thus the characterisation of a particulate system is summarised in Table IV the macroscopic properties listed being only examples of the many which can be measured or possibly predicted from the primary properties.

TABLE IV

Relationship of properties of particulate systems

Primary Properties	State	Macroscopic Properties	Behaviour
Particle Size Distribution	Porosity	Permeability	Flow of Fluid
–	–	–	–
	Anisotropy & Homogeniety	Shear Strength	Flow of Powder
Properties of Solid and Interstitial Fluid	–	–	–
	Moisture Content	Conductivity	Flow of Heat and Electricity
	–		
	Surface Properties		

86.

The basic difference in the behaviour of a subdivided solid and a homogeneous solid is the interaction of the constituent particles and this is dependent on the distribution of size and shape of the particles. The particle size distribution of the particles is thus the primary property of a powder which differentiates it from homogeneous solid. If the size and shape of each particle in a sample of powder were known, then these measurements would be sufficient to differentiate it from any other powder. However, they would not be sufficient to predict the macroscopic properties of the system, since the same set of particles can be arranged geometrically in different ways with respect to each other to produce completely different behaviour. Thus, the porosity of the bed must be known and also the moisture content of the powder if a three phase system is involved. A further complication is added in that, although the porosity of a bed does not uniquely depend on the particle size distribution of the particles, they are nevertheless not completely independent. A particular set of particles in the packed state has upper and lower limits of porosity which are a unique function of the particle size distribution. The actual porosity may lie between these two values depending on the manner in which the particles have been packed. Under some circumstances, the porosity of the bed may be a unique function of the particle size distribution. For example, if powder is flowing, then it must be at its critical porosity.

The complexity, then, in describing the behaviour of a particulate system is usually because several mechanisms are involved. An attempt to correlate the behaviour of a powder directly to its particle size distribution is usually not possible and the mechanisms must be separated and related individually to the size distribution, taking into account the state of the system. Illustrating this point with Table IV   the behaviour of a powder can only be related to the particle size distribution by passing through the two other columns of macroscopic property and state.

4.2.   Particle Size Distribution

The traditional methods of defining particle size is as the size of a sphere equivalent in some geometrical property such as area or volume or equivalent in behaviour such as settling speed. The particle shape is then inherent in the definition of size. Shape factors are then the ratios of the various defined sizes, either for one particle or an average shape factor for a system.

The alternative definition of particle size is a statistical diameter. Well known examples are those due to Martin and Feret.

In addition to the problem of defining tne size of an individual particle, there is a further problem of expressing the distribution of particle size, for example by number or by weight. If particle size is defined as an equivalent sphere, then the moments of the various distributions which can be plotted have significance and may sometimes be related. On the other hand, if the Martins or Feret diameter is used, the physical significance of the distributions is more obscure.

It is obvious that for most aspects of particle behaviour, there is no single equivalent size of spherical particle to which the behaviour of an irregular particle can be uniquely related. Nor even can a single statistical diameter contain all the information about the geometry of a particle. The limitation of the approaches is that of imagining a single particle to be the primary unit of a powder system. An alternative set of measurements will now be proposed which completely characterise a particle system.

Consider an irregular particle as shown in Fig. 29. That particle can be imagined to be split into laminae which are of finite but small thickness. The shape of each laminae is irregular but each has a definite area. Therefore, a number distribution curve of the area of the laminae can be plotted. If the orientation of the particle is changed and the process repeated, then a different set of laminae will be produced. If the laminae in every possible orientatior or direction are measured, then they may all be added together to produce a distribution curve which is characteristic of the particle.

This distribution is a unique function of the particle but the reverse is not necessarily so. Thus, two different particles could conceivably produce the same distribution curve. The laminae may now be broken down again into smaller units.

88.
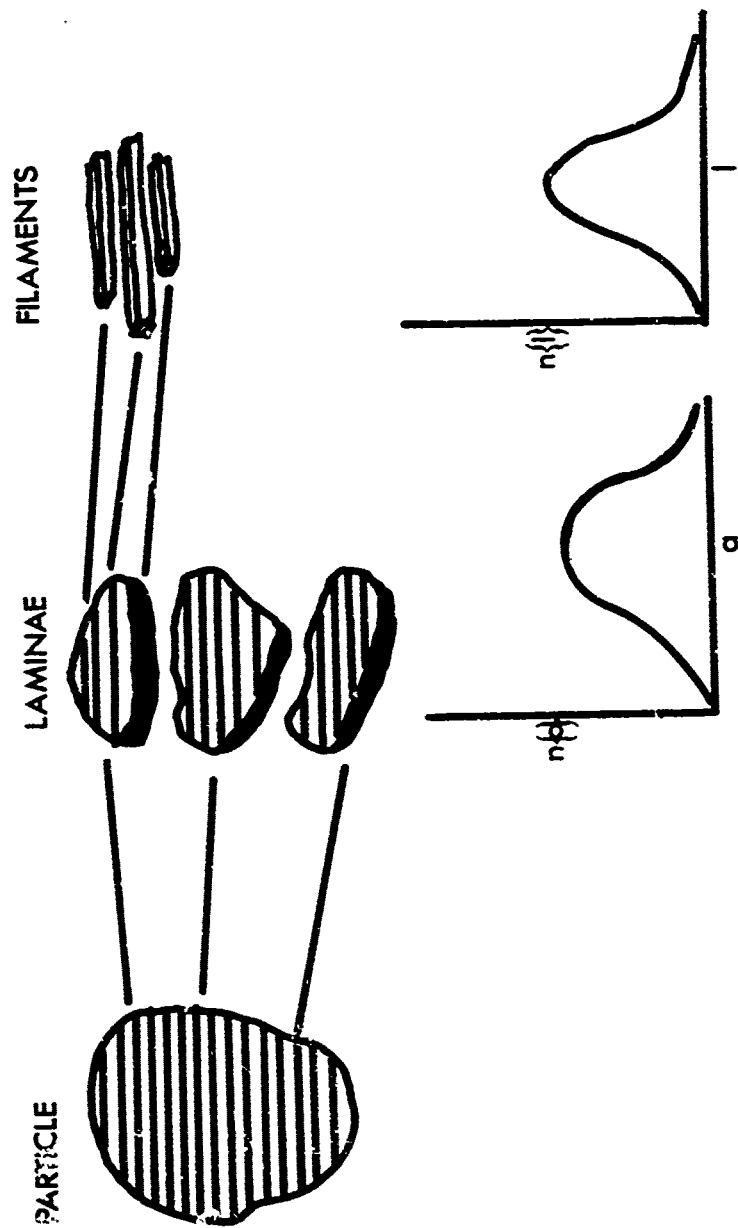
FIGURE 29 Characterisation of a single particle

Each lamina will be split into filaments which have a square cross-section of small but finite value. These filaments vary now only in their length and a distribution curve, again by number, of their lengths is a characterisation of the particle. The filaments may be taken in one direction or alternatively they may be taken in all possible directions and these various distributions added together to produce a compound distribution. This distribution must then be normalised so that the first moment of the distribution is equal to the volume of the particle divided by the cross-sectional area of a filament.

If, instead of considering a single particle a powder is considered, the number distribution of laminae and filaments can be plotted as a characterisation of the whole system. A further distribution must be added in order to make this characterisation unique and that is the number to volume distribution of the particles.

It is proposed, therefore, that a system of particles is completely characterised by three distributions:-

number	:	volume of particles
number	:	area of laminae
number	:	length of filaments

In the limit, as the thickness of the laminae and filaments tends to zero, the distributions transpose from a histogram to a continuous curve and the laminae and filament distributions become area and chord distributions respectively.

This characterisation of a particulate system is illustrated in Fig. 30 and is now a unique characterisation. Although two different sets of particles could produce the same distribution of one or even two of these variables, if all three distributions are the same for two samples, then they are the same powder.

The curves must now be normalised such that the first moment of the number to volume curve is equal to some convenient value. This will probably be either unity or the volume of particles per unit volume of bed. The area and chord distributions must then be normalised such that the first moment of the distribution is equal to the same normalising volume. This point is better illustrated in Fig. 31 where each lamina has been taken and they have been shuffled until they stand in order of ascending size. Then this curve in fact represents the number
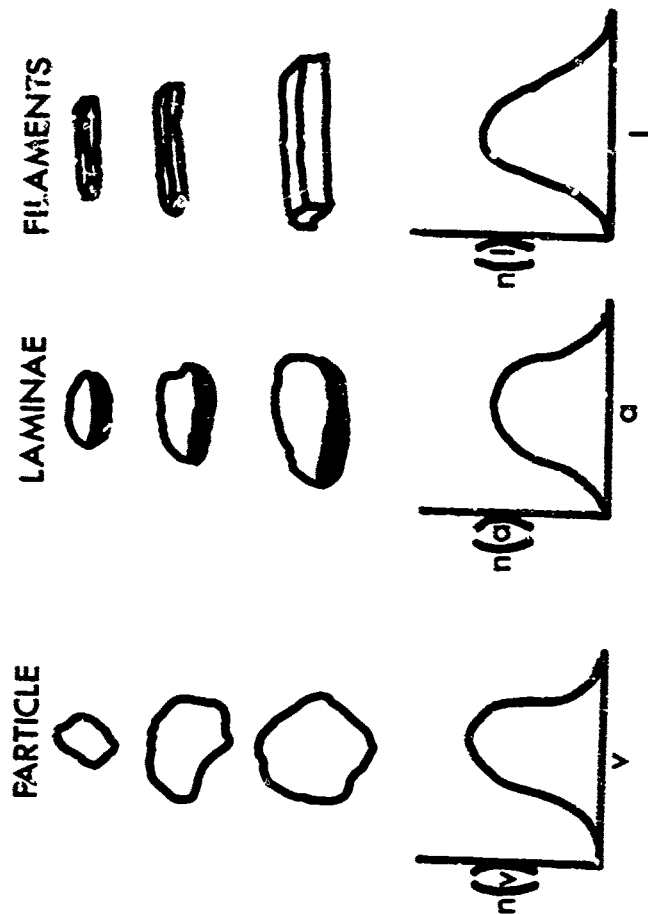
FIGURE 30 Characterisation of a system of particles

91.

The top graph shows a shaded area under a decreasing curve with:
$$\int n(l)\,l\,dl \doteq \frac{V}{\Delta t^2}$$

$$\int n(l)\,dl$$

cum % oversize (from O to A)

cum % undersize (from A to O)

The bottom graph shows a shaded area under a decreasing curve with:
$$\int n(a)\,a.da = \frac{V}{\Delta t}$$

$$\int r(a)\,da$$

cum % oversize (from O to V)

cum % undersize (from V to O)
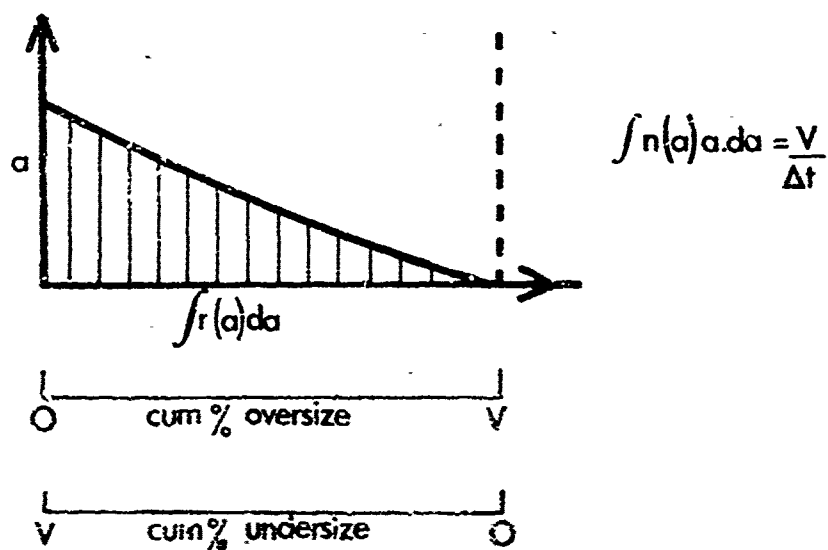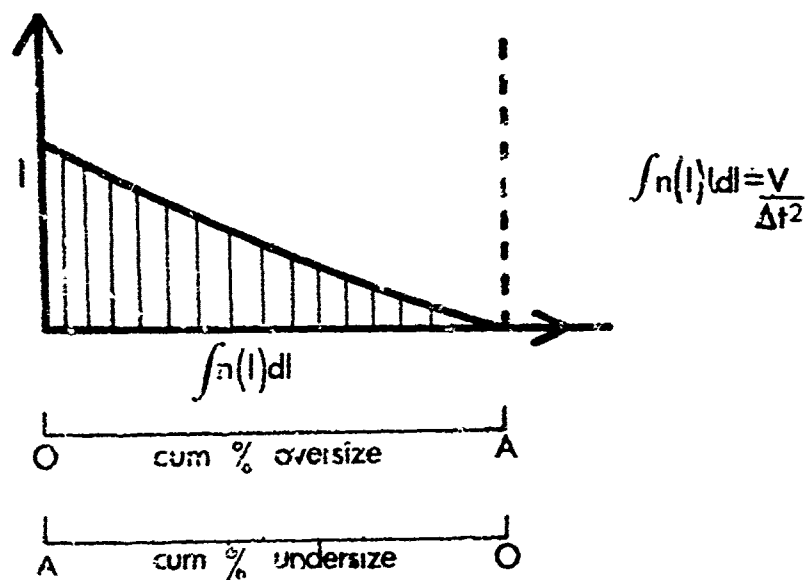
FIGURE 31 Cumulative distributions

distribution curve of laminae plotted as a cumulative distribution. The area under the curve is the volume of the particles divided by the thickness of one lamina and is also equal to the first moment of the primary distribution curve. The same argument applies to the distribution of filaments as illustrated in Fig. 31

Thus:-

$$\int_{\text{all } v} n(v) \; v \; dv \; = \; V$$

$$\int_{\text{all } a} n(a) \; a \; da \; = \; \frac{V}{\Delta t}$$

$$n(\ell) \; d \; = \; \frac{V}{(\Delta t)^2}$$

where Δt = thickness of a chord or filament

4.3.   Pore Size Distribution

The pore space between the particles is a continuum and is not sub-
divided like the particles. It can, however, be characterised in the same manner as
the particles by splitting it into filaments of small but finite cross-section.
Each filament will terminate on a particle surface. This is illustrated in Fig. 32
The number distribution of filament lengths is then a characterisation of the void
space and it must be normalised to a total length. Usually this will be the total
length of filament in unit volume of bed. Thus:-

$$\int_{all\ k} n(k)\ k\ dk \quad = \quad \frac{1-\varepsilon}{(\Delta t^2)}$$

The filaments may be taken in one direction or may be taken in all possible
directions. If the particles are touching, the distribution curve must pass through
the origin, but in a disperse system this is not necessarily so.

The mean filament size of the pores is easily related to that of the
particles if the bed is both random and isotropic. Thus, if a long straight line is
passed through the bed of particles then it samples both the particle and void
filaments. The fractional length of the line occupied by the void filaments is equal
to the voidage of the bed and the total number of solid filaments equals the total
number of void filaments. This, of course, includes the void filaments of zero
length when two particles touch. This fact has been used for some time by met-
allurgists, biologists and geologists   to measure the fractional volume of
constituent parts by microscopic traversing techniques.

The relationship is then as follows:-

Let   l   be a particle filament

    n(l)   be the distribution function by a number of filaments.

     k   be the length of a void filament

    n(k)   to be the distribution function of void filaments.

Since in any total length of line the number of solid filaments is equal to
the number of void filaments.

$$\int n(l)dl \quad = \quad \int_{o}^{B} n(k)dl$$
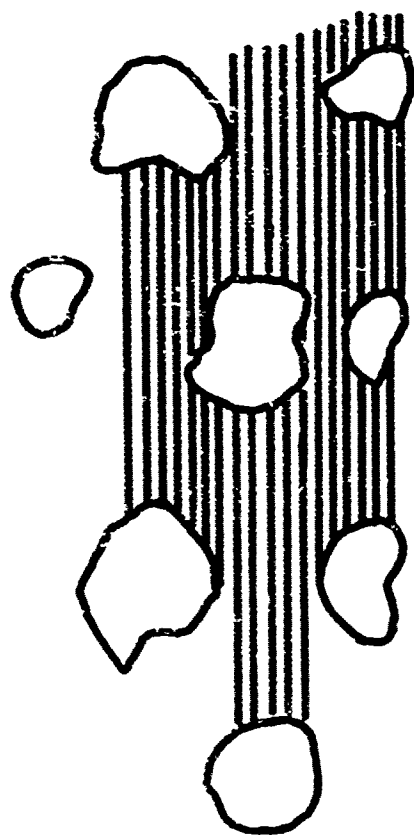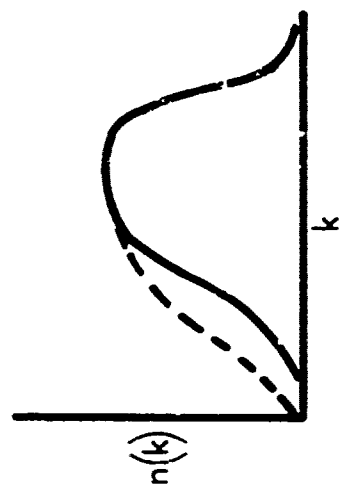
FILAMENTS

FIGURE 32 Characterisation of pore space

95.

$$\int n(l)l.de = 1-\epsilon$$

$$\int n(k)k.dk = \epsilon$$

$$\frac{\bar{l}}{\bar{k}} = \frac{1-\epsilon}{\epsilon}$$

∴ pt Contacts – Chord of zero length

FIGURE 33 Particlo and Voidage filaments

Since the fractional length of void filaments is

$$\frac{\int n(l)\,l\,dl}{\int n(k)\,k\,dk} = \frac{1 - \Sigma}{\Sigma}$$

$$\therefore \frac{\dfrac{\int n(l)\,l\,dl}{\int n(i)\,dl}}{\dfrac{\int n(k)\,k\,dk}{\int n(k)\,dk}} = \frac{\overline{l}}{\overline{k}} = \frac{1 - \Sigma}{\Sigma}$$

$$\therefore \quad \overline{k} = \overline{l}\,\frac{\Sigma}{1 - \Sigma} \quad \ldots\ldots\ldots\ldots\ldots\ldots\ldots \quad (1)$$

where the bar indicates the mean values by number.

4.4. Description of Anisotropy

If the bed is isotropic, then the chord size distribution of both the particles and the void space will be the same in all directions. However, in an anisotropic bed, the distributions may be measured in two or more directions depending on the problem to be solved. Thus, for example, in calculating the flow of electricity through the solid particles or the flow of liquid through the pore space, it would be necessary to know the distributions in the direction of flow and also those perpendicular to the flow.

It should be noted that a bed of particles can be anisotropic due to differences in the shape of the filament distributions. Physically this means that the particles are preferentially orientated. However, the fractional space occupied by void and by particle is the same regardless of direction and the ratio of the mean values is always given by equation (1). The distributions of an anisotropic bed are illustrated in Fig. 34
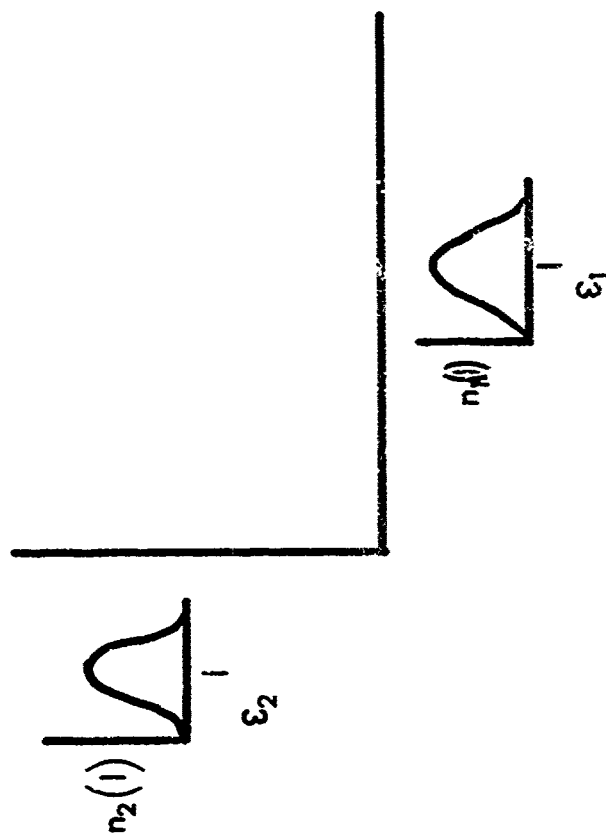
1. PARTICLE ORIENTATION $n[l] \neq n_2[l]$

2. PARTICLE SPACING $\varepsilon_1 = \varepsilon_2$

FIGURE 34 Description of anisotropy

99.

4.5. Characterisation of Agglomerates

If the particles are agglomerated together into clumps, then the behaviour of the system is affected and further information must be added to the description of the system. This is done by expressing the number distributions of volume, area and chord which describe the agglomerates as well as those for the individual particles. There are now also two porosities which are needed to describe the state of the particles. The porosity of an individual agglomerate describes the packing of the particles. If the agglomerates are now considered to be solid, then the fractional volume of the space between them describes their spatial arrangement. This is illustrated in Fig. 35.
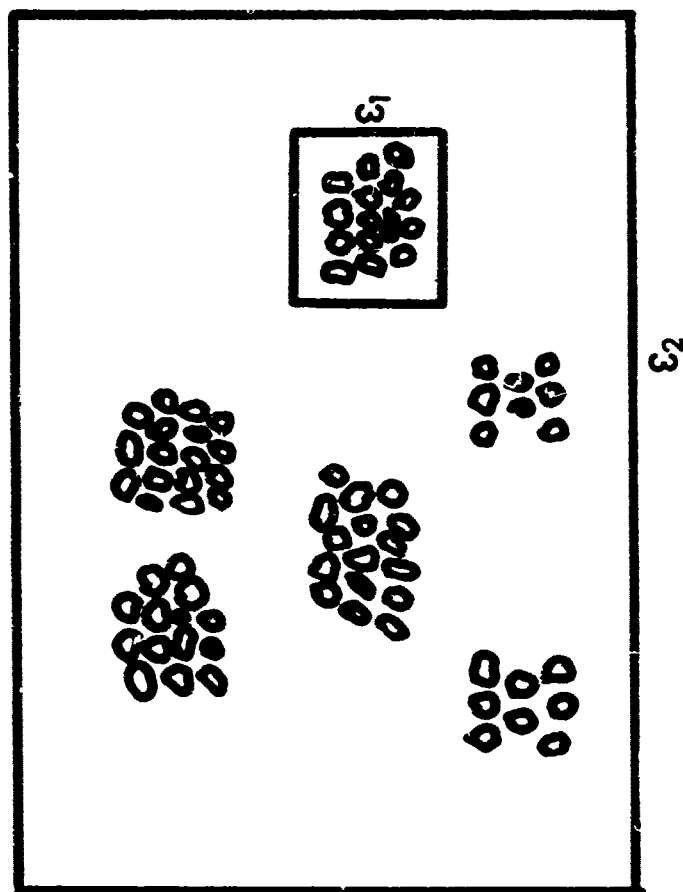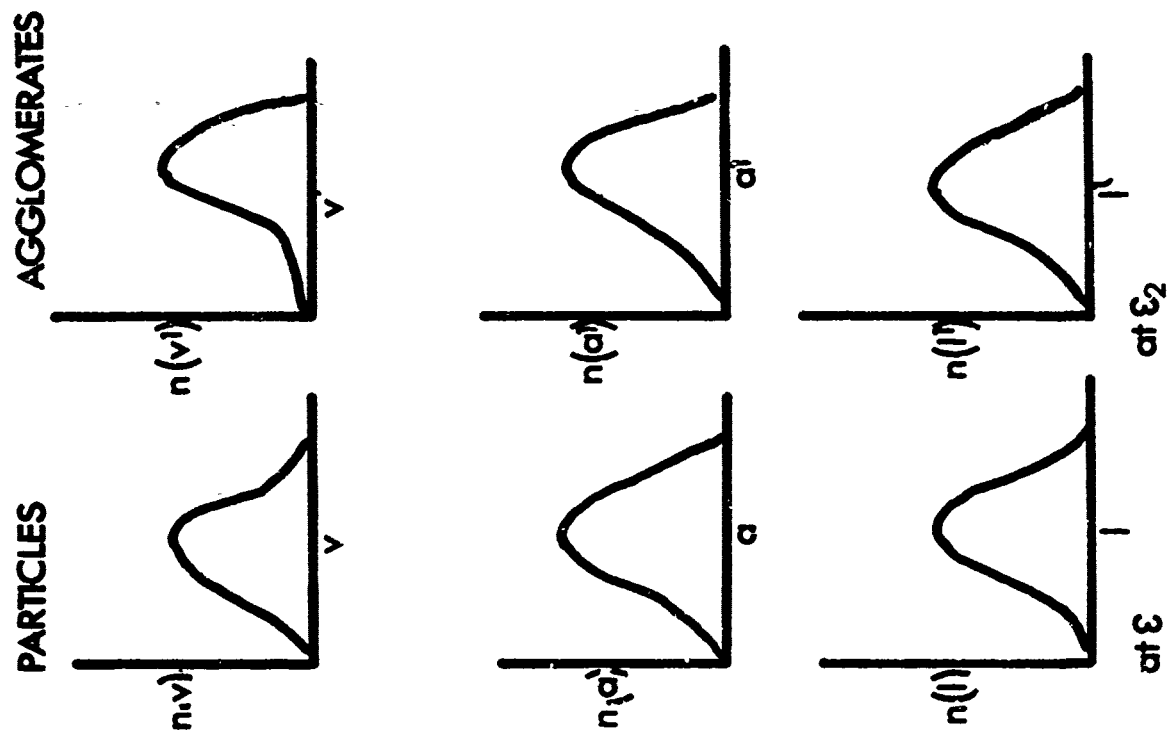
FIGURE 35 Characterisation of agglomerates

4.6. Conclusion

(a) A system of particles can be completely characterised by the following three distributions:-

number	:	length of chords
number	:	area of areas
number	:	volume of particles

(b) The arrangement of the particles can be expressed as the porosity of a bed or concentration of a suspension if the arrangement is isotropic and random. If directional or spatial variation exists, the distributions also have to be measured in different directions or different localities.

(c) Although without rapid automatic techniques this method of analysis is not suitable for routine work, it does enable relationships to be established between the conventional particle size analysis parameters and properties of the particle system. Work is in progress on the mathematical nature of these relationships.

Chapter   5

Particle Size Analysis

5.1 Introduction

Many methods of measuring the size of fine particles have been advocated and the principal ones are listed in Table V.

TABLE V   Techniques for measuring particle size

Class of Technique	Technique	Approx. size range commonly measured (μm)	Parameter Measured
Field Scanning	Optical Microscopy	> 0.5	Longest dimension equivalent area dia. statistical dias.
	Electron Microscopy	10^{-3} - 5	as optical microscopy
	Scanning Electron Microscopy	0.05 - 50	
	Light Scattering	10^{-3} - 1	surface area
Stream Scanning	Coulter Counter	1 - 100	volume
	Hiac Counter	2 - 2000	projected area
	Light Scattering	0.5 - 50	surface area
Classification	Sieving	> 5	sieve diameter
	Air Classifiers	2 - 50	Stokes diameter
Sedimentation	Pipettes	1 - 60	Stokes diameter
	Balances	1 - 60	Stokes diameter
	Photosediment-ometers	0.2 - 60	Stokes diameter
	Centrifugal methods	0.05 - 10	Stokes diameter
Surface Area	Gas Adsorption	> $10m^2g^{-1}$	
	Permeability	> $50m^2g^{-1}$	

The parameters listed in the final column are only equal for spherical particles. For irregular particles their ratios are characteristic of the shapes of the particles although these relationships are very complex. Several workers, notably Heywood (Chem. and Ind. 1937, 56, 149 and other papers), have defined shape factors in terms of the ratios of principal dimensions of particles. This method, whilst giving a very good description of the components of a system does not permit of an analytical synthesis of the system properties from the properties of these individual components. One such possible method is described in Chapter 4 of this report where the particles are considered as being made up of more elementary one and two dimensional units which can be expressed in terms of distribution functions.

Of the methods of size analysis listed in Table V many can be eliminated by the nature of the problem in analysing particles in mineral based hydraulic oil. The characteristics of this particular system are:

(i)   Low concentration of particles

(ii)   Size range $>100 - 5\mu$ m (and possibly less)

(iii)   A mineral based fluid containing several additives

(iv)   A range of material densities

(v)   A suspending fluid of relatively high viscosity.

Considering these properties in relation to the methods listed in Table V , several techniques may immediately be eliminated, e.g.

Methods	Undesirable Characteristic above
Sieving	(ii)
Sedimentation	(i), (ii), (iv), (v)
Surface area	generally impracticable
Air classifiers	" "

This leaves the field and stream scanning techniques. The standard methods in use today are manual field scanning by optical microscopy (e.g. ARP 598 and I.P. (draft) method (U.K.) and surveys have shown these methods to be of less than desirable accuracy and extremely time consuming and fatiguing. A.R.P. 598 is discussed in 5.2 below. Automatic scanning systems have been developed to remove the manual effort from this type of analysis and all current instruments are of the spot scanning type. These include the Millipore/Bausch & Lomb TTMC (U.S.A.) counter which measures a parameter approximating to the

maximum length specified in ARP 598 and I.P. (draft) methods, the Quantimet Image Analysing Computer (U.K.) developed originally for metallographic analysis and German instruments manufactured by Leitz/Bosch and Zeiss. All of these instruments rely on a television camera to scan the specimen and have digital or analogue computing facilities of varying complexity. The major problem in designing instruments of this type are grey level discrimination, re-entrant particles and touching particles. The latter is a very difficult problem beyond the current range of commercially available machines.

For a more detailed analysis a more complete collection of data is required and any machine making use of a television camera producing up to say 25,000,000 items of information per second is operating too fast for most practical data logging systems. This type of analysis requires a mechanical or flying spot scanning system and as such is, together with its computing facilities, both slower and more expensive than the current type of equipment. An outline of the operation of one system is described below in 5.5.

The best known example of a stream scanning particle size analyser is the Coulter Counter. In a stream scanning apparatus particles are passed one at a time through a sensing zone which produces a signal which is then recorded and interpreted in terms of particle size. In the Coulter Counter this transducer is an orifice through which an electrically conducting fluid containing the particles is drawn. A potential is applied across the orifice and the change in electrical resistance due to the presence of a particle measured. Section 5.4 describes a detailed investigation of this device and illustrates some of the general problems to be investigated in any stream scanning device. Because of the requirement of an electrically conducting fluid, the Coulter Counter is not suitable for Mil-H 5606 systems. Although mineral oils can be made electrically conducting by addition of certain suitable solvents and electrolytes this is extremely difficult with Mil-H.5606 probably due to the additives present. During a short but intensive survey no completely satisfactory electrolyte system was found for Shell Aero Fluid No. 4, DTD 585 (approx. U.K. equivalent of Mil-H.5606) and this impression was confirmed by discussion with a representative of the manufacturer.

An instrument which is becoming increasingly used for hydraulic fluid analysis is the HIAC Counter (High Accuracy Products Corpn., Clafemont, Calif.) in which the amount of light obscured by a particle crossing a light beam is measured. It is assumed that the amount of light obscured is proportional to the

cross sectional area of the particle. A brief report on this instrument appears in 5.3 below. Because it can be used with the hydraulic oil as the sole suspending fluid it has possibilities for use in hydraulic systems as an on-line real time analyser.

Many other forms of stream scanning counter have been described making use of electrical capacitance, light scattering, ultrasonic reflection or attenuation amongst the properties studied. The production of one of these devices in a form suitable for use in an operating hydraulic system would involve an intensive program of development work.

One problem to be faced in defining the size of particles is that presented by aggregates. For example it is known that Mil-H.5606B fluid that was within specification when packed may be found to contain particles $>100\mu$m after storage and that these particles are flocs of smaller primary particles. Although these particles will be counted by ARP 598, their resistance to shear would be very low and they would not be expected to manifest themselves under operating conditions. If this problem were of any magnitude in approving fluids, it might be advisable to introduce the application of some shear work to the fluid prior to analysis although how this could be done, apart from vigorous agitation of the sealed container, without introducing more contaminant is difficult to see. This problem might be less significant with stream scanning devices where shear occurs during the course of analysis.

5.2   ARP 598

        re: Procedure for the determination of Particulate Contamination of
            Hydraulic Fuels by the Particle Count Method

        Objective

(1)   To investigate the validity of the assumption implicit in the procedure
        that the particles counted over small number of randomly chosen grid
        squares could be used to express the total particle count.

(2)   To evaluate critically the experimental procedure of ARP 598.

        Results

        A closely sized fraction (Alpine MZ classifier) of A.C. Fine test dust in the
range 35 - 40μm was prepared and a suspension of the particles in Aero-Shell 4
hydraulic fluid was prepared.   Samples of this suspension were filtered following
the procedures of ARP 598.   Two uncertainties were found in the method.

(1)   Instruction 8.2.2.5 is a little misleading as it did not indicate whether
        the petroleum ether should be layered on the oil or whether some mixing
        should be obtained by pouring in the petroleum ether more vigorously.

(2)   Particles were observed to deposit on the shoulders of the filter funnel.
        No quantitative tests were made of the loss incurred but it was observed
        that with particles of the size used only vigorous washing would dislodge
        them.

        The results of 4 separate experiments are presented in Tables VI
IX.   Care was taken with each experiment to locate the membrane filter grid in
the position with respect to the glass sinter substrate.   Thus the counts in each
square can be added and the result of this addition is given in Table X   where
only the complete grid squares are represented.   The mean particles for a square
is 108 with a standard deviation of 13.   It should be noted that only three
results are outside the range of mean size $\pm$ 2 x standard deviation and all are
within $\pm$ 3 x standard deviations.   This is consistent with a random distribution
of particles.

        Table XI   shows in each corner of each square the number   of counts x 100
divided by the mean for that experiment.   No systematic high counts or low counts

108.

are apparent.   If present, systematic high or low counts might indicate heder-
ogenerties in the porous membrane support.

Conclusions

Since no control was maintained on the concentration of the suspension used
in these experiments, it has not proved possible to apply variance analysis between
the experiments.   The indications are that on the apparatus used the particles are
distributed at random.

Two further points should be noted:

(1)   The approximate standard deviation on a number of counts N is $\sqrt{N}$ and for
small N, $\sqrt{N}$ is large (for N = 100, $\sqrt{N}$ = 10).   Since at 95% confidence
limits there can be a   acceptable range of $N \pm 2\sqrt{N}$ in the number of counts
or $\pm \dfrac{2\sqrt{N}}{N}$, i.e. a total range of $\dfrac{4\sqrt{N}}{N}$ (e.g. 40% in the case above).   Thus
the scale-up from counting the number of particles on a few squares may
lead to large over or under estimates of the true count.

(2)   It is possible that the washing procedure used during the test might lead
to an excess of particles at the periphery.   As however the number of
complete squares very close to the edge is very small, not enough data was
collected to test for this particular form of maldistribution.

TABLE VI   Numbers of Particles Counted in Squares on membrane filter 1

(Superfix x indicates an incomplete square.)

The counts are arranged as a honeycomb pattern of squares; each labelled square heads a column of counts (reading down each diagonal column):

2^x	16^x	29^x	32^x	19^x	1^x

19^x	50^x	44	40	44	37	42^x	8^x

15^x	43	48	62	31	36	27	38	33	9^x

5^x	59	36	36	50	42	40	29	31	36	37^x

17^x	39	39	42	39	45	39	28	21	29	30	9^x

23^x	41	42	28	35	29	33	32	26	32	38	23^x

18^x	40	50	38	33	34	46	28	34	32	34	21^x

11^x	35	35	25	28	23	32	25	23	27	38	20^x

1^x	39	41	37	27	31	33	26	25	35	37	5^x

24^x	42	41	38	28	29	39	25	41	17^x

29^x	24^x	40	20	26	35	50	33^x	1^x

3^x	23^x	41^x	36^x	27^x	7^x

110.

TABLE VII Numbers of Particles Counted in Squares on membrane filter 2

1[x]											
4[x]	6[x]	1[x]									
4[x]	16[x]	23	23	18	18	15[x]	1[x]				
6[x]	13[x]	15	10	15	13	15	14	17[x]	7[x]		
3[x]	24[x]	11	16	11	11	9	14	22	9	18[x]	10[x]
3[x]	19	17	14	9	16	22	16	10	16	12	15[x]
16[x]	11	21	18	21	13	19	10	18	7	12	17[x]
13[x]	20	14	16	8	14	10	9	10	17	12	10[x]
14[x]	15	22	22	15	17	14	15	17	13	18	2[x]
2[x]	19	19	16	9	7	9	11	20	9	17	
14[x]	19	14	18	15	22	21	15	11	15[x]		
15[x]	12	19	20	13	14	10	21[x]	1[x]			
4[x]	19[x]	18[x]	19[x]	14[x]	4[x]						

111.

TABLE VIII   Numbers of Particles Counted in Squares on membrane filter 3

6^x	1^x	10^x	29^x	19^x	18^x	3^x	15^x	26^x	3^x
55^x	40^x	49	40	44	48	42^x	15^x	26^x	3^x
47	46	53	57	42	45	50	66^x	44^x	11^x
40	42	45	38	40	46	56	50	59	31^x
47	42	33	58	50	49	37	54	37	26^x
51	35	65	43	60	50	46	51	37	18^x
50	42	39	51	52	53	39	41	41	8^x
42	35	52	49	47	37	45	41	41	
58	39	53	48	29	43	36	44	15^x	
23^x	39	41	41	37	53	27	42		
2^x	58	54	40	37	57	58	27^x		
	24^x	34^x	33^x	27^x	6^x				

20^x			
35^x	9^x		
39	18^x		
61	19^x		
46	15^x		
43			
43^x			
14^x			

112.

TABLE IX   Numbers of Particles Counted in Squares on membrane filter 4

	4^x	6^x	14^x	14^x	9^x	16	6^x	6^x	4^x
	9	13	20	25	13	16	9	11	
	15	11	15	16	15	10	15	11	5^x
	16	18	13	11	12	8	15	11	12^x
	7	16	14	4	10	18	9	12	8^x
	6	14	7	14	6	17	10	11	3^x
	12	15	17	12	20	13	10	9	
	17	14	22	15	14	16	8	13	
	9	14	12	21	14	14	14	9^x	
	14	17	7	11	16	10	6^x		
	8^x	13	11	6	11	14	1^x		
	2^x	5^x	15^x	5^x	9^x	2^x			

	6^x		
	15		
	23		
	12		
	17		
	9		
	12		
	8		
	14		
	2^x		

9^x	11^x	14	13	16	15	16^x	2^x

1^x 5^x 8^x 14^x 4^x

113.

TABLE X

Sum of Particles in Corresponding Squares in Tables V1-X, Complete Squares only

120	137	124	113						
133	124	110	109	104	102				
108	110	110	94	103	95	101	98		
120	120	119	97	140	115	110	98	103	109
112	135	97	128	92	120	113	104	87	101
129	122	105	95	122	120	99	94	97	89
111	117	105	102	96	119	91	97	109	124
120	117	91	101	94	98	95	82	126	
120	125	103	102	111	89	109			
129	89	87	99	114					

TABLE XI count for each square for membranes 1 to 4.

mean count for all squares

5.3 A Preliminary Report on the Hiac Particle Size Analyser

5.3.1 Introduction

The laboratory had the use of a Hiac counter for 10 days and during that time made a brief examination of the performance of the instrument. The tests were carried out using spherical pollen particles 42 μm dia. and the pulse shapes recorded on a Tektronix Storage Oscilliscope type 564B. Because of the very short time available this report is necessarily extremely tentative.

5.3.2 Pulse Shape

42 μm pollen was introduced to the counter and the pulse shape presented at the output socket of the counter was recorded. Preliminary investigations suggest that this output is the transducer signal amplified and that the pulses have not been shaped. The pulse shape was not of the expected flat topped type, i.e.

But of the form
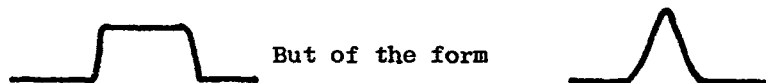
Observation confirmed the statement in the instrument manual that the pulse height was a variable of particle residence time in the counting head (figs. 36, 37). If as has been suggested, particles spin whilst in the sensing zone, elongated particles would be expected to produce approximately flat-topped pulses with a series of maxima on them, whilst spherical particles should produce a flat-topped pulse. The claim that flat-topped pulses are produced implies that the rise time of the dector is small compared with the residence time of the particle within the secsor. Both the shape of the pulse and the dependence of pulse height upon particle flow-rate would appear to contradict this.

5.3.3 Background Count

Clean water triply filtered through 0.2 μm aperture membrane filters was used to attempt to reduce the particle count at the small size end. Some reduction did occur but the counter continued to register counts including the occasional particle in excess of 20 μm. There are two possible explanations for this (a) that some particles remained from previous counts, (b) that the registered counts were due to noise in the counter. From the work carried out it was not possible to differentiate between these effects although the fact that the counter, in spite of making use of integrated circuitry, took 2 hours to stabilize, suggested that there
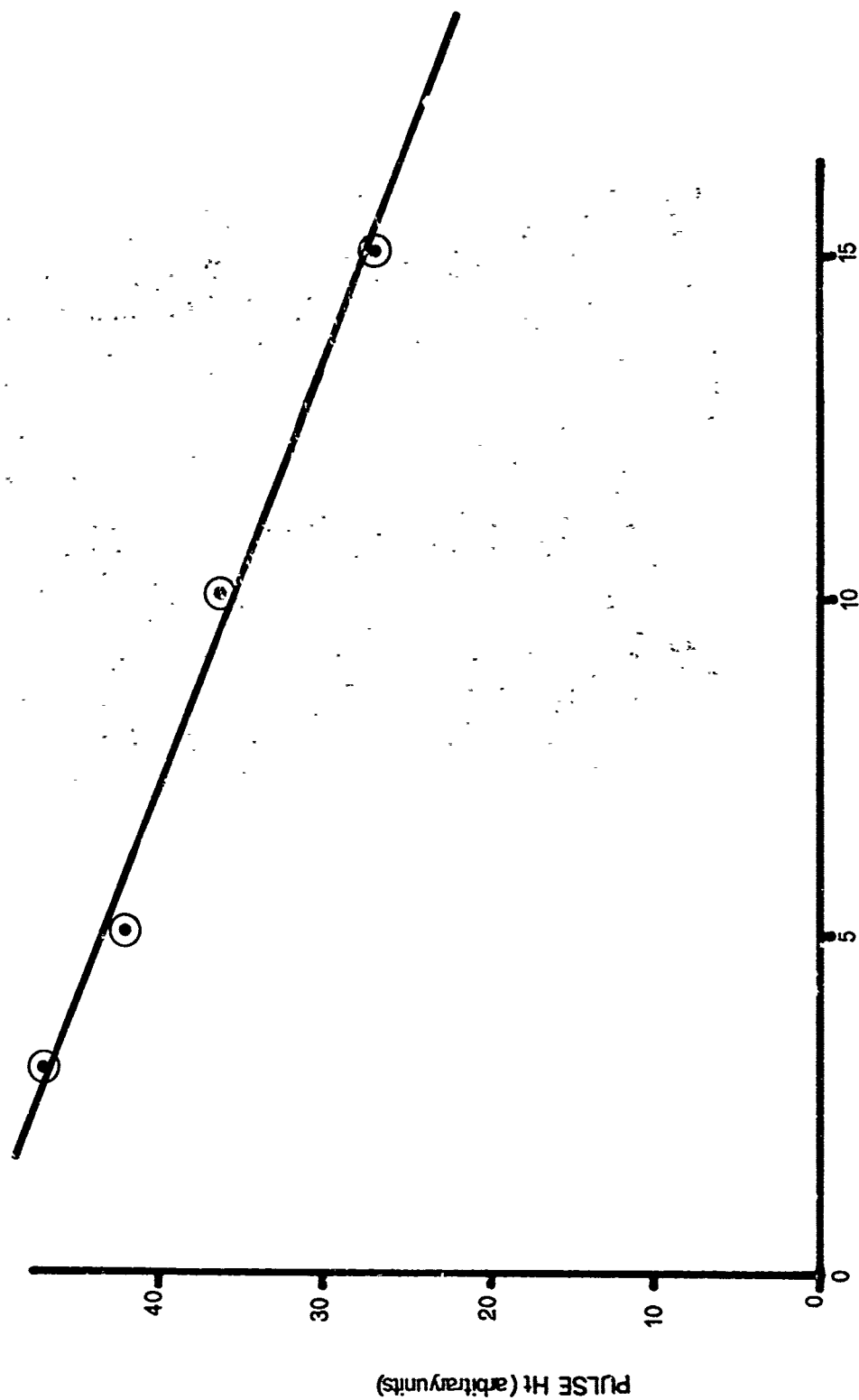
116.

FIGURE 36. Pulse height vs flow rate of HIAC Counter

FLOW RATE (arbitrary units)
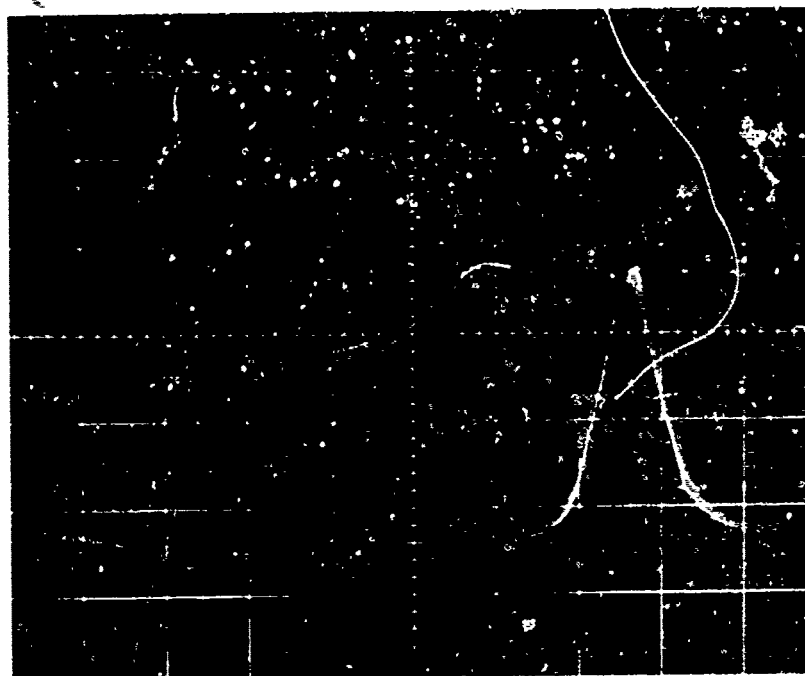
PULSE Ht (arbitrary units)

117.

FIGURE 37 Typical HIAC Counter pulse for spherical particles

might be some electronic noise within the system.

5.3.4 : Pulse Shapes Produced by Irregular Particles

Runs were carried out using 40µm sieved aluminium flake particles. The pulses observed were identical to those produced by spherical particles.

5.3.5 Conclusions

The extremely good reproducability obtained suggests that this instrument is probably an extremely good comparative method of counting particles, but its value as an absolute counting device has yet to be confirmed. More work is needed on analysis of pulse shapes and the effect of operating parameters of the results obtained. The present conclusions assure that the pulses observed were not shaped before the output socket. This assumption needs to be checked by experiment and reference to circuit diagrams.

5.4   The Coulter Counter

5.4.1   Introduction

One of the features of new developments in methods of particle size analysis is the increasing importance of stream scanning methods whereby a particle is sized and counted as it passes through a sensing zone. This field is dominated by the extremely successful Coulter Counter (1) in which the change of resistance between two electrodes immersed in an electrolyte, is monitored as a particle passes through a small orifice separating the electrodes. Other developments are in the use of the measurement of the light scattered from individual particles as the means to count and identify particles. Both of these types of measurement have the ability to count and analyse large numbers of particles and so give a statistically meaningful analysis. However, no matter how dilute the suspension used there is always a finite chance that two or more particles will arrive in the sensing zone simultaneously. The response of the instrument to such an occurrence is important as it can give rise to an inaccurate analysis. It is the purpose of this paper to examine the response of the Coulter Counter type of instrument to two or more particles within the sensing zone.

The earliest correction for coincidence is that developed from the paper by Mattern et al (1) and is the correction recommended by the manufacturers. The undercount, n^{11} the number of particles not counted is related to the actual count n^{1}, the orifice diameter D and the volume sampled V

$$n^{11} = 2.5 \left(\frac{D}{100} \right)^3 \left(\frac{500}{V} \right) \left(\frac{n^1}{1000} \right)^2$$

This expression contains the realisation that a correction must depend on the orifice dimensions and the volume sampled but its origins are not explicit.

The second approach was that by Wales and Wilson (2) who realised that the response of the instrument could give rise to two types of coincidence.

(a)   All pulses from two or more coincident particles add so as to produce a single pulse whose maximum is the sum of the individual pulses.

or (b)   the pulses from two or more simultaneous particles produce a single pulse whose maximum corresponds to the largest particle.

120.

They considered the sensing of particles to be equivalent to the successive filling and emptying of the sensing volume v. The chance of finding n particles in such a volume is obtained by the application of Poisson's Law.

$$p(n) = \frac{\epsilon^n \, e^{-\epsilon}}{n!}$$

where ϵ is the expectation of finding one particle in the volume v

$$\epsilon = \frac{v}{V} \cdot No \qquad \text{where No is the number of particles in the volume V.}$$

The probability of no count is $p(o) = e^{-\epsilon}$ and the probability of some count is therefore $p(n > o) = 1 - p(o) = 1 - e^{-\epsilon}$

They finally conclude that the number of particles counted will be

$$n = \frac{No}{\epsilon} \cdot (1 - e^{-\epsilon})$$

This equation is in error since if the true number per volume V is No and n is the number counted, the probability of a count is $\frac{n}{No}$ and not $\frac{n\epsilon}{No}$ Wales and Wilson continue to examine coincidence as a function of response level (threshold) for each of their assumptions.

where

$$n(t) = No \, e^{-\epsilon} \left[f_i + t_2 \, f_2 + \frac{t^2}{6} f_3 + \cdots \cdots \right]$$

where f_i are dependent on their assumptions (a) or (b). A solution can only be obtained for assumption (b) when

$$N_o(t) = \frac{n(t)}{1 - \frac{1}{2} \frac{n(t)}{V}}$$

This paper was criticised by Kubitschek (3) who stated that only assumption (a) was valid and this lead to a further paper by Princen and Kwolek (4) who assumed that the 'time distance' Ti between particles was distributed randomly. From the mean 'time distance' $\overline{\tau}$ between particles, they calculated that a fraction $\frac{t}{2\tau}$ will be separated by a distance less than t the time spent in the sensing volume and so they calculate the correction

$$n = N - CN^2 \qquad \text{where n is the number counted and N is the true number.}$$

C is a constant $= \frac{v}{2V}$. This relation has been used experimentally by Edmanson (5).

It is the purpose of this paper to re-examine the assumptions of Wales and Wilson and to derive correct coincidence corrections for the Coulter Counter.

5.4.2   Response of the Coulter Counter

The predictions of the resistance change in the orifice due to the presence of a particle have been presented in papers by Batch (6) and by Gregg and Steidley (7).   The analysis depends on the particle being in a region of uniform field and the approaches differ only in the methods solving the integral.   The solution obtained by Gregg and Steidley for the sphere is

$$R = \frac{2\rho_0}{\pi D} \left[\frac{\tan^{-1} K (1-K)^{\frac{1}{2}} - K}{(1 - K^2)^{\frac{1}{2}}} \right]$$

This equation is approximated by:

$$\Delta R = \frac{\rho_0 v}{A^2} \frac{1 + 0.3 K^2 + 0.13 K^4 + \ldots)}{1 - K^2}$$

and illustrates that provided K is small the resistance change is proportional to the volume of the particle.   The difference between the assumption that the resistance is proportional to the volume and the Gregg and Steidley result has been examined by Allen (8) and has been examined experimentally by Eckoff (9).

Grover et el (10) with an alternative approach apply Maxwell's expression for the resistance of a composite medium to the case of a particle in a uniform field and obtain an expression for the relative change in current obtained for the presence of a particle

$$\frac{-\Delta I}{I} = \frac{1.5\delta}{1 - \delta}$$

where δ is the ratio of particle volume to that of the orifice.   Provided

$$\left(\frac{r_1}{R_1} \right)^{10} < \frac{1}{3}$$

where R is the radius of the concentric sphere in which the field is uniform in the absence of the particle.   This expression is examined experimentally in a subsequent paper by Grover et al (11).

5.4.3   Coulter Analogue Results

(a) 1   The Response to Single Particles

Because of the physical dimensions of the orifice it is difficult to
obtain precisely the resistance change with position in a real situation.
However, an electrically similar analogue can be built in which the phys-
ical dimensions are scaled up and an electric field is maintained across
the enlarged orifice.   Large diameter particles can now be physically
drawn through the orifice and the resistance change with position,monitored.
The physical dimensions are illustrated in fig. 38   which also demonstrates
the pulley system used to pull the particle through the orifice.   As in
operation of the Coulter orifice a constant current was maintained across
the orifice and the change in voltage required to maintain the current
constant was recorded graphically on an x-y plotter.   The position of the
particle was monitored by movement of a spiral wound potentiometer attached
to the pulley system.

A typical response of voltage against position is illustrated in fig.39
for spherical particles.   From these curves the peak response can be
obtained as a function of particle volume.   This variation is presented
in table 1 and illustrated by fig.40   which shows that the proportion-
ality between peak response and particle volume is good for spheres up to
50% of the orifice diameter, a figure in excess of that previously accepted.

The results also show that the resistance of the orifice is changed by a
particle well outside the physical limits of the orifice and that the sens-
itive region is a function of particle size.   To investigate the reason for
this further,the orifice and the electrode system have been represented on
graphited paper.   A potential placed between the electrodes enable lines of
equipotential to be obtained.   A particle approaching the orifice is now
represented by the removal of a disc of the conducting paper and the lines
of equipotential obtained once again.   The results are sketched in fig.
41   and show how the distribution of potential is changed by the presence
of the particle.   Whilst it is not suggested that the electric field
obtained in this way is the field in the cylindrical geometry of the Coulter
Counter, it is interesting to note the change in field occurs and to note

123.

TOP ELECTRODE

PARTICLE

PERSPEX ORIFICE BLOCK

CENTRAL P.V.C. SHEET

P.V.C. TANK

TEN TURN POT WITH PULLEY

TUBULAR GUIDE

COUNTER-BALANCE WEIGHT

VARIABLE SPEED FORWARD-REVERSE MOTOR

60cm

60cm

8·1cm

11·4cm

ELECTRODE/ORIFICE ARRANGEMENT
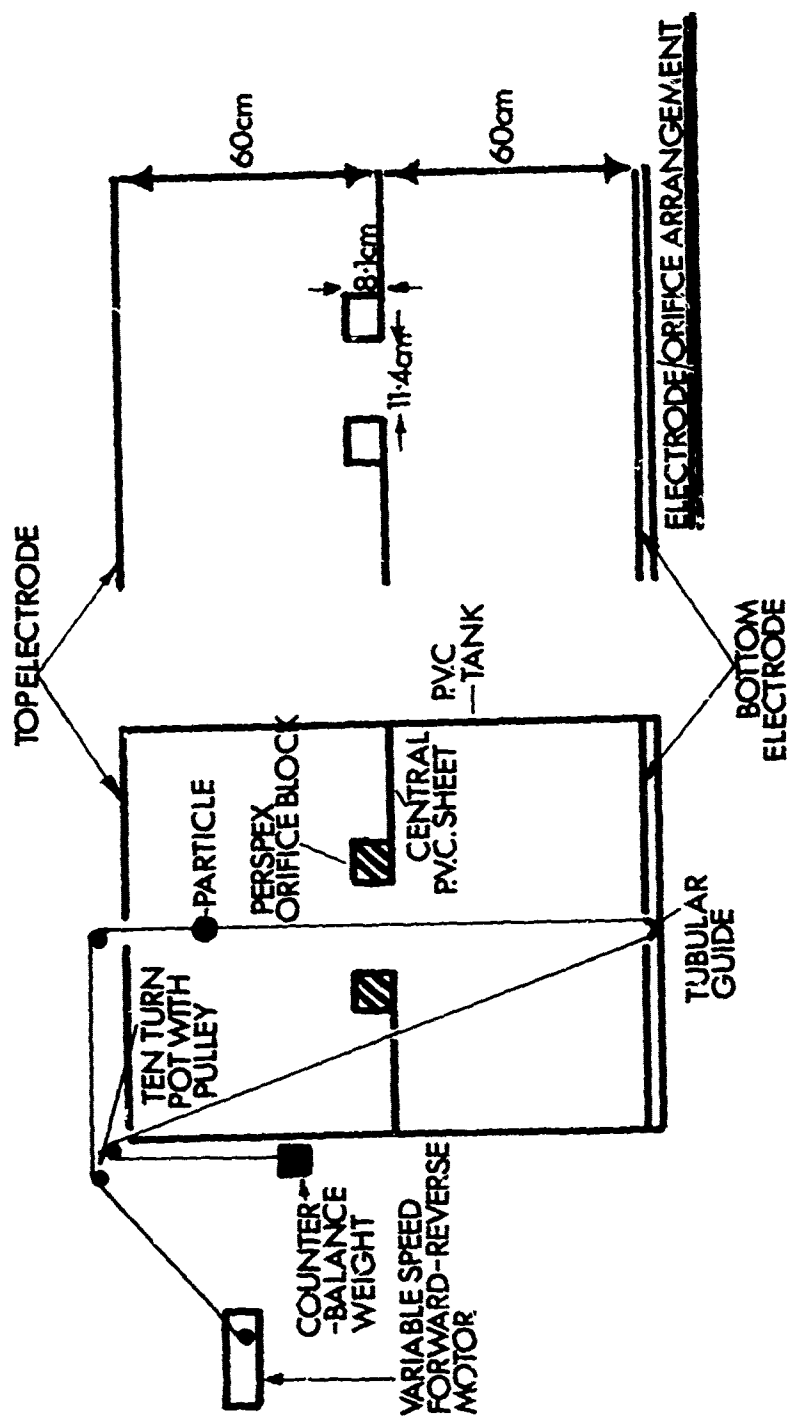
BOTTOM ELECTRODE

FIGURE 38   Analog Coulter Counter - general diagram
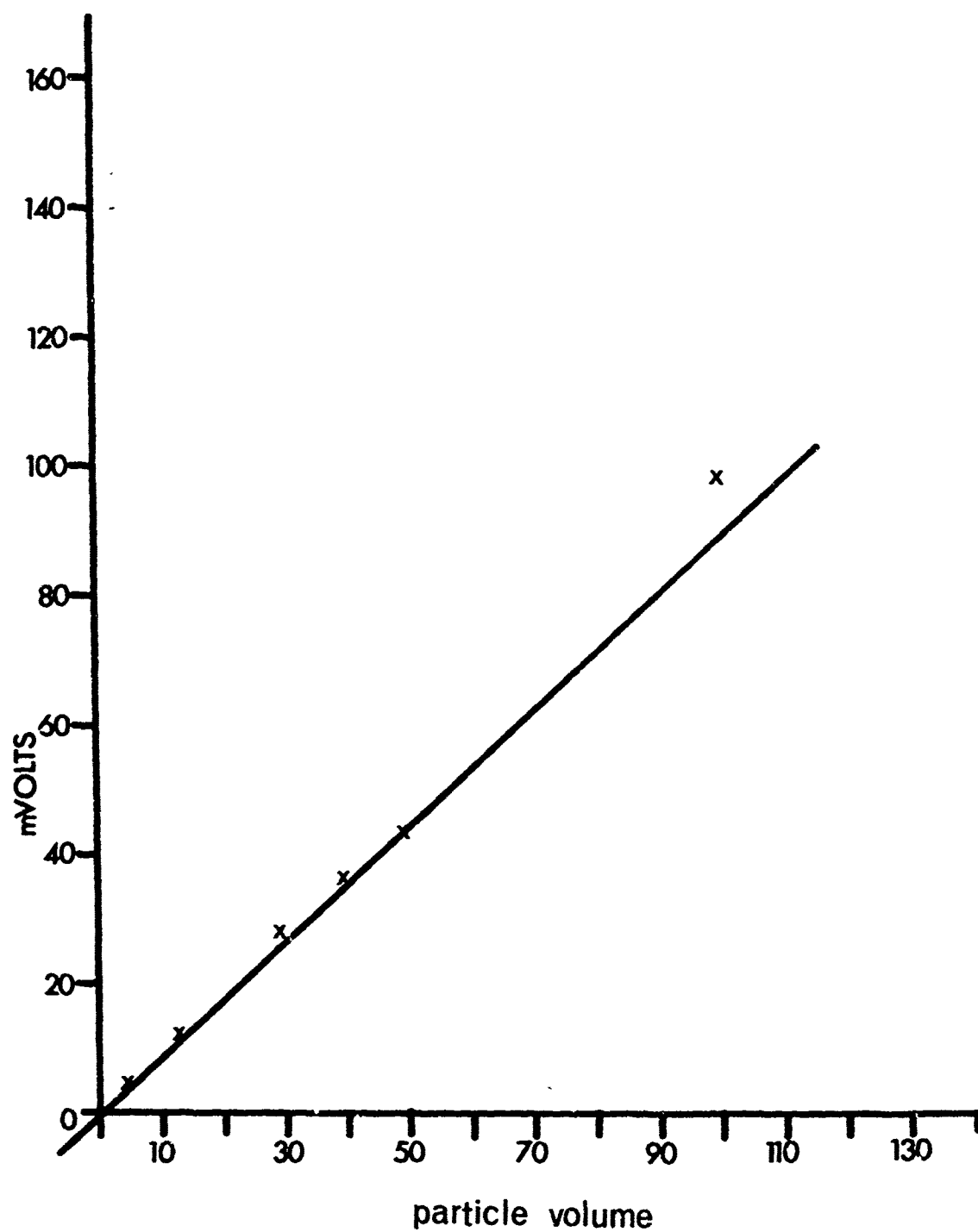
124.

FIGURE 3⁹ Response of Coulter Counter to Spherical Particles
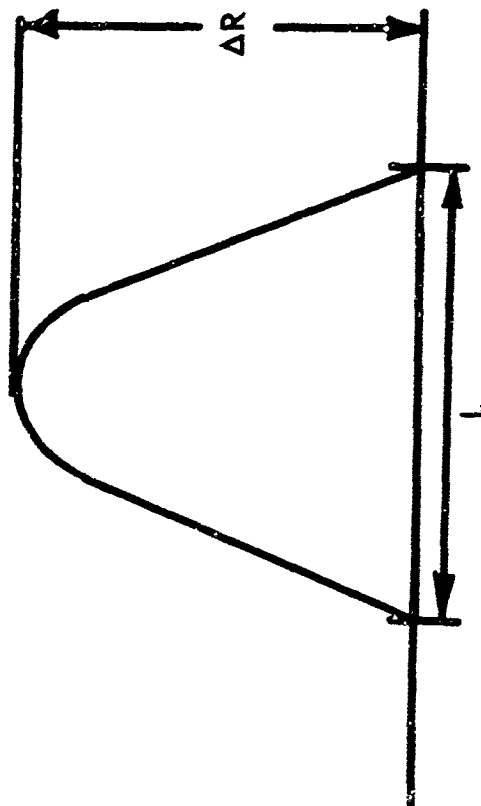
125.

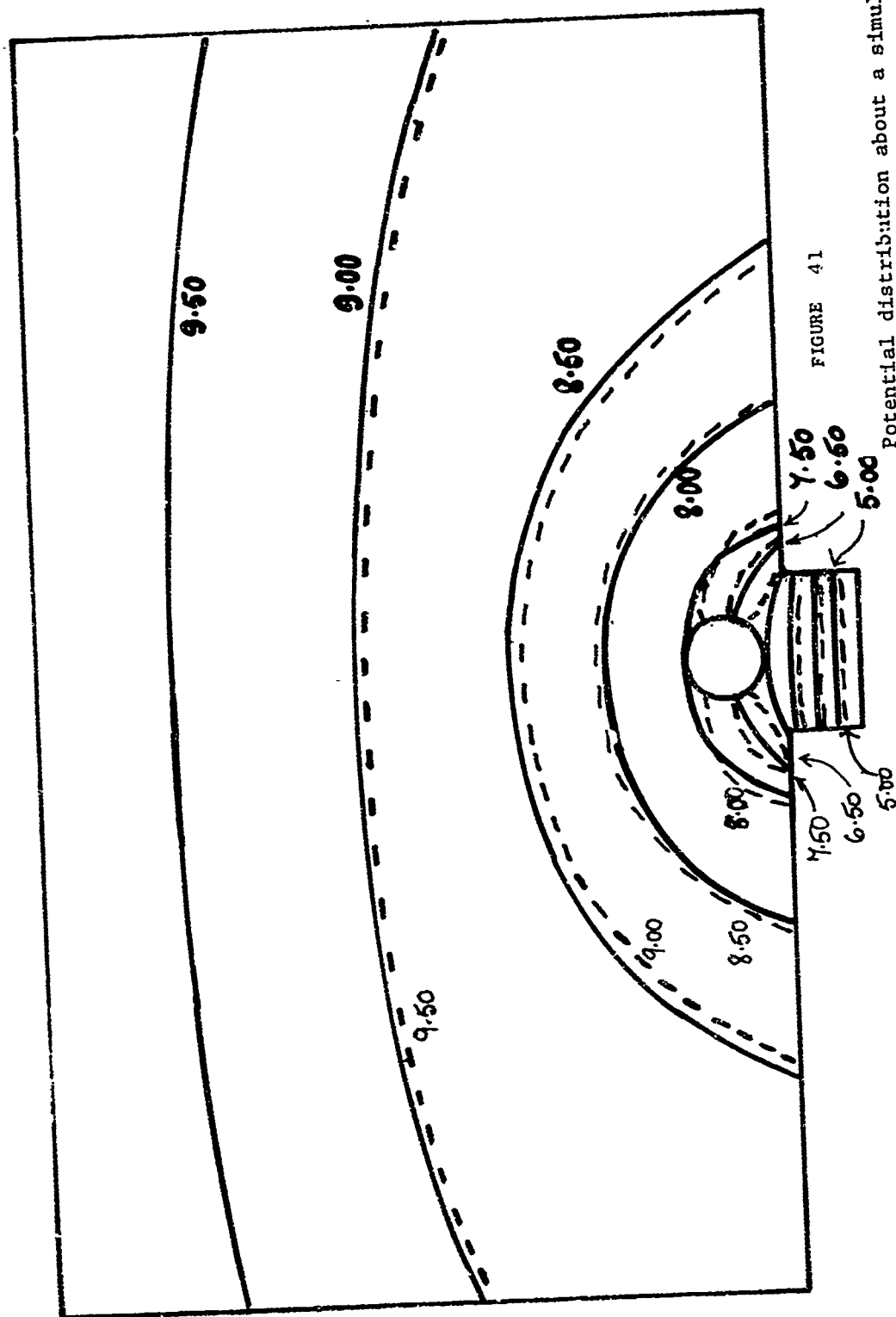FIGURE 40   Typical response to a spherical particle

126.

FIGURE 41

Potential distribution about a simulated orifice

the influence of the particle outside the physical limitations of the orifice. These results suggest that the sensitive region can be divided into two regions shown in fig. 42. Region I is the region of uniform field in which a particle will give the peak resistance change. Region II is a region in which there is a response due to the presence of the particle but that response will depend on the position of the particle. Outside region II, is the electrolyte in which the presence of particles will not cause a resistance change. In fig. 42 the two regions labelled II are shown as being symmetrical but this will only be so if the electrodes are placed symmetrical to the orifice. These conclusions were shown to be valid by further experiments in the Coulter Analogue. Figure 43 demonstrat.s the effect of doubling the orifice length. The pulse becomes more flat topped but is otherwise symmetrical, thus indicating that the region of uniform field is proportional to the orifice length.

(b)   The response to two or more particles

When two equal sized particles separated by a distance d are drawn through the orifice, the response is complex and is illustrated in fig. 44. The peak resistance change is plotted as a function of the separation in fig. 45 These resistance changes can be reconstructed by adding together the spacial response of single particles with the peak responses separated by the distance between the particles fig. 46. Further complex responses will be obtained if three or more particles are found in the sensitive regions at the same time. Predicted pulse shapes are shown in fig. 47 for three particles and figs 48-53 show oscillographs of pulses obtained using pollen in a Model A Coulter Counter.

5.4.4   The Interactions between monosized particles

The following interactions can now be seen to occur.

1.   A single particle separated from all other particles by a distance will produce a peak response, ΔR, proportional to its volume within the limitations discussed earlier. Where the distance ℓ_2 is equal to the distance between the outer limits of the two regions II see fig. 54.
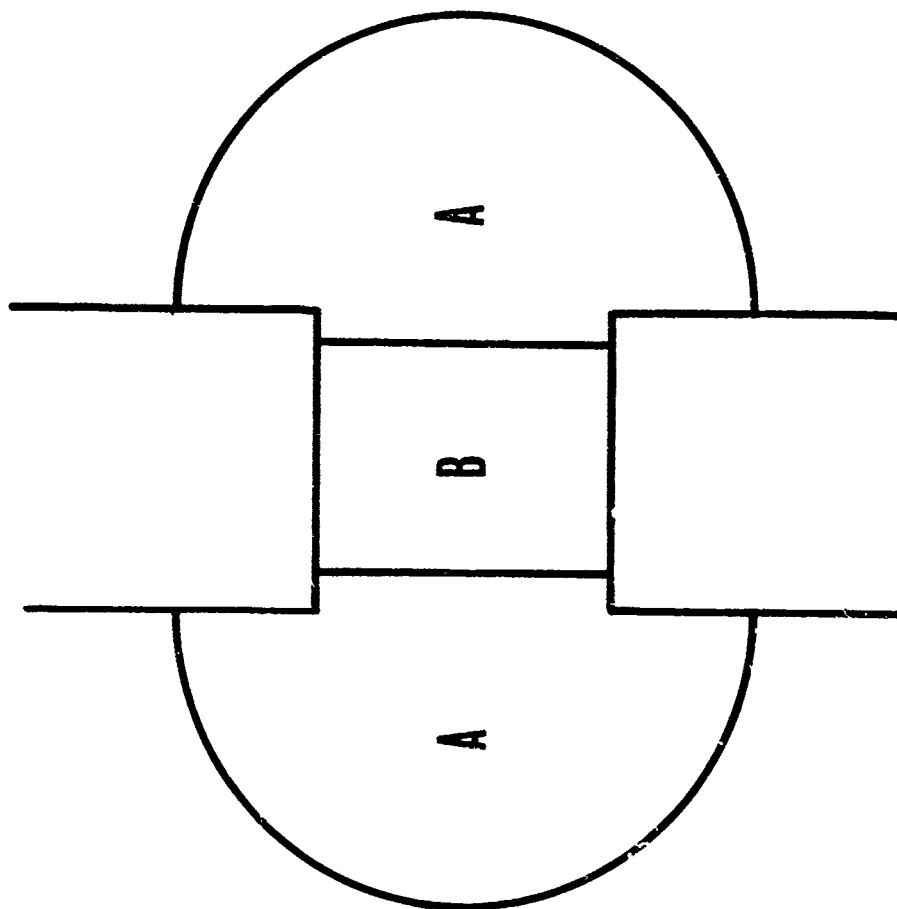
FIGURE 42 Regions of field about orifice

129.
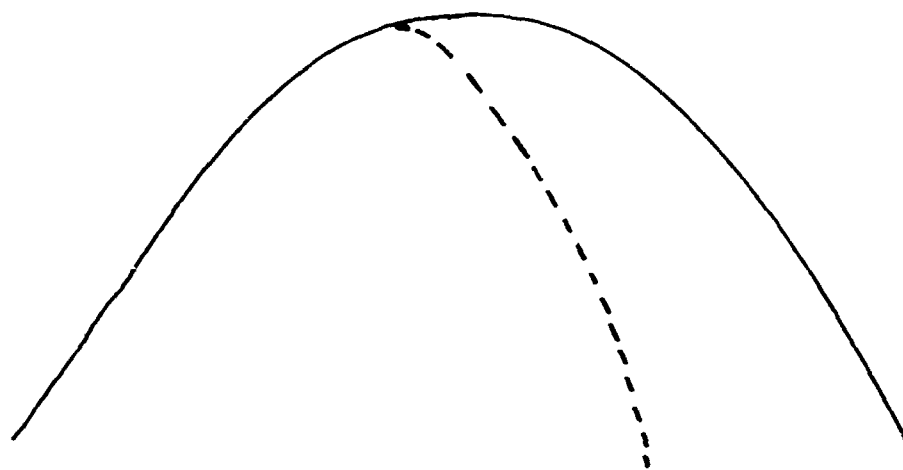
FIGURE 43   Effect of doubling orifice length

130.

Touching 2cm. separation

4cm. 6cm.

8 cm. 10 cm.

12 cm. 14cm.
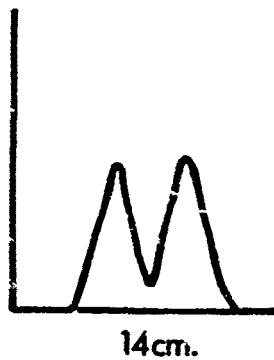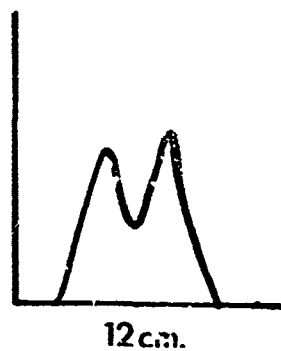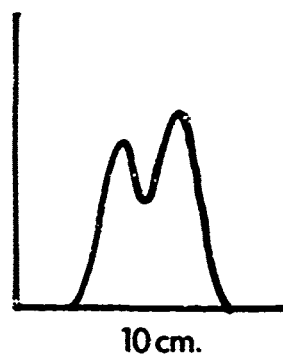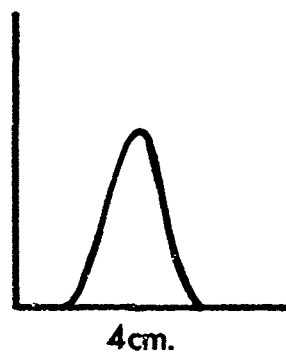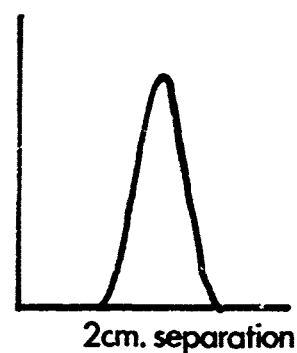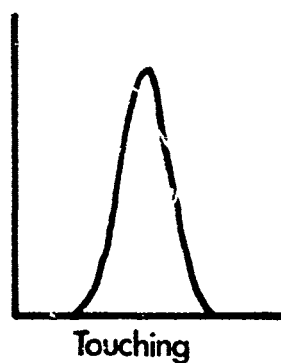
FIGURE 44. Response to two particles passing orifice

131.
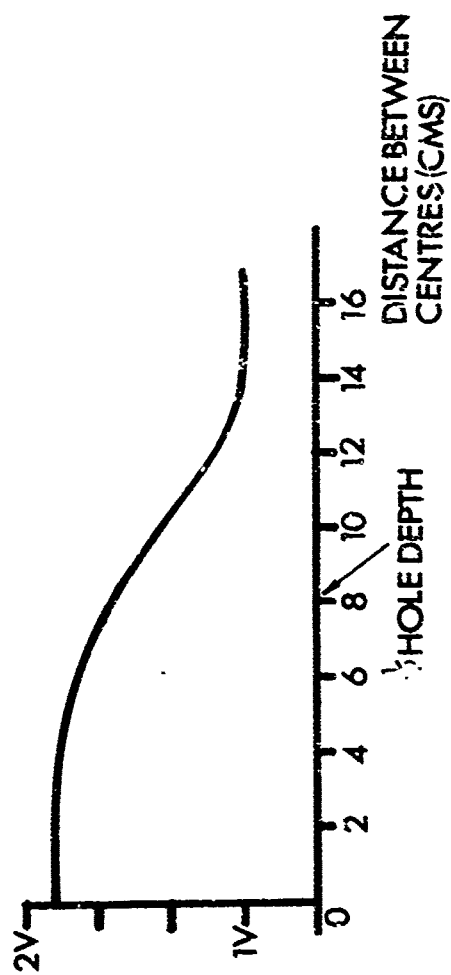
FIGURE 45   Peak voltage response as a function cf particle separation
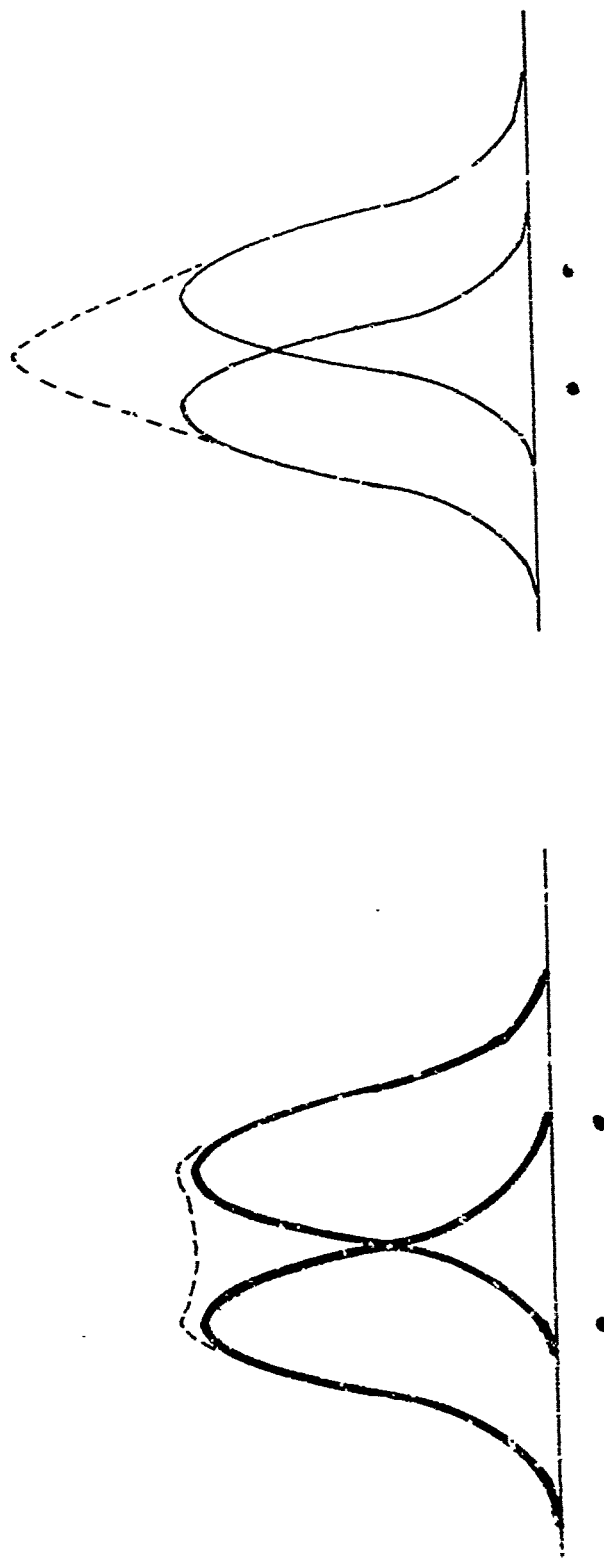
FIGURE 46   Pulse shapes given by two particles

133.
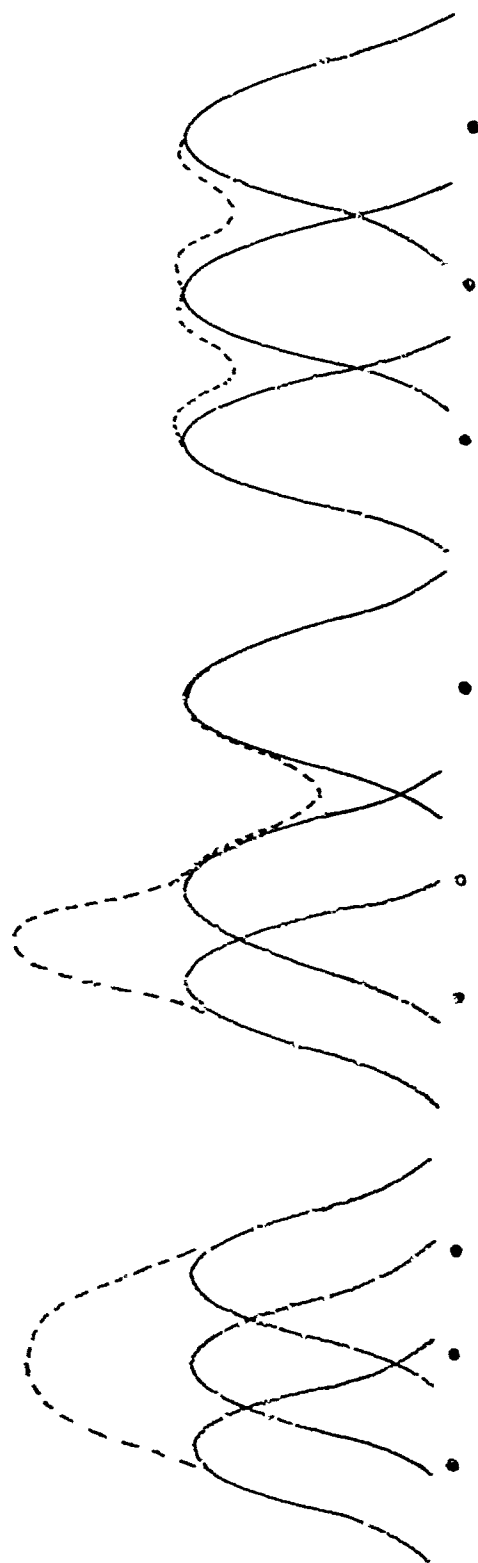
FIGURE 47   Pulse shapes given by three particles

134.
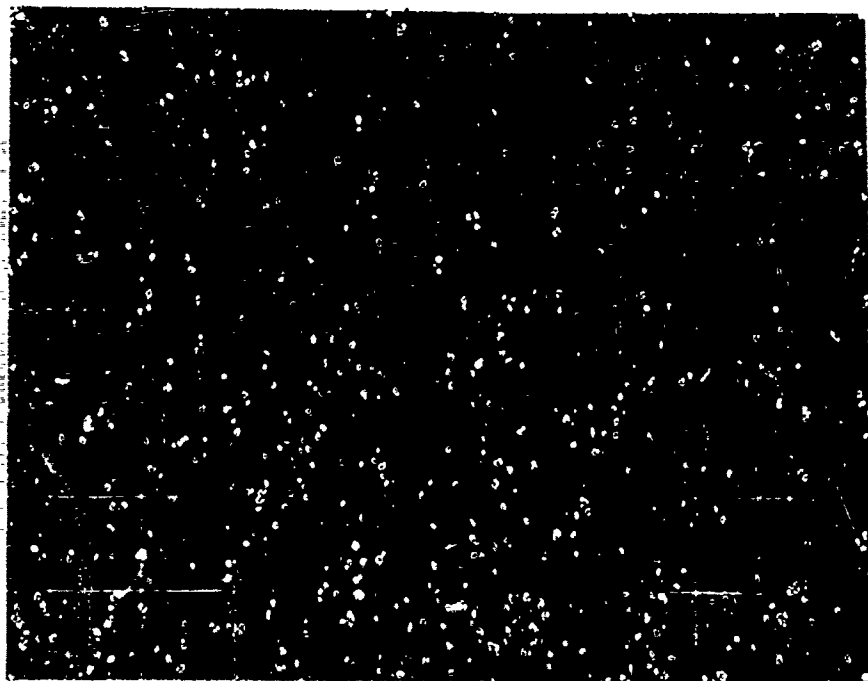
FIGURE 43

Pulse Shape from Single Particles

135.
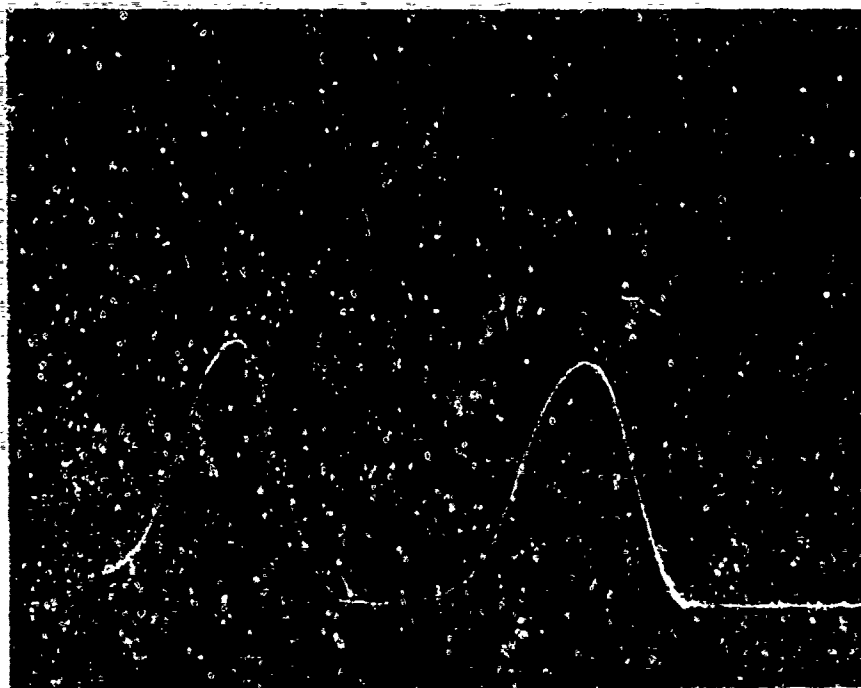
FIGURE 49

Two Particles Passing Through Orifice in Close Proximity
But Giving Singlet Response

136.
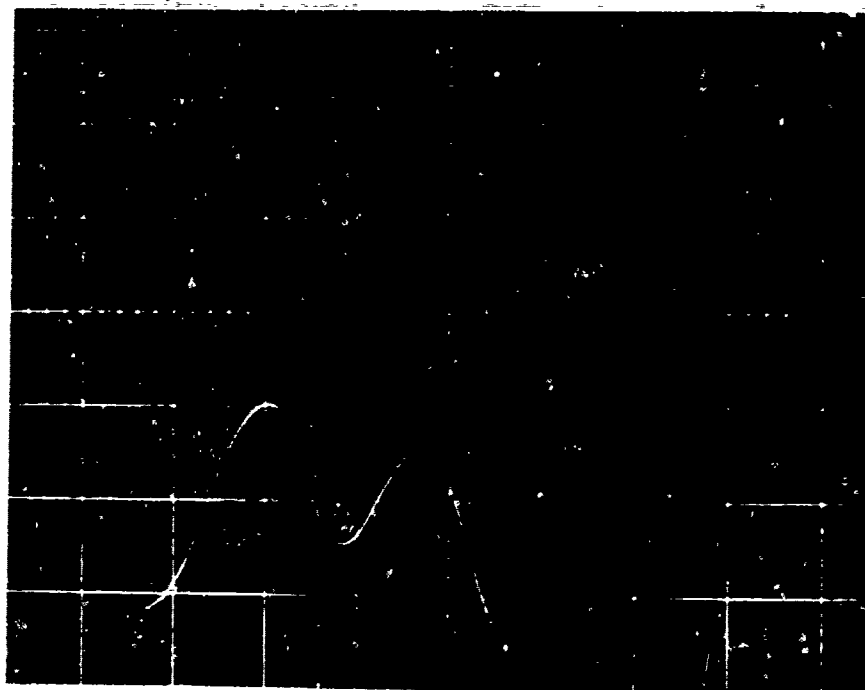
FIGURE 50

Two Particles Showing Intermediate Response

137.
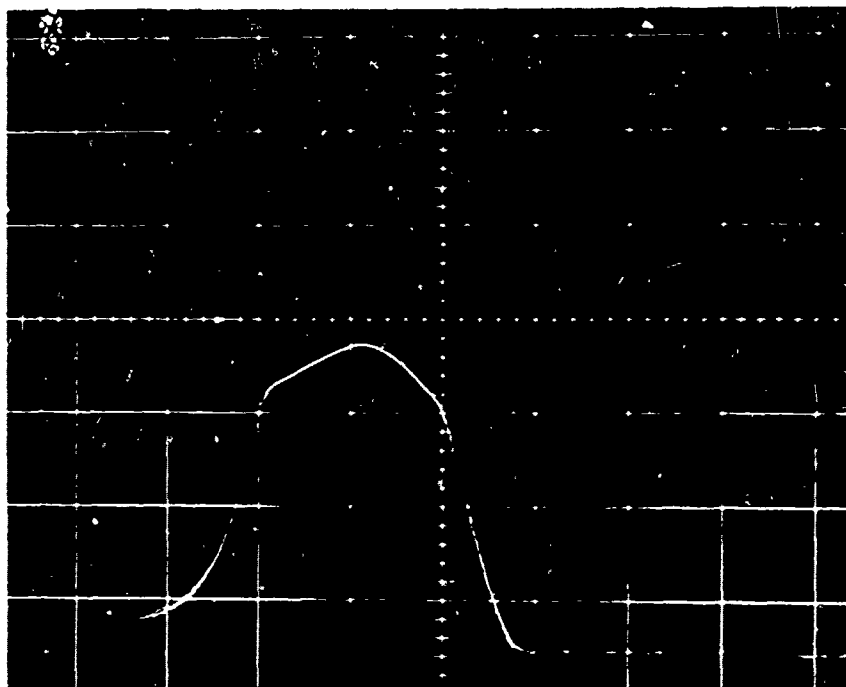
FIGURE 51

Two Particles Showing Almost True Doublet
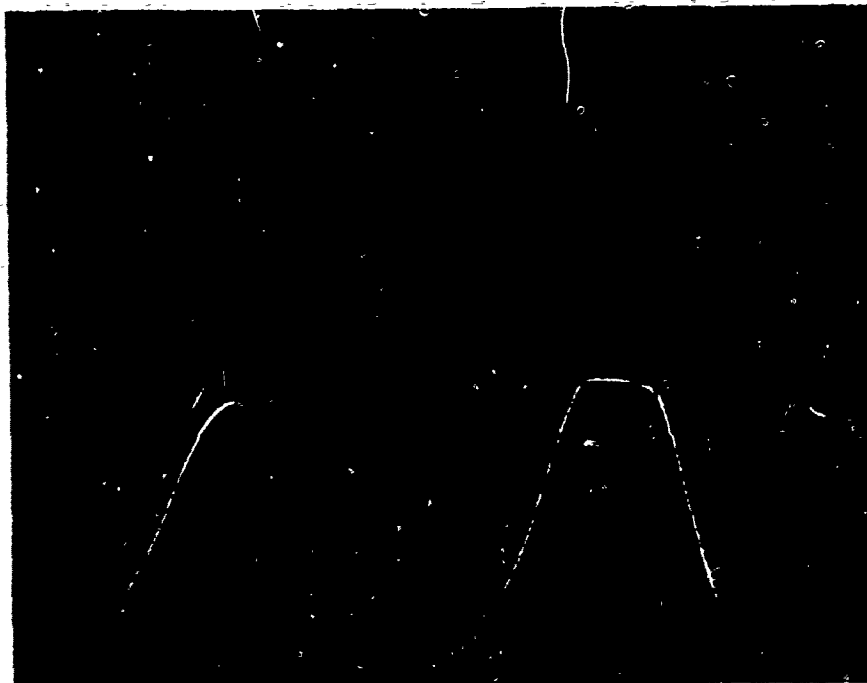
FIGURE 52

Single Particle Followed by Intermediate Doublet

139.
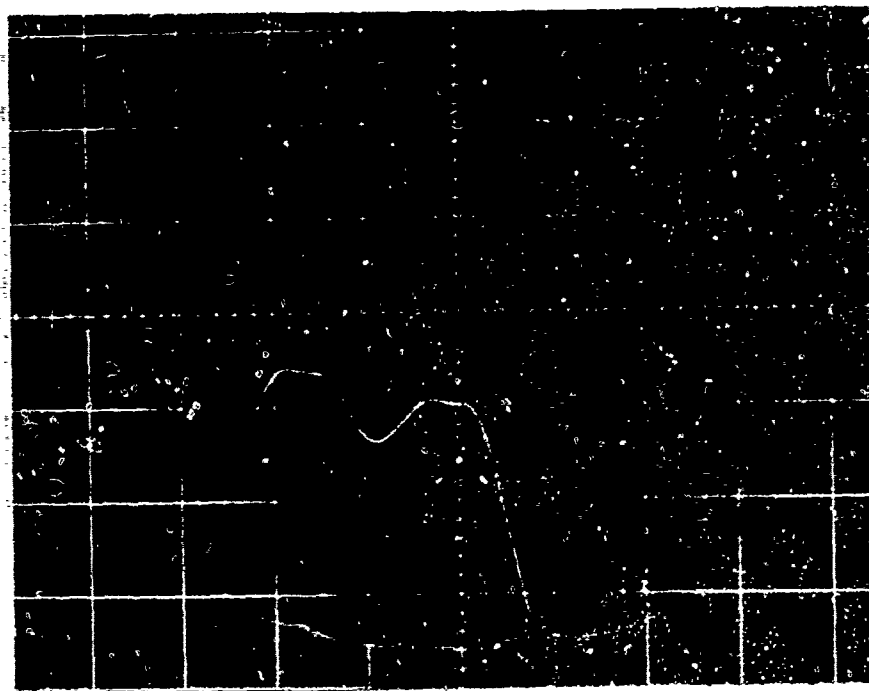
FIGURE 53

Intermediate Doublet followed by Intermediate Doublet

140.
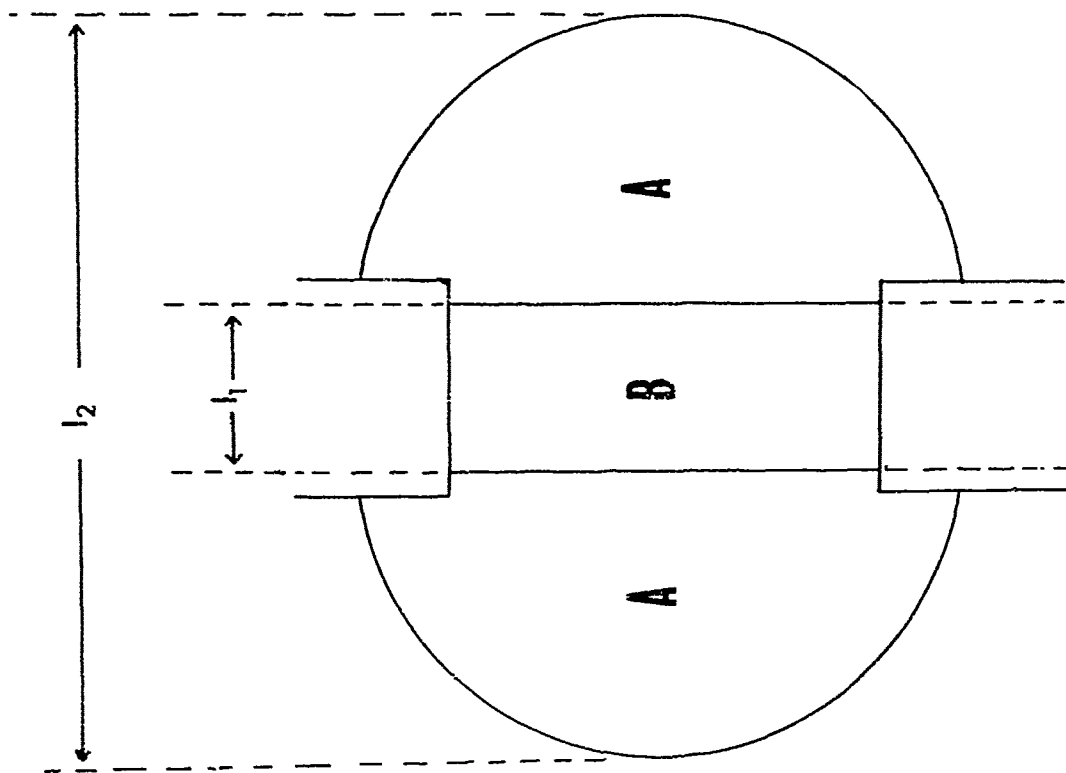
FIGURE 54   Idealised field showing length of uniform field and sensitive region l_2

141.

2.   Two or more particles found within a distance, ℓ defining region I and with
all other particles at a distance greater than ℓ_2 away will give a 'vertical
interaction' response.   The response will be proportional to the total
volume of the particles within the region.

3.   With two particles at a distance apart between ℓ_1 and ℓ_2, all other part-
icles being at a distance gr∈ .ter than ℓ_2 away , the response will be inter-
mediate between that for a particle of unit volume and that of double volume,
and will be dependant on the precise separation.

4.   With three or more particles within a distance ℓ_2, all other particles
being greater than ℓ_2 apart, the response is complex and will depend on
the geometry.

It is interesting to note that the horizontal interaction of Wales and
Wilson does not occur but on more complex response giving rise to 'apparent' part-
icles of volumes intermediate between that of integral number of particles is
obtained.   This is further demonstrated by the apparent size distribution obtained
when counting concentrated dispersions of monosized particles.   Figure 55   demons-
trates the apparent change in size distribution of 27 μ pollen in a 140 μ orifice,
where the only difference is the concentration of the particles.

5.4.5   The Theory of Coincidence

If the suspension from which particles are drawn has sufficiently large
volume so that the removal of some particles does not materially change the con-
centration of particles and if there are no other physical conditions affecting
the separation between particles, the distance between particles will follow the
Poissonian distribution.

The probability of finding a separation between x and $x + d_x$ is

$$dP(x) = \mu \, \exp \, (- \mu x) \, dx$$

where μ is the reciprocal mean separation

$$\frac{\pi d^2 \, No}{V}$$

142.
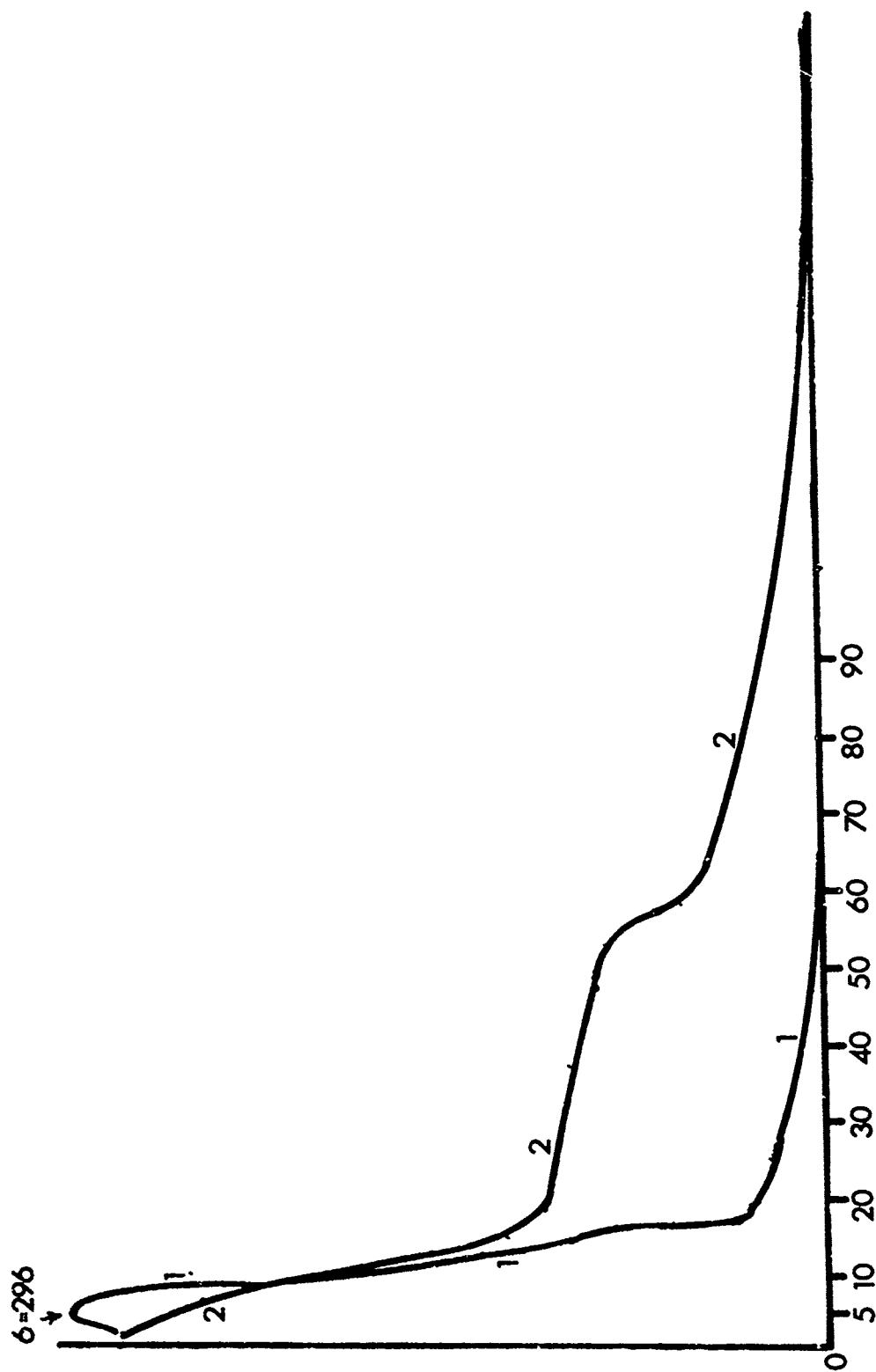
FIGURE 55   Apparent change in size distribution of a monosize pollen
due to a large increase in concentration

143.

Interaction I True single pulses

Since true pulses occur if there is a separation greater than ℓ_2 on each side of the particle the probability of a true singlet will be

$$P(1) = \int_{\ell_2}^{\infty} \mu\exp(-\mu x)\, dx \quad \int_{\ell_2}^{\infty} \mu\exp(-\mu x)\, dx$$

$$\therefore \quad P(1) = \exp(-2\mu\ell_2) \qquad \ldots\ldots(1)$$

and the probability of particles not being counted as a single particle

$$= 1 - P(1) = 1 - \exp(-2\mu\ell_2) \quad \text{an approximate form of equation (1)}$$

$$\text{is} \quad P(1) = 1 - 2\frac{\pi d^2}{V} N_o \ell_2$$

so $\quad N = N_o(1 - C N_o)$ the equation of Princen and Kwolek

Interaction II True multiplet pulses

(a) Doublet

If two particles are found at a separation less than ℓ_1 and on either side of the doublet there are separations greater than ℓ_2, then the response will be that of a doublet.

$$P(2) = \int_{\ell_2}^{\ell} \mu\exp(-\mu x)\, dx \quad \int_{0}^{\ell_1} \exp(-\mu x)\, dx \quad \int_{\ell_2} \exp(-\mu x)\, dx$$

$$\therefore \quad P(2) = \exp(-2\mu\ell_2)\,(1 - \exp(-\mu\ell_1))$$

Triplet

If three particles are found within the distance ℓ_2 then the response will be a true triplet.

$$P(3) = \int_{\ell_2}^{\infty} \mu\exp(-x)\, dx \quad \int_{0}^{\ell}\int_{0}^{y} \mu^2\exp(-\mu x)\exp(-\mu(y-x))\, dx\, dy \int_{2} \mu\exp(-\mu x)\, dx$$

144.

$$\therefore \quad P(3) = \exp(-2\mu \ell_2)\,(1 - \exp(-\mu \ell_1)\,(1 + \mu \ell_1))$$

Quadruplet

Similarly

$$P(4) = \int_{\ell_2} \mu \exp(-\mu x)\,dx \int_0^{\ell_1} dy \int_0^y \int_0^{y-x} \mu^3 \exp(-\mu x)\exp(-\mu z)$$

$$\exp(\mu(y-x-z)) \; x \; dy \; dz \int_{\ell_2} \mu \exp(-\mu x)\,dx$$

$$\therefore \quad P(4) = \exp(-2\mu \ell_2)\,(1 - \exp(-\mu \ell_1)\,(1 + \mu_1 + \frac{\mu^2 \ell^2}{2} + \dots))$$

Multiplet

The probability of finding n particles in length ℓ_2 with separations greater than ℓ_1 on either side is

$$P(n) = \exp(-2\mu \ell_2)\,(1 - \exp(-\mu \ell_1)\,(1 + \sum_1^{n-2} \frac{(\mu \ell_1)^n}{n}))$$

Probability of Intermedidate Response

Interaction III

Doublets with separation between ℓ_1 and ℓ_2

$$P^1(2) = \int_{\ell_2}^{\infty} \mu \exp(-\mu x) \, dx \int_{\ell_1}^{\ell_2} \mu \exp(-\mu x) \, dx \int_{\ell_2}^{\infty} \mu \exp(-\mu x) \, dx$$

$$P^1(2) = \exp(-2\mu\ell_2) \left(\exp(-\mu\ell_1) - \exp(-\mu\ell_2) \right)$$

and the probability of a separation between d and d + dd

$$dP^1(2) = \exp(-2\mu\ell_2) \, \mu \exp(-\mu d) \, dd$$

Interaction IV

Three further types of response are possible and are illustrated in Fig. 56.   All other possibilities are allowed for in interactions previously considered.   The pulse recorded will depend on the mechanism of pulse height selection used but it appears (12) that pulse (a) will be recorded as an interaction III, a doublet with intermediate response, pulse (b) will also be recorded as a doublet with intermediate response whilst (C) will be recorded as a triplet with intermediate response between two and three.

Probability of pulse type (a) is

$$P^1(3_a) = \int_{\ell_2}^{\infty} \mu \exp(-\mu x) \, dx \left[\int_{\ell_1}^{\ell_2} \mu \exp(-\mu x) \, dx \right]^2 \int_{\ell_2}^{\infty} \mu \exp(-\mu x) \, dx$$

$$= \exp(-2\mu\ell_2) \left[\exp(-\mu\ell_1) - \exp(-\mu\ell_2) \right]^2$$

Pulses of the shape 3(b) and 3(c) will have the same probability

$$P^1(3b) = \int_{\ell_2}^{\infty} \mu \exp(-\mu x) \, dx \int_{\ell_1}^{\ell_2} \mu \exp(-\mu x) \, dx \int_{0}^{\ell_1} \mu \exp(-\mu x) \, dx \int_{\ell_2}^{\infty} \mu \exp(-\mu x) \, dx$$

$$= \exp(-2\mu\ell_2) \left[\exp(-\mu\ell_2) - \exp(-\mu\ell_1) \right] \left[1 - \exp(-\mu\ell_1) \right]$$

Interaction I

$I>I_1 \quad I>I_1$
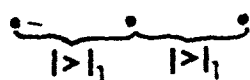
singlet

Interaction II

$I>I_1 \quad I<I_2 \quad I>I_1$

Doublet

$I>I_1 \quad I<I_2 \quad I>I_1$

Triplet

$I>I_1 \quad I<I_2 \quad I>I_1$
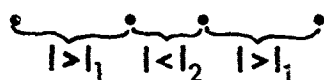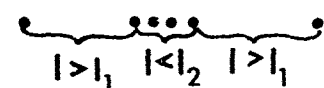
Quadruplet

Interaction III

$I>I_1 \quad I_2<I<I_1 \quad I>I_1$
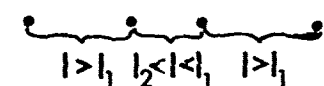
Doublet with
Intermediate response

Interaction IV

(a)
Triplet with response
$\Delta R \leqslant V \leqslant 2\Delta R$

$I>I_1 \quad I_2<I<I_1 \quad I_2<I<I_1 \quad I>I_1$

(b)
Combination
Singlet/Doublet
$\Delta R \leqslant V \leqslant 2\Delta R$

$I>I_1 \quad I_2<I<I_1 \quad I<I_2 \quad I>I_1$
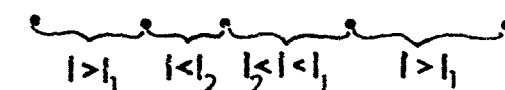
(c)
Combination
Doublet/Singlet
$2\Delta R \leqslant V \leqslant 3\Delta R$

$I>I_1 \quad I<I_2 \quad I_2<I<I_1 \quad I>I_1$

FIGURE 56   Classification of coincidence into 4 types of interaction.

147.

Similar analysis will apply to interactions of four or more particles.

5.4.6   The Magnitude of the Coincidence Correction

This theory can be used to investigate the magnitude of the coincidence effect if values can be assigned to the critical lengths l_1 and l_2. The former l_1, is the length of uniform field within the orifice and to a first approximation may be assumed to equal the length of the orifice. This approximation to the critical length will be too large and will slightly over emphasise the occurrence of true multiplets but the true effective distance of uniform field will depend on the shape of the orifice and the position of the electrodes and is in practise difficult to determine.

The total effectively sensitive distance may be obtained by observing the shape of the pulses obtained when monosized particles are drawn through the orifice as in the usual calibration procedure. By overlaying the pulses obtained on the display of an oscilloscope, an effective time of passing of the particle is obtained. If one now assumes that the particle is travelling at the average velocity of the fluid through the orifice an estimate of the sensitive distance l_2 is obtained. Table XIII represents the results obtained when calibrating pollens of different sizes are passed through a range of orifices. Particles of diameter small compared to the orifice diameter give rise to a fairly consistant estimate of the sensitive length. Large particles however give much larger estimates of the length. This is due to the complex paths of large particles approaching the orifice and to the incorrect assumption that these particles will be travelling at the fluid velocity. Values of the sensitive distance obtained with the smaller particles have been taken as more representative of the above theory.

These values for the sensitive distances have been substituted in the equations presented above and estimates of the occurrence of the singlets, intermediate doublets, doublets etc. made for a series of initial particle concentrations. The results are presented in a series of tables XIII, XIV, XV, XVI. These tables illustrate that the probability of coincidence is not only a function of concentration of the particles but is also a function of the orifice tube diameter. Moreover, it illustrates that particles not counted as single particles will be

148.

counted as multiple particles and so that the distribution obtained from the counting of concentrated suspensions may well be in serious error. The tables estimate the probable extent of that error.

5.4.7   Use of a Multichannel Pulse Height Analyser

Whilst there exists a Coulter Counter which will divide a distribution into 15 channels (Model T), this is not yet available in the U.K. and so could not be evaluated. Ideally however, the voltage pulse obtained when a particle passes through the orifice across which a constant current is maintained should be divided into a larger number of channels. A convenient instrument is the Lætern Pulse Height Analyser which will analyse the pulses into 100 channels.

However, the analyser has a unique analogue to digital converter sequence which makes it superior to other types of analyser   See supplement.

In collaboration with the manufacturers a suitable interface has been designed which will permit the instrument to accept the long pulses and also to permit the voltage level across the 100 channels to be adjusted to a convenient level.

The experimental arrangement has so far proved satisfactory. The time for a complete analysis is short of 20-30 secs. and shows that this instrumental set-up is ideal for rapid particle size analysis. However, there is a need for the comparison between particle size analyses obtained on this instrument and those obtained on the conventional Coulter Counter.

Because the Coulter principle measures the particle volume a 100 channel analyser is restricted in the range of particle diameters that can be resolved accurately because of the scale compression at the lower size end. In order to overcome this, a logarithmic amplifier preceeded by an impedance converter has been placed between the Coulter orifice and the multichannel analyser. This arrangement increases the input impedance of the amplification chain to $\sim 20M\Omega$ which facilitates the use of non-aqueous electrolyte systems as are necessary when analysing mineral oil base fluids.

A further logarithmic stage would enable a cube root of the pulse height to be analysed thus giving a linear scale in terms of equivalent spherical diameter.

149.

5.4.8 Summary and Conclusions

The response of a Coulter Counter to spherical particles has been examined and it has been found that the peak resistance change of the orifice is a linear function of particle volume up to 50% of the orifice diameter. However, the resistance begins to change as the particle approaches the orifice. The effect of this resistance change as two or more particles approach with different separations has been measured and it has been illustrated how complex pulse shapes can be obtained.

The change in resistance in response to the approach of particles has been classified into four main areas and the probability of occurrence of each event has been calculated. Estimates of the critical lengths have been obtained for a series of orifice diameters. These results are presented in tabular form and illustrate that the problem of coincidence is not only the problem of lost counts as previously considered but is really the problem of the distortion of the particle size distribution obtained due to the additive responses that can be obtained. The analysis has only been applied here to monosized particles. The analysis will be more complex with many sized particles as there will be more possibilities of additive response. However, the general solution will still apply. The easiest way of reducing the problems associated with coincidence is to count with a low concentration suspension and this will be true for multi-sized dispersions as well as mono-sized dispersions and the tables presented can be used to select acceptable concentration levels.

A suitable interface has been designed to enable the orifice 'transducer' to be connected to a pulse height analyser and tests indicate that the arrangement is suitable. Further work is proceeding.

150.

Bibliography - Section 5.4

(1)   Mattern C.F.J. and Brackett F.S., Olsen B.J.   J.Appl.Physol. 1957 10, 50.

(2)   Wales M., Wilson J.N., Rev.Sci.Inst. 1961 32 1132.

(3)   Kubitschek H.E.,   Research 1960, 13 128.

(4)   Princen L.H., and Kwolek W.F., Rev.Sci.Inst. 1965 36 646.

(5)   Edmunson I.C. Nature.1966, 212, 1450

(6)   Batch B.A.   J.Inst. Fuel 1964, 37 455.

(7)   Gregg E.C., Steidley K.D.   Biophys. J. 1965 5 393.

(8)   Allen T.   Proc.S.A.C. Conference on Particle Size Analysis 1966.

(9)   Eckoff, R.K.   J. Sci. Inst. 1969 2.

(10)   Grover N.B., Nauman J., Ben-Sasson, S., Doljanski F., Biophys. J. 1969,
                                                    9 1398.

(11)   Grover N.B., Nauman J., Ben-Sasson, S., Doljanski F., Nadev E.,
        Biophys. J. 1969 9 1415.

(12)   Lines R.W.   Private Communication.

TABLE XII

Analogue Response to Single Spheres

Particle diameter cms	Particle diameter / Orifice diameter	Particle volume ml	Peak response mv 1	Length of response 1 $^{c}\mu$
1.2	.105	0.9	0.9	-
2.0	.175	5.1	5.2	-
3.0	.264	13.5	12.4	-
3.36	.295	20	17.0	34
3.86	.339	30	29.0	36
4.24	.372	40	37.0	39
4.50	.395	50	44.0	43
5.76	.505	100	99.0	46
6.60	.579	150	150.0	46
7.26	.637	200	210.0	48
8.30	.728	300	324.0	49
9.10	.808	400	450.0	50
9.84	.863	500	620.0	50
10.46	.918	600	750.0	50

1.   Analogue current maintained at 0.5 amp.

152.

TABLE XIII

Length of Sensitive Regions

Orifice Diameter	Depth of Hole	Sensitive Region (1 mμ			
μm	2 μm	pollen 3.13μm	pollen 13.5μm	pollen 27.3μm	pollen 42.5μm
70	48.0	172.8	193.1	675.9	-
140	55	-	199.8	279.8	549.5
200	90.0	-	209	209	313
280	115.0	-	-	259.8	417.5

153.

TABLE XIV

Coincidence Effects for 140μm Tube

No/cc	1000	3000	5000	10,000	30,000	50,000	100,000	300,000
Singlets	993.9	2945.0	4848.2	9402.1	24,934.3	36,376.3	53,982.3	47,192.8
Intermediate Doublets Class III	3.9	34.6	94.7	365.3	2,843.4	6,834.7	19,085.8	42,110.0
Intermediate Doublets Class IVa	-	0.2	1.0		179.9	693.2	3,514.7	15,969.0
Intermediate Doublets Class IVb	-	0.1	.4	3.1	71.3	283.1	1,548.3	9,439.2
Doublets	.8	7.5	20.5	79.2	624.9	1,521.6	4,379.1	10,578.6
Intermediate Triplets Class IVc	-	0.1	.4	3.1	71.3	283.1	1,548.3	9,439.2
Triplets	-	-	-	0.3	7.9	32.0	182.6	1,285.7
	-	-	-	-	etc.	etc.	etc.	etc.

154.

TABLE XV

Coincidence Effects for 200.0μm Tube

No/cc	1000	3000	5000	10,000	30,000	50,000
Singlets	987.0	2,884.7	4,684.0	8,775.8	29,275.7	26,025.3
Intermediate Doublets	9.2	82.0	224.1	857.2	6,371.1	14,276.8
Doublets	2.7	24.3	65.7	244.5	1,647.7	3,428.6
Intermediate Triplets	–	.7	3.0	22.5	438.9	1,475.2
Triplets	–	.1	.5	3.4	68.8	236.5
	–	–	–	etc.	etc.	etc.

155.

TABLE XVI

Coincidence Effects for 280μm Tube

No/cc	1000	3000	5000	10,000	30,000	50,000
Singlets	974.7	2,778.3	4,399.4	7,741.7	13,920.0	13,904.8
Intermediate Doublets	19.5	170.3	457.8	1,677.5	10,194.4	18,360
Doublets	6.9	58.4	152.9	528.9	2,662.3	4,143.3
Intermediate Triplets	.1	3.4	15.0	102.3	1,478.4	3,717.0
Triplets	-	.6	2.7	18.5	272.6	689.8
	-	-	etc.	etc.	etc.	etc.

5.5 Automated Particle Size Analysis Using a Digital Computer

5.5.1 Summary

A Research programme has recently been started at Loughborough with the object of developing improved methods of automatic particle size analysis.

This paper discusses preliminary work on an image analysing system that is based upon digital computation and shows how this system can be used for particle sizing.

The images from optical, and electron, microscopes are suitable starting points for particle size analysis. These images, however, contain ambiguities which may be easily dealt with by human operators but not by existing automatic analysers. The data processing capability of the digital computer and its memory are important assets for an image analysing system.

An image scanner is described whose motion can be controlled by digital means and which supplies data that completely defines the projected areas of particles in the field of view.

5.5.2 Introduction

The derivation of various particle parameters from measurements obtained by visual examination of a sample through a microscope is a well established technique. The main drawback is the tedium involved in making these measurements. A great deal of effort has therefore been expended by many workers with the object of automating the measurement process. A number of commercial instruments have been produced but these have achieved varying degrees of success.

The need for automatic particle size analysis, is based upon visual examination, is as important as ever and the present project is an attempt to improve upon existing techniques.

A major problem that has to be overcome in an automatic system is the need to handle large quantities of data. The basic weakness of existing equipment is that the data is derived and processed using analogue computer techniques. Digital data handling, if it is used at all is only utilised at the end of the system after the primary measurements have been made and the format of the data frozen.

157.

Although analogue circuits have a very high data processing rate they suffer from the following limitations.

(a) the equipment increases in size as the number of operations, in a calculation, increases

(b) only very limited data storage is possible if cost is to be minimised

(c) they are not as reliable or as precise as digital equipment

(d) if the calculations are modified then extensive re-construction of the equipment will be necessary.

The value of digital circuitry, and computation, for image processing has already been demonstrated in systems handling cloud cover pictures and identifying man-made objects on aerial photographs.   Additional techniques, relevant to automated particle sizing, have been developed by researchers concerned with machines for computer recognition of texts composed of handwritten, or printed characters.
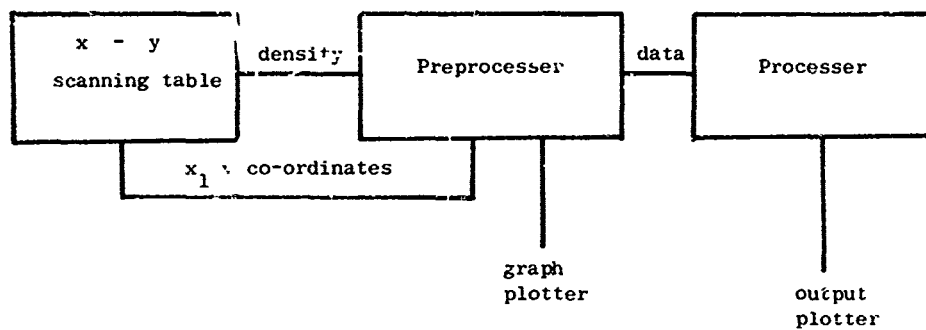
Functional blocks of an automatic image analyser

FIGURE 57
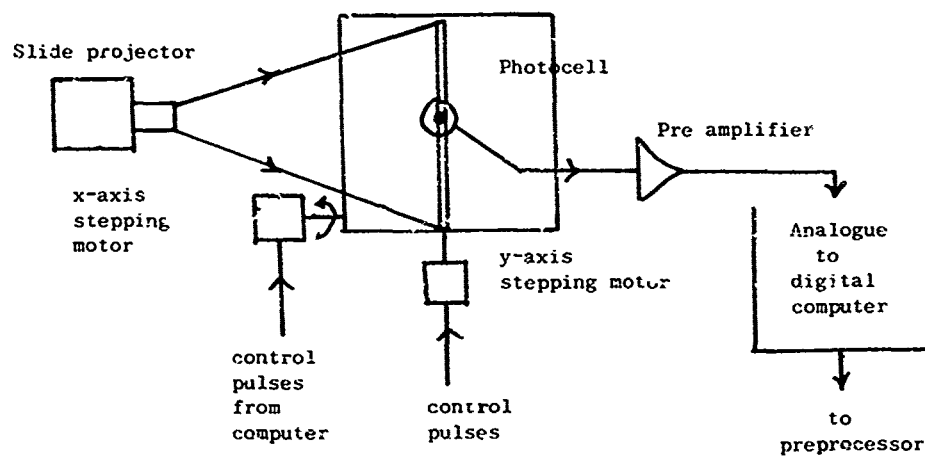
Image Scanner

FIGURE 58

159.

The methods being developed at Loughborough for size analysis are based upon knowing the X, Y coordinates and image density of any point of interest in the image plane. This is subject to a limit of resolution fixed by dividing the image plane into a matrix of square size 400 x 400. The availability of such data means that the perimeter of every particle, in the sample being analysed can be precisely specified. Using this data any desired particle, or population parameter can be computed as long as it has been defined in terms of projected area lengths.

Automated size analysis can be considered under the following headings:

1. Obtaining an image for scanning
2. The scanning equipment
3. Data processing

5.5.2 (i) Obtaining an image

The success, or failure, of the automatic process depends to a large extent upon the quality of image that can be produced from the original particles. Ideally the image should consist of absolutely sharp black objects on a white background or white objects on a black ground. This ideal is, of course, rarely attained.

In the present work an image is formed by projecting a photographic negative of the sample onto the measuring plane of the image scanner. The photographic film is processed to obtain maximum contrast and the projected image is 20 inches square.

5.5.2 (ii) The scanning equipment

The image processing system can be sub-divided into the blocks shown in fig.1.

5.5.2 (ii) a The scanner

At present the outward form of the scanning equipment being used has been dictated by financial limitations but it does, however, contain all the required facilities. A diagram of the equipment is given in fig. 58.

The image scanner is basically a modified X-Y plotting table, fitted with a photocell in place of a pen, linked to a digital computer. At present the computer is being used as a development tool since some of its tasks would be more suitably carried out by special hardware in a final system.

160.

The computer is programmed to:

(a)   position the photocell by sending pulses to the motors

(b)   read the analogue output of the photocell and convert this into a digital number.

(c)   pre-process the photocell readings.

A scanning motion made up of a series of parallel straight lines that cover the field of view is extremely efficient for size analysis. The angular orientation of the scan to the particles can be varied either by rotating the slide or by changing the ratio between the horizontal and vertical increments for the stepping motors.

A scan starts in the bottom left hand corner of the image. After each reading of the image density, the position of the photocell is advanced by one increment in the scan direction. When the end of a scan line is reached, the Y-axis motor is advanced and the X-axis scan re-started. The advantage of using incremental positioning of the photocell is that the X, Y coordinates are readily available in digital form for each measured value of image density.

Interleaved with the program for positioning the photocell and reading the photocell output is a ; ogram which carries out some preliminary processing.

This pre-processing routine detects particle edges and measures the particle interceptions with each scanned line of the image field.

The simplest form of boundary detection is to use a fixed reference density to determine whether the photocell is currently positioned on a particle or the background. This procedure has been used in many automatic instruments and is used in the present project when the image contrast is adequate and no anomalies are present.

The reference level is chosen by making a number of exploratory traverses across the image, recording the photocell output with a chart recorder, and deciding on a suitable value after visual examination of the results.

Once the photocell has traversed a particle, the X, Y coordinates of its initial intersection with the line of scan are recorded together with the length of the intersection.

Since each particle intersects an appropriate number of scan lines, and all of these intersections are recorded, its two dimensional projected image in the plane of the photographic emulsion is fully defined in terms of X,Y coordinates and chord lengths.

5.5.2 (ii) b The processor

Typical output data from the preprocessor are given in table XVII pictorially in fig. 59   The essential difference between the table and the figure, however, is that in fig. 59   the re-recording onto X,Y coordinates was established for a human observer which chord belongs to which particle   Table XVII gives the data as it is held in the computer core store and it is not apparent to the machine which chords constitute a particular particle.

The first routine in the processor is therefore a sorting routine to find out how many particles there are and which chords belong to each particle. The criterion for determining the association of chords with particles is shown in fig. 60.

5.5.3 Computation of size parameters for individual particles

Table XVII lists the chords for the particle shown pictorially in Fig. 61 The boundary of this particle is defined, in terms of X,Y coordinates only, in Table XIX   Table XIX is computed by using the length of a chord and its X,Y co-ordinates at the left hand end to obtain the right hand coordinates.

162.

TABLE XVII   Output from preprocessor for particles in Fig. 59

X	Y	L	X	Y	L	X	Y	L	X	Y	L
153	2	7	127	25	34	4	35	20	160	41	13
149	3	14	61	26	13	61	35	13	4	42	30
145	4	20	128	26	34	120	35	36	122	42	29
142	5	23	58	27	17	161	35	7	162	42	11
142	6	24	125	27	37	4	36	22	4	43	30
140	7	27	59	28	17	63	36	11	122	43	28
141	8	27	126	28	36	121	36	36	161	43	12
139	9	29	58	29	19	161	36	10	5	44	32
140	10	30	124	29	36	3	37	24	123	44	27
138	11	32	12	30	2	65	37	9	163	44	10
138	12	32	60	30	18	120	37	34	5	45	31
135	13	34	124	30	37	160	37	13	122	45	26
134	14	35	7	31	12	5	38	24	163	45	10
133	15	35	60	31	17	65	38	8	7	46	31
133	16	35	122	31	37	122	38	32	123	46	25
131	17	35	7	32	14	160	38	13	165	46	8
132	18	34	61	32	17	4	39	25	7	47	31
129	19	35	123	32	36	65	39	5	123	47	24
131	20	35	5	33	17	121	39	31	165	47	8
129	21	34	60	33	16	159	39	14	8	48	31
130	22	33	121	33	37	5	40	26	124	48	24
62	23	3	163	33	4	68	40	2	166	48	7
129	23	33	5	34	19	122	40	31	9	49	29
63	24	7	62	34	15	161	40	12	124	49	3
130	24	32	121	34	37	4	41	28	131	49	15
61	25	10	163	34	6	122	41	28	168	49	3

163.

Y AXIS

X-AXIS

Scan Using 05 Increments

Scan using 05 Incroments
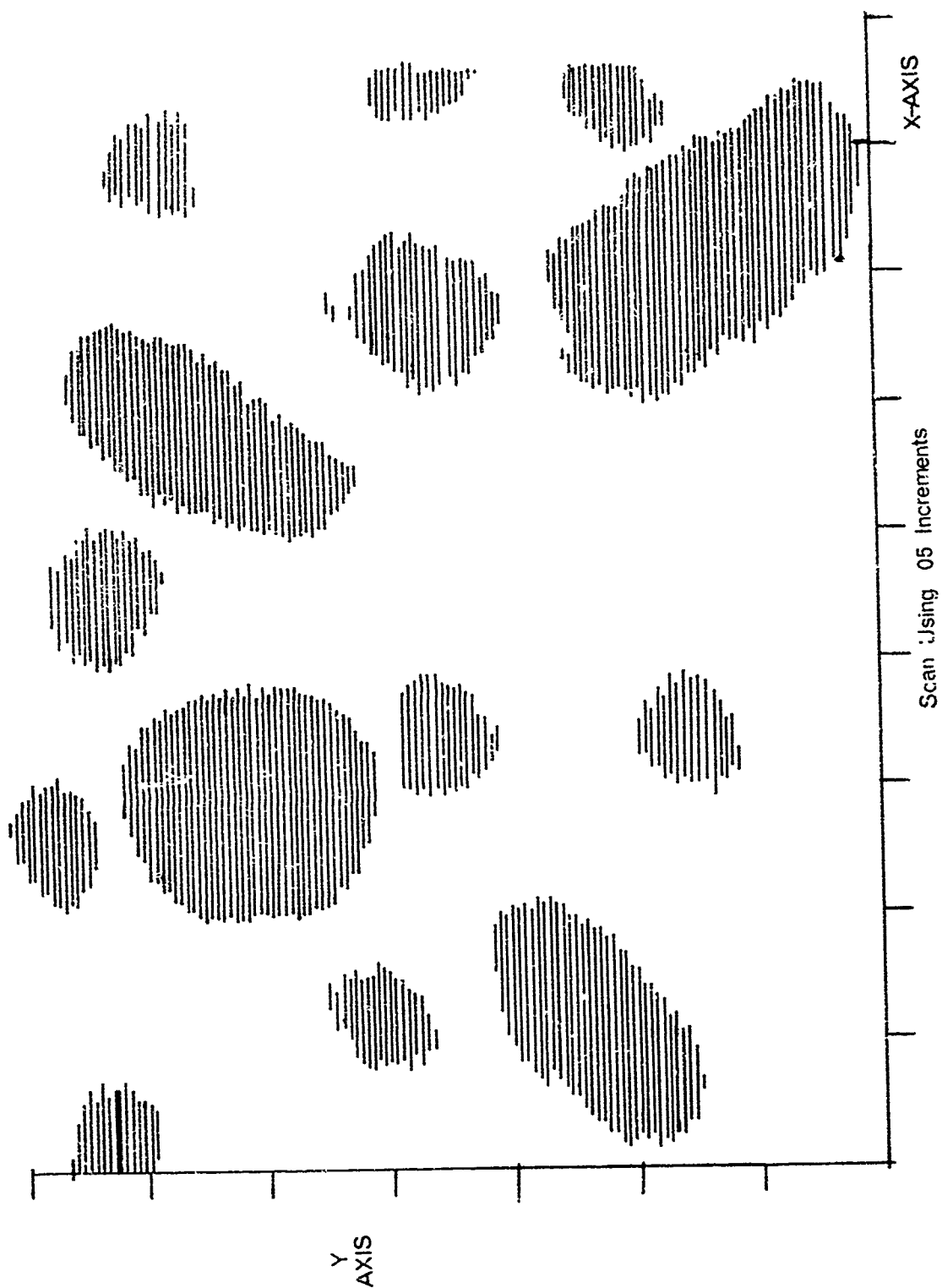
FIGURE 59   Scan using 05 Incroments

164.

$$\overset{\xleftarrow{\hspace{1em}\ell_2\hspace{1em}}}{\underset{(x_2y_2)}{\text{X}\rule{3cm}{0.4pt}}}$$

$$\overset{\xleftarrow{\hspace{0.5em}\ell_1\hspace{0.5em}}}{\underset{(x_1y_1)}{\text{X}\rule{2cm}{0.4pt}}}$$
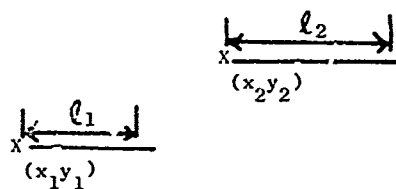
These chords belong to separate particles since x does not equal x and in fact is less than x_2. Also ℓ_1 is not long enough 1 to overlap x_2. 2

$$\underset{(x_2y_2)}{\text{X}\ \underline{\ \ell_2\ }}$$ $$\underset{(x_1y_1)}{\text{X}\underline{\quad\ell_2\quad}}$$
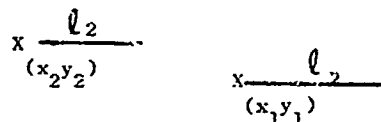
still separate particles since

$x_1 \not> x_2$ and L_2 still too short

$$\text{X}\ \underline{\quad\ell_1\quad}\ \overset{\text{X}\ \underline{\ell_2}}{}$$
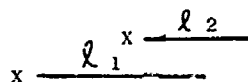
same particle since ℓ_1 is long enough to cause overlap

$$\text{X}\underline{\quad\ell_2\quad}$$
$$\text{X}\ \underline{\quad\ell_1\quad}$$
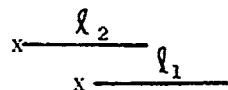
same particle since ℓ_2 is long enough to cause overlap

$$\text{X}\ \underline{\qquad\ell_3\qquad}$$
$$\text{X}\underline{\ \ell_1\ }\qquad\text{X}\underline{\ \ell_2\ }$$
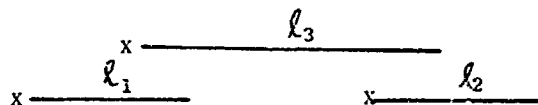
A re-entrant case since ℓ_3 is long enough to joing ℓ_1 and ℓ_2

FIGURE 60   Associating chords to form particles

TABLE XVIII   Chords for particles shown in Fig. 61.

(increments of 0.1 " for X and Y)

X	Y	L
77	1	7
74	2	11
73	3	13
73	4	14
72	5	16
71	6	16
69	7	18
68	8	18
67	9	17
67	10	17
67	11	16
66	12	17
65	13	18
65	14	18
63	15	19
63	16	19

X	Y	L
63	17	18
63	18	17
63	19	16
64	20	15
63	21	14
64	22	13
63	23	13
65	24	11
69	25	6
73	26	1

166.
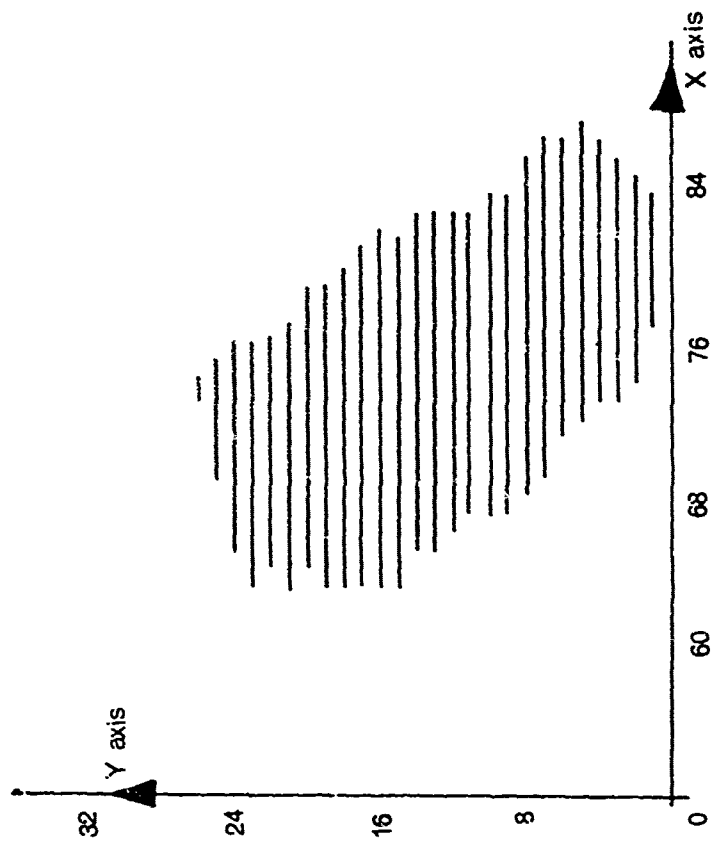
FIGURE 61   Chords for a single particle

167.

TABLE XIX

The boundary of particles (Fig. 61) in terms of x, y co-ordinates

X	Y	X	Y	X	Y	X	Y	X	Y
77	1	65	14	74	26	83	13	83	1
74	2	63	15	75	25	83	12	82	1
73	3	63	16	76	24	83	11	81	1
73	4	63	17	76	23	84	10	80	1
72	5	63	18	77	22	84	9	79	1
71	6	63	19	77	21	86	8	78	1
69	7	64	20	79	20	87	7		
68	8	63	21	79	19	87	6		
67	9	64	22	80	18	88	5		
67	10	63	23	81	17	87	4		
67	11	65	24	82	16	86	3		
66	12	69	25	82	15	85	2		
65	13	73	26	83	14	84	1		

Once a particle boundary has been defined by a set of X, Y coordinates it is possible to compute any defined parameter. Such parameters might be

3.1.1   The diameter of the circle of equal projected area

3.1.2   The diameter of a circle having the same projected perimeter

3.1.3   The Feret diameter for any viewing angle in the 2-D plane

3.1.4   Martin's diameter

(a)   Circle of equal projected area

The projected area of the particle is given by

$$A = \left(\sum_{1}^{N} \ell_n \right) I$$

where ℓ_n = length of the n th chord in terms of x-axis increments

     N = the total number of chords for the particle when scanned using x and y increments of size I

The circle of same projected area is given by

$$d_a = \sqrt{\frac{4A}{\pi}}$$

(b)   Circle of equal projected perimeter

The perimeter of a particle P (fig. 62) can be found using the set of X, Y coordinates defining the particle edge. The circle of equal projected perimeter is then given

$$d_p = \frac{P}{\pi}$$

(c)   Feret diameters

Feret's diameter can be readily calculated for a viewing axis which is parallel to either the x or y axis. Fig. 63 illustrates these situations. If the viewing axis is parallel to the y-axis then Feret's diameter is given by

$$d_f = (x_2 - x_1)$$

169.

point x, y, on the particle perimeter is the point with the smallest x-co-ordinate and the point $x_2 \ y_2$ is the point with the maximum x-coordinate.

When the viewing axis is parallel to the x-axis the points are chosen on the basis of minimum and maximum y-coordinates.

(d) <u>Martin's diameter</u>

The area of a particle in terms of increments is given by

$$A = \sum_{1}^{N} \ell_n$$

FIGURE 62
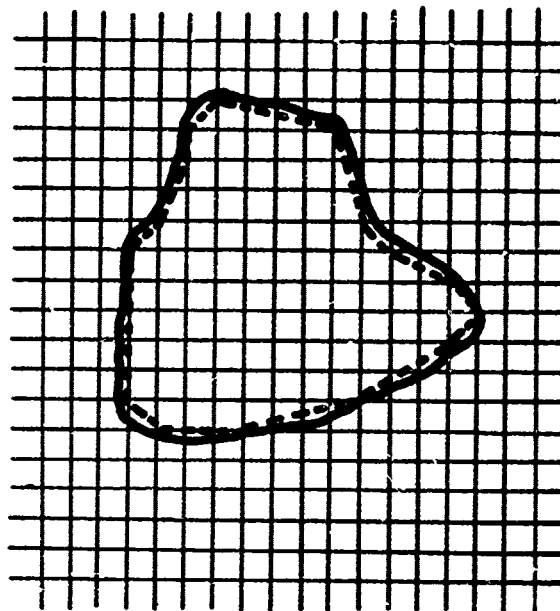
Perimeter of a particle

Accuracy depends upon the ratio between the x, y increments and the particle itself.

$$P = \sum_{i=1}^{N} d_n$$

where

$$d_1 = \sqrt{(x_1 - x_2)^2 + (y_1 - y_2)^2}$$

$$d_2 = \sqrt{(x_2 - x_3)^2 + (y_2 - y_3)^2}$$

etc

Feret Dia.
given by
$$(x_{max} - x_{min})^i$$

Feret Dia

given by

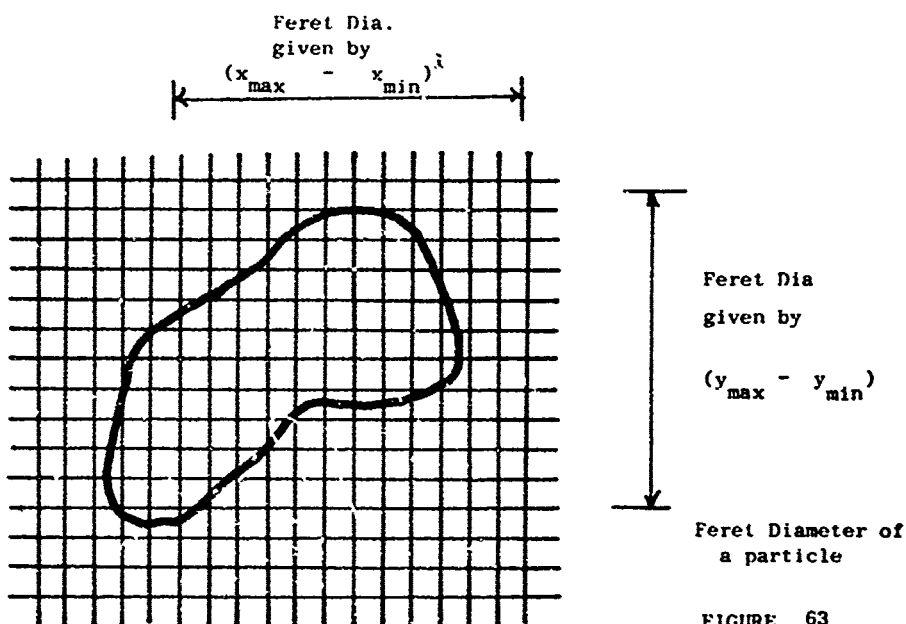$$(y_{max} - y_{min})$$

Feret Diameter of
a particle

FIGURE 63

171.

Therefore to find the Martin's diameter parallel to the x-axis it is only necessary to find the r th chord where

$$\frac{A}{2} = \sum_{1}^{r} \ell_n$$

The computation of Martin's diameter when the viewing axis is parallel to the x-axis requires slightly more work. A set of chords for a scan direction parallel to the y-axis must be computed using the initial set of chords. After this the calculation is the same as before.

5.5.4 Population parameters

The commonly accepted frequency distributions for the scanned sample can be computed from the results for individual particles. Since the total number of particles on the slide has already been computed it is straightforward calculation to obtain t'e mean value and standard deviation.

5.5.5 Conclusion

At present the procedure for size analysis using the automated procedure is:-

(a) photograph the sample using either a microscope or direct photography with a camera.

(b) project the negative and, using the data from the scanner and pre-processor generate the type of drawing shown in fig. 59. This is done automatically with an incremental graph plotter.

(c) use the main processing programme to compute the relevant parameters.

Our entire system obviously requires much effort before we can feel satisfied with it. Apart from changes in the outward form of the hardware the software must be improved. Some particular areas of interest are:-

(a) touching particles

(b) filtering out the effect of dust and scratches

(c) particles surrounded by a halo or containing areas of the same contrast as the background.

(d) better methods for edge detection

(e) on-stream three dimensional analysis

172.

Chapter 6

Filtration

173.

6.1.   Introduction

Filtration is a means of separating solids from liquids and is made use of
in hydraulic systems to remove contaminant particles from the hydraulic oil. Many
parameters are involved in this operation and the design of filtration equipment is
an attempt to optimise these for a particular situation. This chapter consists of
two sections, the first using the technique described in chapter 4 to describe the
flow of liquid through a porous bed which could be either a filter cake, filter
medium or combination of the two. The second section proposes a retention efficiency
curve for characterising the efficiency of a filter and describes how this curve may
be obtained.

The pressure distribution in a bed of particles is complex and is amenable
to control for two main reasons. On a particulate scale, the force is handed on
from particle to particle through the point contacts. An individual particle may
deform elastically, plastically or it may fracture. Its behaviour will depend upon
its own size and geometry, its own physical properties and those of its surrounding
neighbours. Thus, the pressure distribution in a bed can be greatly controlled by
changing the form of the original particles or alternatively mixing in other
particles. This is the process which is commonly known as pretreatment.

On a more macroscopic scale, the pressure distribution is completely con-
trolled by the geometry of the equipment. Whenever there is a solid boundary, the
pressure distribution is redistributed due to friction against the boundary and there
is here great scope for more sophisticated design of filtration equipment where
traditionally almost all of the mechanical pressure is allowed to be transmitted to
the septum.

The movement of particle beds would seem to be important in the design of
filtration equipment also for two reasons. Firstly, the pressure distribution in a
static bed of particles is immediately changed when the bed starts to flow. More
important, the residual moisture in a dried cake is held in the form of pendular
moisture at the point contacts. It is clear that if this moisture is to be further
reduced substantially, then the particles must move relative to each other and thus
release this moisture. The relative movement can be caused by a variety of forces,
for example body forces, mechanical shear forces or vibration.

174.

The third mechanism which would seem to be of interest to filtration engineers is that of explaining the complex fluid flow patterns in a separation system. For example, the fluid flow pattern in a deep bed filter must clearly be contrived to bring each particle into contact with a solid surface. Thus, a tortuous bed is required rather than straight channels and a precise description of the fluid flow pattern in terms of the pore distribution is required. This description is also necessary for those types of separator, such as centrifugals, in which the particle trajectories are calculated on the assumption that the pressure of the particles does not disturb the fluid flow pattern. It is known that at very modest concentrations that the pattern is disturbed and that return flow occurs but this cannot yet be predicted quantitatively.

In the following section an example is given of the type of statistical solution which can be made of fluid flow patterns. In this type of solution, it is not necessary to be able to calculate the velocity and pressure at each point in a system. Quite simple geometries pose major mathematical problems in order to obtain a classic solution of this kind. However, a statistical solution deals only with a knowledge of the distribution curve of the variables and in many cases only the mean values. This approach has been accepted for many years in describing the properties of a gas by the kinetic theory. However, in that case the geometry of the container is not important. Starting with a statistical characterisation of the geometry such as proposed in 4.1 this can be effected.

6.2. Viscous Flow of Fluid in an Irregular Pipe

6.2.1. This technique of characterising a void space will first be applied to a pipe which is irregular in cross-section but which is straight. In this case, the fluid velocity and the pressure gradient lie in the same direction at all points and are both parallel to the axis of the tube. It is only necessary to consider the effect of the shape of the cross-section on the flow pattern and the filaments will only be drawn within the plane of this cross-section. The filaments will be drawn in every possible direction within this plane but the distribution will be normalised so that first moment of the distribution is proportional to the cross-sectional area, A, of the pipe. Thus, for all the filaments lying in any one direction

$$\int_{\Delta t} \mathbf{N}(J) \, J \, dJ \quad = \quad A \qquad \cdots \cdots \cdots \quad 6.2.1$$

where

$$\Delta t \quad = \quad \text{thickness of the filaments}$$

$$J \quad = \quad \text{length of filament}$$

$$\mathbf{N}(J) \quad = \quad \text{number distribution of filaments}$$

When the distribution of filaments is plotted for all possible directions it will be normalised back to conform with equation 6.2.1.

The pressure gradient is equal at all points in the cross-section and is given by the equation:

$$- \frac{1}{\mu} \frac{dp}{dz} \quad = \frac{d^2 u}{dx^2} \quad + \quad \frac{d^2 u}{dy^2} \qquad \cdots \cdots \cdots \quad 6.2.2$$

Consider a filament AB, lying in the cross-section of the channel as shown in Fig. 64. The velocity, u, of the fluid varies with position along the length of this filament and may be plotted as a velocity profile stretching between points A and B. It is tacitly understood that the velocity is perpendicular to the cross-section and, therefore, may be considered to be a scalar quantity within the plane of the cross-section. The first and second gradients of the velocity are, however, parameters which vary along the line AB and which determine the shape of the velocity profile between AB. Considering now the fluid to be flowing through all the possible filaments, any element of fluid is passing through an area in which there is a statistical distribution of three parameters which are velocity and the first and second gradients of that velocity. For convenience we shall denote $\frac{du}{dx}$ by $\overset{\bullet}{u}$ and $\frac{d^2 u}{dx^2}$ by $\overset{\bullet\bullet}{u}$. It
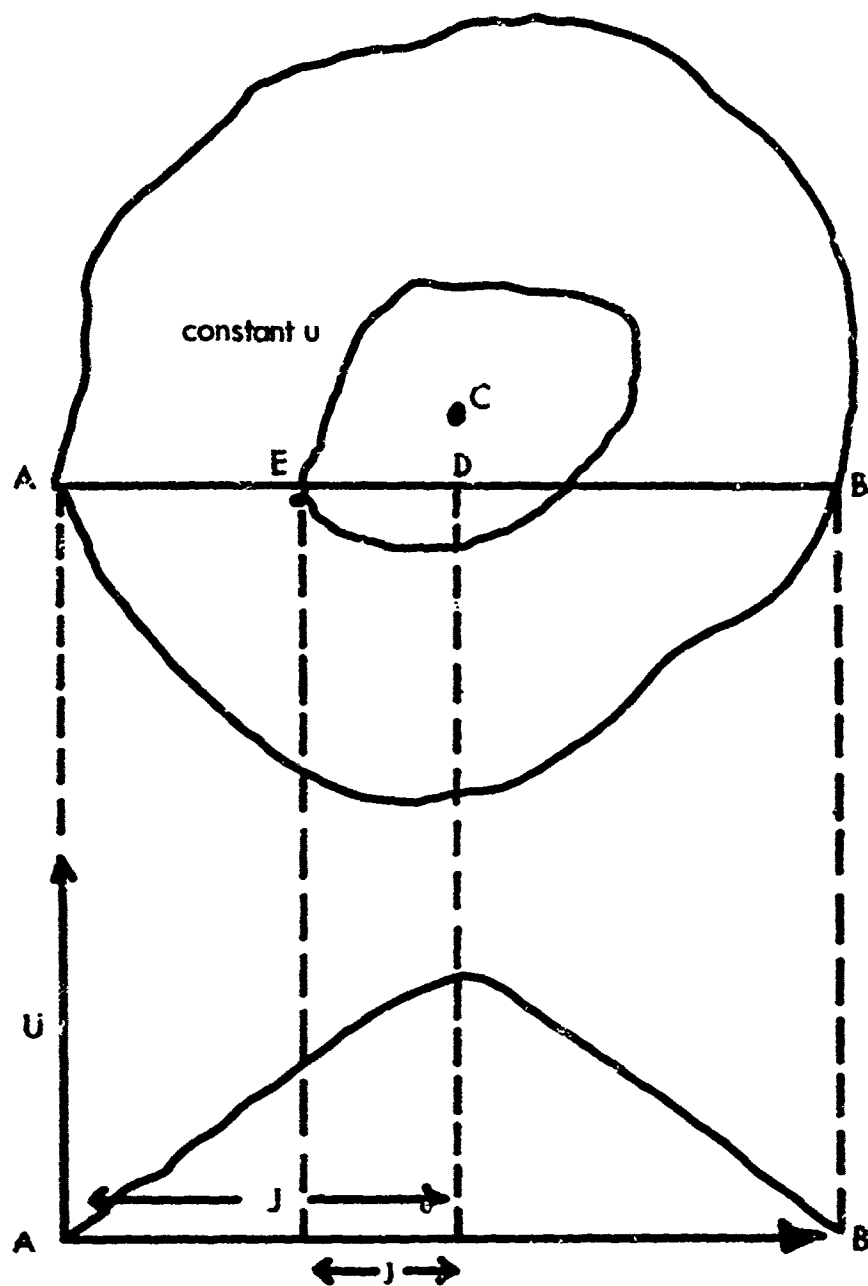
176.

constant u

FIGURE 64   Flow profile in an irregular pipe

177.

is emphasised that this in no way implies a variation with time but, in this context, is used to denote the gradients of a velocity profile which is itself a section of the total velocity profile. Each of the three parameters has a distribution function which expresses the probability of finding a particular value of the parameter at some point on one of the filaments. These distributions are illustrated in Fig. 65.

The velocity u will at all points be positive, the distribution of the first gradient will be symmetrical about the origin and the second gradient will be at all points negative if they are measured in a consistent direction.

The total area under each distribution function must be the same since it is equal to the total length of line contained in this area.

Thus:-

$$\int_{all\ A} p\ (u)\ du = \int_{All\ A} q\ (\ddot{u})\ du = \int_{All\ A} r\ (\ddot{u})\ d = \frac{A}{\Delta t}$$

Where Δt = the thickness of one filament.

We shall show that since the three fields must fit together into the same space, it is possible to relate the mean velocity to the mean value of the second differential by relating each to the first differential. Thus, the relationship between the flowrate and pressure drop in the channel will be deduced, since the second differential is related to the pressure gradient by (6.2.2.). Since the filaments traverse the area in every possible direction then the x - y co-ordinates are no longer relevent, and we shall consider the distance along a filament from some reference point to be the only co-ordinate. This distance will be denoted by x.

When all the possible filaments are drawn in the cross-section, each point is traversed once and only once in each direction. Since the pressure gradient, $\frac{dp}{dz}$ is also a constant at every point, then equation 3 reduces to:-

$$\frac{\overline{d^2 u}}{dx^2} \qquad \frac{\overline{d^2 u}}{dy^2} = -\frac{1}{2}\ \frac{1}{\mu}\ \frac{dp}{dz} = \overline{\ddot{u}} \quad \dots\dots\dots \quad 6.2.3.$$

where the bar denotes the average value of the second gradient taken over all directions. This relationship applies to any smaller area drawn within the cross-section which is tranversed by filaments in every direction.
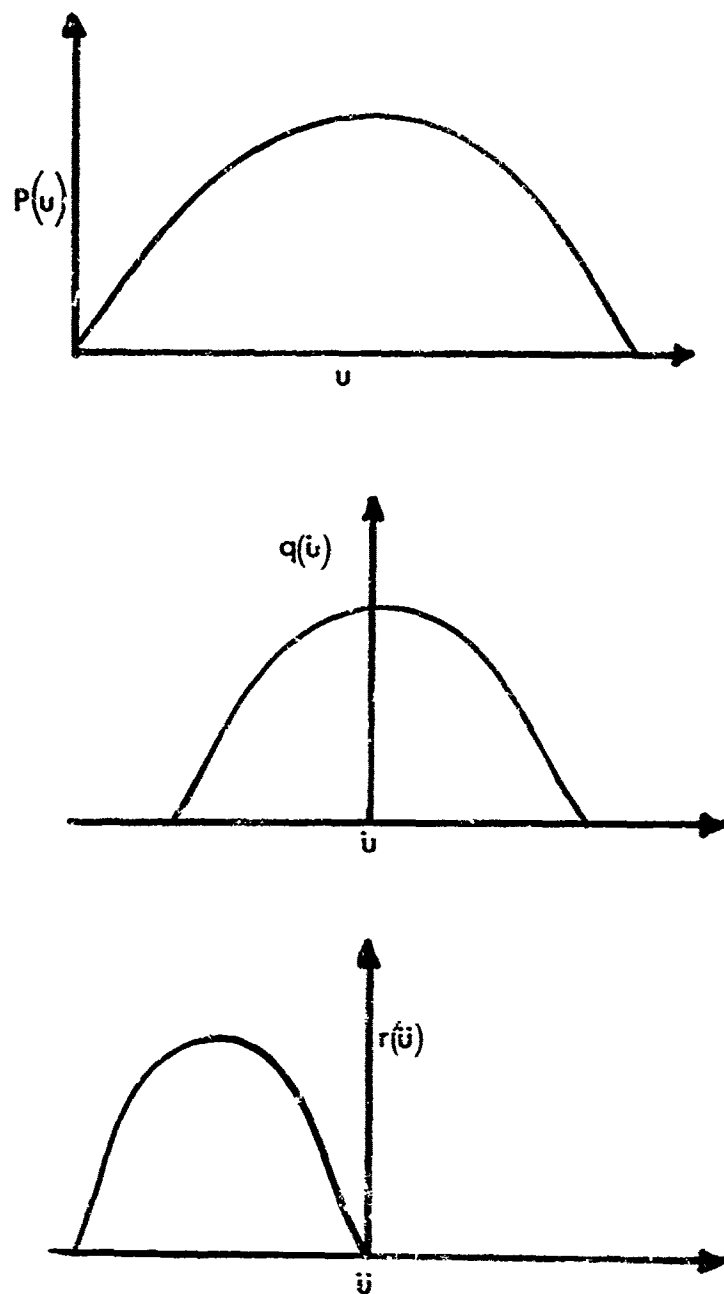
178.

FIGURE ·65   Velocity distribution and its derivatives in an irregular pipe

In order to choose the reference point, consider again the velocity profile shown in Fig. 64 stretching between two points AB. We then know two facts. Firstly that the velocity is zero at points A and B. Secondly, that there must be some intermediate point at which the first gradient is zero and hence the velocity is a maximum. This point will be denoted D and will be taken as the reference point for this filament. The reason for this is that the second gradient can be integrated along the filament from this point to any other point to give the first gradient.

The velocity is a maximum at this point only for this particular filament. For the other filaments which traverse the same point in a different direction it will not be the maximum point except for the special point which is the point of maximum velocity for the whole profile. In this derivation, only channels which have a single point of maximum velocity, C, are considered. Channels which are very complex in shape may have several such points and the implication of this is that some of the filaments will have several maxima in their velocity profile.

The mean value of the second gradient which is proportional to the pressure gradient by equation 6.2.3., will now be related to the mean velocity. Consider the point E on the line AB which is distance j from the reference point D.

$$\text{Then:-} \qquad -\dot{u}j \qquad = \int_{o}^{j} \ddot{u}\ dx \qquad \cdots\cdots\cdots \quad 6.2.4$$

where $\dot{u}j$ is the first gradient of the profile at point E. Considering still Fig. 64 draw a line of constant velocity, u, which encloses a portion of the cross-section and allow this area to be traversed by all the possible filaments in every direction. Then the relationship given in (6.2.4) applies to each of these filaments. However, each filament is divided into two parts by a point corresponding to point C and the sectioned filaments will have a number distribution function which can be denoted by n, (j), j . Then summing equation over all the section filaments:-

$$-\int_{\text{all } j} n\ (j)\ \dot{u}_{j}\ dj \quad = \quad \int_{\text{all } j} n\ (j) d\ j \ \text{\tiny $\cdot$} \int_{o}^{j} \tilde{u}\ dx$$

$$\therefore \quad - \frac{\displaystyle\int_{\text{all } j} n\ (j)\ \dot{u}_{j}\ dj}{\displaystyle\int_{\text{all } j} n\ (j)\ j\ dj} \quad = \quad \frac{\displaystyle\int_{\text{all } j} n\ (j) d\ j \ \text{\tiny $\cdot$} \int_{o}^{j} \tilde{u}\ dx}{\displaystyle\int_{\text{all } j} n\ (j) j\ dj}$$

180.

The right hand side of this equation is simply the second gradient integrated along all the filaments divided by the total length of filament.

$$\therefore \quad -\frac{\int\limits_{all\ j} n(j)\ \ddot{u}_j\ dj}{\int\limits_{all\ j} n(j)\ j\ dj} \quad = \quad \ddot{u} \quad = \quad constant$$

$$\therefore \quad -\frac{\int\limits_{all\ j} n(j)\ \dot{u}_j\ dj}{\int\limits_{all\ j} n(j)\ dj} \quad = \quad \frac{\bar{\ddot{u}} \int\limits_{all\ j} n(j)\ j\ dj}{\int\limits_{all\ j} n(j)\ dj} \quad = \quad \bar{\ddot{u}}\ \bar{j}$$

The term $\bar{j}$ is the average length of the sectional filaments.

The left hand side of this equation is the average value of the first gradient at the ends of the filaments.

$$\therefore \quad -\ \dot{u}_j \quad = \quad \bar{\ddot{u}}\ \bar{j} \qquad \bullet\bullet\bullet\bullet\bullet\bullet\bullet\bullet \qquad 6.2.5$$

This value of the first gradient is the average with respect to number at the end of the filaments. However, it is not the average with respect to the perimeter of the line of constant u, since the various filaments cut the perimeter in different directions. Consider an element of the perimeter, ds, as shown in Fig. 66.

Suppose that the first gradient normal to this element is given by $\frac{du}{dr} = \dot{u}_r$ which can be considered to be constant for the element ds.

Then, in direction θ,

$$\dot{u} \quad = \quad \dot{u}_r \ \cos\theta$$

and the number of filaments which cut ds at this angle is given by:-

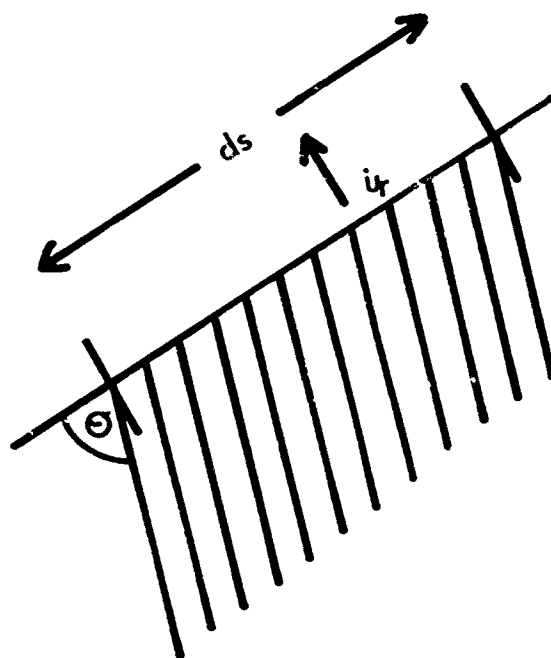$$dn \quad = \quad \frac{ds}{\Delta t}\ \cos\theta$$

181.

FIGURE 66   Element of perimeter of a pipe

182.

Thus the number mean of $\dot{u}$ taken over all directions is given by:-

$$\overline{\dot{u}_N} = \frac{\displaystyle\int_o^\Delta 2\dot{u}dnd\theta}{\displaystyle\int_o^\Delta 2dnd\theta} = \frac{\dfrac{\dot{u}rds}{t}}{\dfrac{ds}{t}} \cdot \frac{\displaystyle\int_o^\Delta 2\cos^2\theta d\theta}{\displaystyle\int_o^\Delta 2\cos\theta d\theta}$$

The mean of $\dot{u}$ with respect to perimeter is given by:-

$$\overline{\dot{u}_s} = \frac{\displaystyle\int_o^\Delta 2udsd\theta}{\displaystyle\int_o^\Delta 2dsd\theta} = \frac{ds}{ds}\cdot\frac{\dot{u}r\displaystyle\int_o^\Delta 2\cos\theta d\theta}{\displaystyle\int_o^\Delta 2d\theta}$$

$$\therefore \quad \overline{\dot{u}_N} = \frac{\dot{u}r\pi}{4}$$

$$\overline{\dot{u}_s} = \frac{\dot{u}r^2}{2}$$

$$\therefore \quad \overline{\dot{u}_s} = \frac{8\dot{u}}{2N\pi} \qquad\qquad 6.2.6.$$

Substituting equation (6.2.5)

$$\overline{\dot{u}_s} = \frac{8}{2\ddot{u}J} \qquad\qquad 6.2.7.$$

This relationship applies to each element of the perimeter, ds, and is therefore true for the whole perimeter.

In order to deduce the flow through the channel it would be possible to integrate this first gradient of velocity twice more to give velocity and then flow. However, it is easier to integrate the volume contained under the velocity profile with respect to velocity rather than with respect to area. Thus, if the velocity has a value u when the area contained within the line of constant us is a, then:-

$$Q = \int uda \qquad\qquad 6.2.8a$$

$$\text{or} \quad Q = \int adu \qquad\qquad 6.2.8b$$

183.

This is illustrated in Fig. 67 and we shall take the (6.2.8b) as being the easier to evaluate.

The variables involved are now superficially a and u. Both these variables are functions of the number, n, and the mean length j of the filaments cutting the area contained by the line of constant velocity. From (6.2.1) it is clear that:-

$$nj \quad = \quad \frac{a}{\Delta t} \qquad\qquad 6.2.9$$

Now consider the surface of constant u and one of (u - du) which enclose an area da as shown in Fig. 67 The mean value of the first gradient of velocity in this area da is, in the limit, the same as the mean with respect to the perimeter. This is illustrated in Fig. 68 if it is realised that the total length of line traversing the element ds dr is the same in every direction.

If all lines traversing the element da are taken then the velocity difference between the ends of each is -du except for the few lines which have both ends terminating on the (u-du) line. In the limit these lines disappear and:-

$$\int_{\text{all } n} \dot{u}_s \, dx = \frac{\bar{\dot{u}}_s \, da}{\Delta t} \quad = \quad -ndu \qquad\qquad 6.2.10$$

Differentiating equation 6.2.9

$$da \quad = \quad \Delta t \, (ndj \; + \; jdn) \qquad\qquad 6.2.11$$

Combining (6.2.10) and (6.2.11)

$$-du \quad = \quad \frac{\bar{\dot{u}}_s}{n} \quad (ndj + jdn) \qquad\qquad 6.2.12$$

(6.2.7) and (6.2.12) may be combined to give:-

$$du \quad = \quad \frac{8}{\pi^2} \quad \frac{}{u} \quad (jdj + \frac{j^2}{n} \, dn) \qquad\qquad 6.2.13$$

Combining equations (6.2.8b), (6.2.9) and (6.2.13)

$$dQ \quad = \quad \frac{8}{\pi^2} \quad \frac{}{u} \Delta t \, (nj^2 \, dj + j^3 \, dn) \qquad\qquad 6.2.14$$

Mathematically, n and j are independent variables but physically they will combine to produce the maximum value of Q which can satisfy (6.2.14). The condition
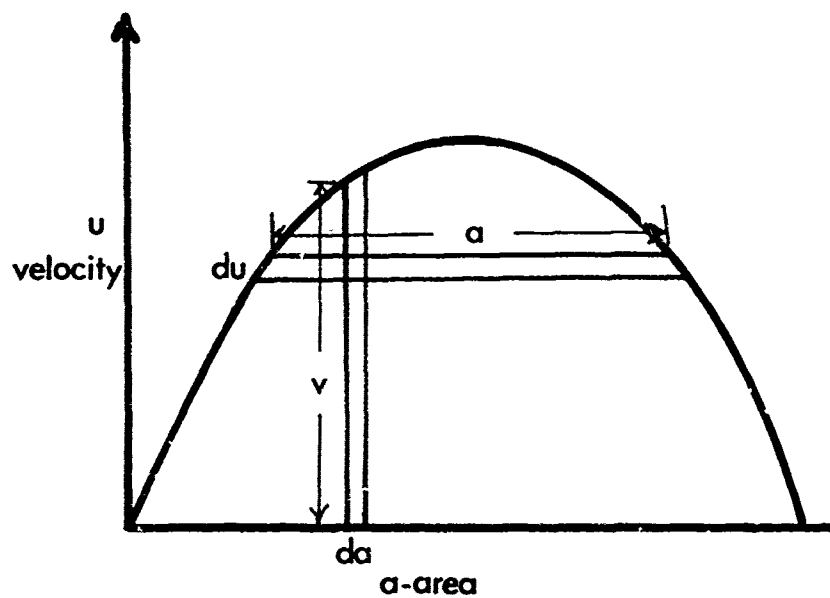
184.

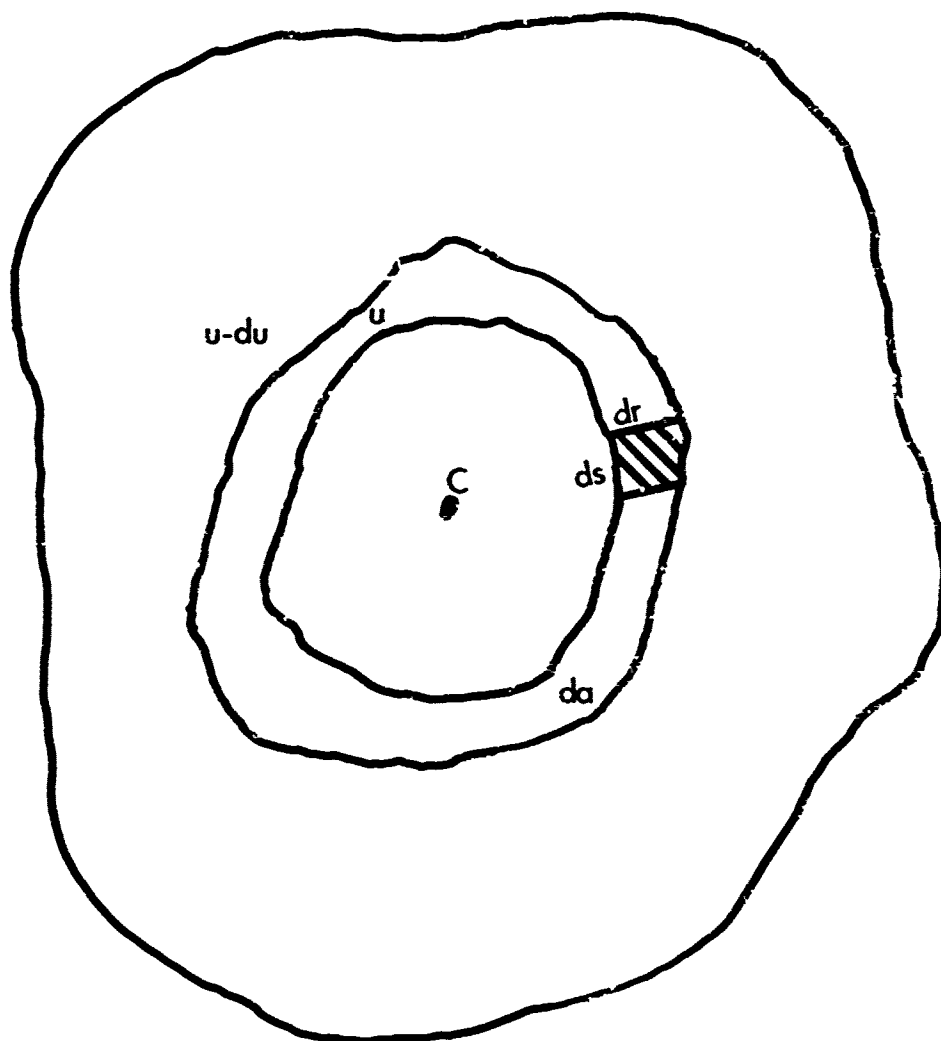FIGURE 67   The relationship of $\int uda$ to $\int adu$

FIGURE 68 Relationship between du/da and du/ds

for maximum Q is seen to be that:-

$$\frac{n}{\bar{J}} = \frac{N}{\bar{J}} \quad dJ \qquad\qquad 6.2.16$$

Substituting (6.2.15) and (6.2.16) into (6.2.14)

$$Q = \frac{10}{\pi^2}\,\bar{u}\quad \Delta t \quad \frac{N}{\bar{J}}\int_{0}^{\bar{J}} j^3\,dj$$

$$\therefore \quad Q = \frac{4}{\pi^2}\,\bar{u}\quad \Delta t \quad N\bar{J}^3$$

Equation (6.2.3) will be substituted in (6.2.17), remembering the total area of the pipe will be substituted by the relationship:-

$$N\,\bar{J}\Delta t = A$$

$$\therefore \quad Q = A\,\frac{1}{\mu}\frac{dp}{dz}\,\frac{2}{\pi^2}\,\bar{J}^2 \qquad\qquad 6.2.18$$

There is one final substitution to make. $\bar{J}$ is not a complete filament. Each complete filament, D, has been divided into two parts to produce J. Therefore the mean filament $\bar{D}$ has twice the value of $\bar{J}$

$$\bar{D} = 2\bar{J}$$

Substituting into equation (6.2.18)

$$\bar{u} = \frac{1}{2\pi^2}\frac{1}{\mu}\frac{dp}{dz}\,\bar{D}^2 \qquad\qquad 6.2.19$$

This equation is a general relationship for a pipe of any shape within the limitation that it has only a single point of maximum velocity. It is easily shown, for example, that for a circular pipe, the mean filament is given by:-

$$\bar{D} = \frac{\pi r}{2}$$

where r is the radius of the pipe.

(6.2.19) then degenerates to the Hagen-Poiseuille equation.

187.

Bibliography - Section 6.2

1. Darcy, H. (1956) les fontaines publiques des la ville de Dijon, Dalmont, Paris.

2. Sheidegger, A. The Physics of Flow through Porous Media, University of Toronto Press (1958).

3. Kozeny, J. (1927) S.Ber.Weiner Ak ad. Abt.IIa, 136, 271.

4. Kozeny, J. (1927) Wasserkr.u.Wasserw.22.86.

5. Kozeny, J. (1932) Kulturtechniker 35-478.

6. Carman, P. C. (1938) Trans.Inst.Chem.Eng. 15, 150.

7. Coulson, J. M.Trans.Inst.Chem.Eng. 27, 237.

8. Brooks, C. S. Purcell, W. R. (1952) Trans.A.I.M.E. 195, 289.

9. Scarlett, B. Eastham, I.E. Stresses in Granular Material due to Applied Vibration. Tripartite Chemical Engineering Conference, Montreal, Canada, 22-25 September 1968.

10. Scarlett., Todd, A.C. The Critical Porosity of Free Flowing Solids Presented to the A.S.M.E. Symposium on Storage, Flow and Handling of Solids October 1966, Boston, Mass.

11. Weibel, E.R. (1963) Morphometry of the Human Lung (Academic Press).

188.

6.3. Filter Testing

6.3.1. Introduction

In the past, the testing of filters has amounted to little more than the determination of the fractional amount of the feed solids which has been retained by the filter with perhaps some attempt to estimate the maxium size of particle which would be found downstream of the filter. This type of testing has involved close definition of the conditions of test and, in particular, specifications of the test solids by nature and size distribution. The results of these tests are useful for the comparison of filters only when the filters are used under similar conditions. For practical use the results have only indicative value since the conditons of use and the solids to be filtered will in general differ widely from those of the test. More informative data of the filter performance can be obtained by determining the actual point efficiency, that is, the fraction of each size of particle which is retained. This can be expressed as a retention efficiency curve (point efficiency plotted against particle size), the parameters of which can be investigated as functions of test variables.

6.3.2. Determination of the Retention Efficiency Curve

Given the mass fraction of the solids retained by the filter and the size distributions (usually cumulative fractional weight oversize or undersize) of the feed and the solids passing or retained, the two commonest methods of determing the retention curve are either to construct a histogram of retention efficiency by considering various size ranges or to calculate the point efficiencies from the mass-frequency distributions. Both methods are straight forward but rely on having accurate size distributions, particularly at the ends of the size distributions. In the histogram method rather wide size ranges have to be considered at the extremes of the ranges in order to obtain accuracy in the calculated mean efficiencies, and in the direct determination method it is more difficult to determine the values of the mass-frequency distributions at extreme sizes so that the calculated point efficiencies are in greater error.

A suggested alternative method is to use "mono sized" fractions of powders so that only the fractional weight retained has to be determined and the point efficiency is found directly. However, objections to this method arise from the difficulty of obtaining fractions of small size range in quantity, that the system

189.

Let D $\quad$ = $\quad$ Particle size

Q(D) $\quad$ = $\quad$ Fractional weight less than D in Feed.

R(D) $\quad$ = $\quad$ Fractional weight less than D in total retained solids.

F(D) $\quad$ = $\quad$ Fractional weight less than D in filtrate.

f $\quad$ = $\quad$ Fraction of feed passing unfiltered to filtrate.

r $\quad$ = $\quad$ Fraction of feed retained by all mechanisms other than retention at the medium.

ψ $\quad$ = $\quad \dfrac{\text{Total weight of retained solids}}{\text{Total weight of feed solids}}$

ψ_r $\quad$ = $\quad \dfrac{\text{Weight of solids retained by the filtering action of medium}}{\text{Weight of feed solids presented to medium}}$

$\eta(D)$ $\quad$ = $\quad$ Overall point retention efficiency

$\eta_r(D)$ $\quad$ = $\quad$ Point retention efficiency due to filtering action of medium.

The distribution of the solids will then be shown in Fig. 70 $\quad$ the quantities Q(D), F(D), R(D), ψ being experimentally determined.

For any size D, we have the mass balance:

$$\psi \frac{dr}{dD} = \eta_r (1-f-r) \frac{dQ}{dD} + r \frac{dQ}{dD}$$

$$\text{6.3.1}$$

$$\text{or} \quad \psi \frac{dr}{dQ} = \eta_r (1-f-r) + r$$

Similarly:

$$(1-\psi) \frac{dF}{dQ} = (1-\eta_f)(1-f-r) + f \qquad \text{6.3.2}$$

Now, for $D \rightarrow 0$, $\eta_f \rightarrow 0$,

$$\text{hence} \quad \frac{dR}{dQ} = r/\psi \qquad \text{6.3.3}$$

$$\text{and} \quad \frac{dF}{dQ} = \frac{1-r}{1-\psi} \qquad \text{6.3.4}$$

For $D \rightarrow \infty$, $\eta_f \rightarrow 1$,

$$\text{hence} \quad \frac{dR}{dQ} = \frac{(1-f)}{\psi} \qquad \text{6.3.5}$$

$$\text{and} \quad \frac{dF}{dQ} = \frac{f}{1-\psi} \qquad \text{6.3.6}$$

190.

is highly idealised, and any effect due to a wide size distribution of the feed solids is eliminated.

For these reasons, therefore, the method which is proposed is an adaption of a technique recently developed in these laboratories for the analysis of the behaviour of classifiers. Essentially this consists of plotting the size distributions of the material retained or passing the filter against the feed size distribution, and analysing the curve obtained, as explained below. A further advantage of the method is that it allows considerably more information about events occurring inside the filter to be obtained than by the previously described methods which present only an overall picture.

6.3.3. Theory of Method

In the simple case, any two of the three size distributions which are obtained from the test are related by the retention efficiency curve. In Fig. 69 the diagonal OA would be obtained if no filtration occurred; if the filtration were such that all material greater than some size given by $(1-\psi) = Q(D)$ were retained, then the lines OB AC would be obtained. ψ then equals the fraction:

$$\frac{\text{mass of solids retained}}{\text{mass of feed solids}}$$ for cumulative undersize distributions.

In practice, curves such as OFA, OGA, will be found.

For the general case, we must also consider the situations when:

(a) the filter is faulty, that is, the medium has broken down at some point or by-passing occurred so that a fraction of solids with the feed size distribution passes with the filtrate;

(b) A fraction of the feed solids is held up, either due to the design of the system or by the action of the cake which has formed. In effect, this material has not been filtered by the medium.

191.

Sufficient data are therefore available to determine f, r, ψ ,. However, as ψ can be experimentally determined, a check of f and r is avail le.

Fig. 71.   illustrates a plot for the general case.

A further check of the tangents is available by consider. ; their intersections, H, K, on Fig. 71   It is easily shown that

$$Q_H = Q_k = \frac{1 - \psi - f}{1 - f - r} \qquad\qquad 6.3.7$$

We have also, that

$$\psi = \psi_r \ (1-f-r) \ + \ r$$

i.e.,

$$\psi_f = \frac{\psi - r}{1-f-r} \qquad\qquad 6.3.8$$

and

$$1-\psi_f = \frac{1-\psi-f}{1-f-r} = Q_H = Q_K \qquad\qquad 6.3.9$$

To determine the point efficiency due to the medium, η_r, equation (6.3.1) or (6.3.2) can now be used with the values of $\dfrac{dR}{dQ}$ or $\dfrac{dF}{dQ}$ determined at the appropriate points.

If the overall point efficiencies are required, these are determined also from (6.3.1) and (6.3.2), putting $r=f=0$.
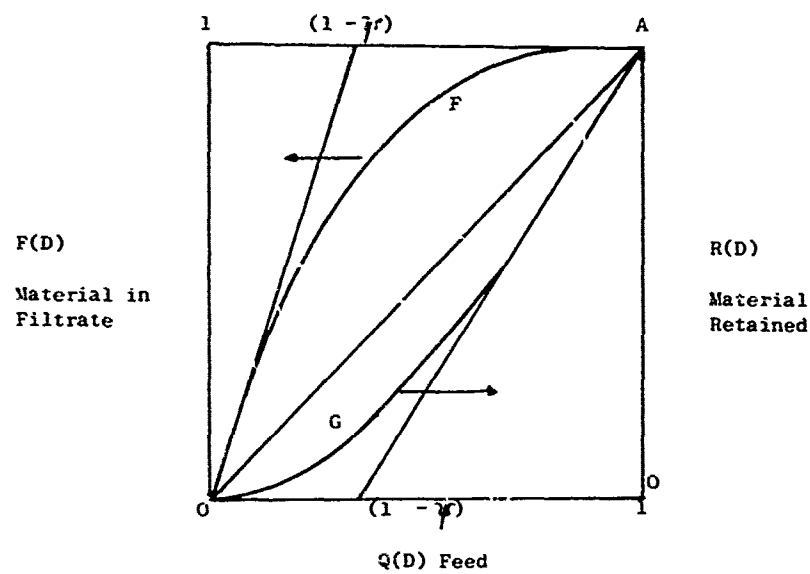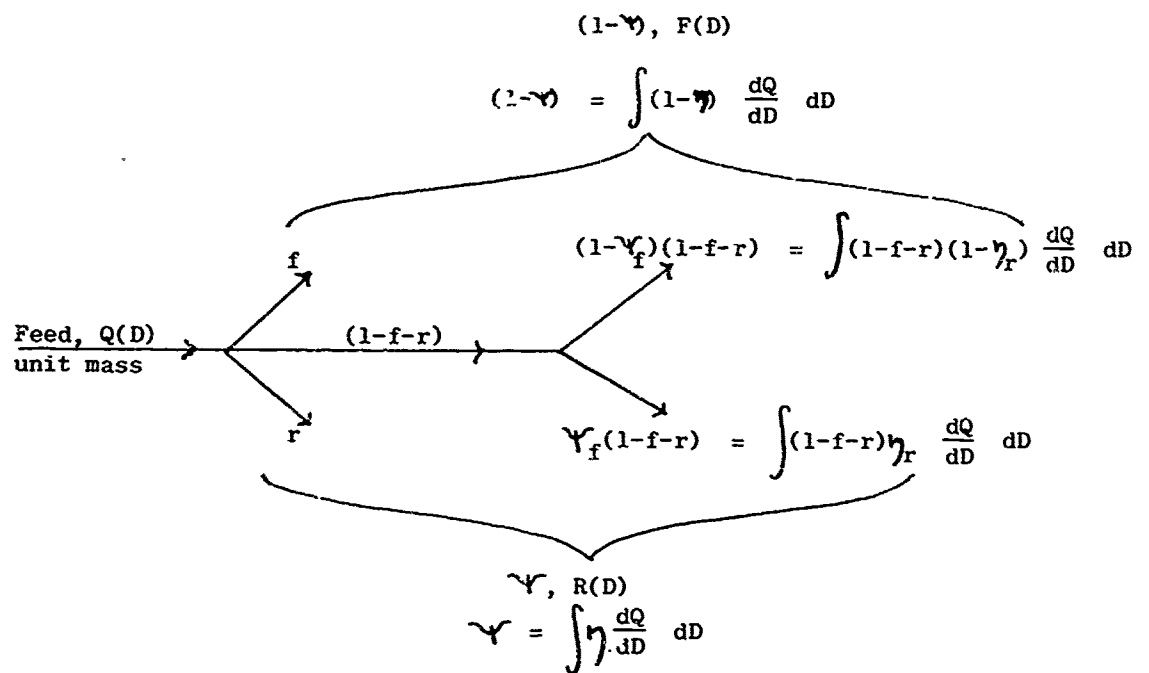
FIGURE G9   Size Distribution Plots

193.

$$(1-\Upsilon), \quad F(D)$$

$$(1-\Upsilon) = \int (1-\eta) \frac{dQ}{dD} \; dD$$

$$(1-\Upsilon_f)(1-f-r) = \int (1-f-r)(1-\eta_r) \frac{dQ}{dD} \; dD$$

Feed, $Q(D)$ unit mass

f

$(1-f-r)$

r

$$\Upsilon_f(1-f-r) = \int (1-f-r)\eta_r \frac{dQ}{dD} \; dD$$

$$\Upsilon, \quad R(D)$$

$$\Upsilon = \int \eta \frac{dQ}{dD} \; dD$$

FIGURE 70   <u>Distribution of solids in filtration</u>
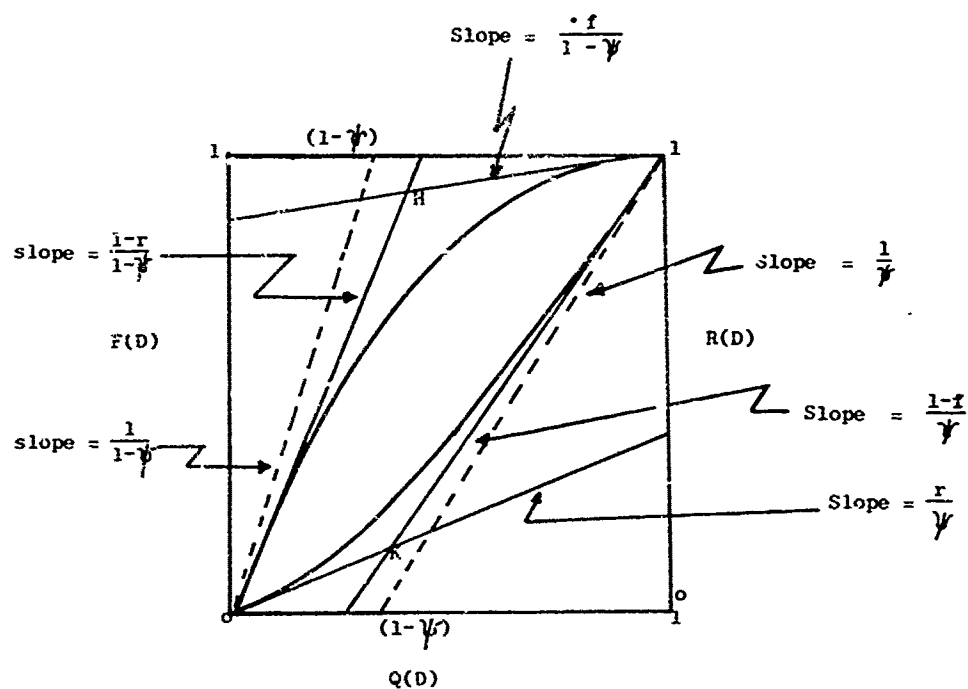
194.

FIGURE 71   Plot for general case

195.

Chapter 7

Techniques

7.1 Identification of Origin of Contaminant Particles

7.1.1 Introduction

Particles presented in hydraulic oils originate from:

(a) "Built-in" dirt. This is swarf from the initial machining of the components, that generated during assembly of the system and dirt of external origin present in components before assembly. It is recognised that any frictional contact will give rise to particles and for this reason very critical components, e.g. propellant valves, are constructed with no screw threads within the system. Although this dirt is usually soon removed from the system by the internal filters it may do great damage during commissioning, if it occurs between a filter and a sensitive component.

(b) Extraneous dirt. This will enter the system through breathers, wiper seals and be picked up on the disconnects of both the system and its servicing equipment. It is characteristic of the environment in which the system is operating and is usually silicacaeous nature with some fragments of cloth, paint, etc. from servicing operations.

(c) System generated dirt. This may be metal particles arising from component wear or elastomer fragments from O-ring and seals.

7.1.2 Identification of Particles

Specifying the origin of particles is facilitated by identifying the materials of which they are composed. For example silica is likely to be extraveous, bronze from a pump or bearing and nitrile rubber from an elastomer seal. Microscopic examination on membrane filters under the reflected light conditions specified in ARP 598 gives some information, e.g. bronzes can be differentiated from white metals, transparent particles may either be silica or shreds of "Teflon", but for example two different types of bronze or aluminium alloy could not be differentiated.

Vickers, Inc., Troy, Mi. (personal communication - R. Leslie) have been successfully using emission spectroscopy to identify the elemental composition of particles of $\geqslant 40\mu m$. However as particles of much smaller dimensions are of great interest in hydraulic oil contamination it was decided to investigate the possibilities of electron probe x-ray analysis.

197.

7.1.3   Electron Probe X-ray Analysis

In this technique of analysis the specimen to be examined is placed in a vacuum environment and bombarded with high energy (10-30 KV) electrons causing the sample to emit x-radiation. The x-rays produced are characteristic of the elements present and may be differentiated using an x-ray monochromater and detector. Many instruments of this type require a flat specimen surface which constrains the geometry of the system. However, this is not possible with particles and hence the instrument chosen was the Stereoscan Scanning Electron Miscroscope Model 2A with x-ray accessories (Cambridge Scientific Instrument Company, Cambridge, England). Fig. 72 is a conventiona -canning electron micrograph demonstrating the topography of the particles and figs. 73 to 76 the scans for Al, Fe, Si and Cr. No Cu was found. This is a preliminary report and improvement in the specimen preparation technique should give better particle distribution in the field. With calibration quantitative analyses would be possible. However these results do show that it is possible to identify at least the major elements present in l_μ particles.

7.1.4   Technique

In electron probe analysis it is necessary to coat non-conducting particles with a conducting layer (usually carbon or Au/Pd alloy) to enable the induced charge to leak away. An attempt was made to examine particles retained on a Millipore filter by mounting the filter onto a specimen mounting stub, coating with Au/Pd and examining. However the particles still charged and the cellulose acetate filter disintegrated in the high beam current necessary to induce x-ray emission.

The next technique tried was an attempt to overcome both of these problems. A piece of silver foil (the specimen mount is aluminium and this was being analysed for) was coated in 'Silver Dag', a colloidal silver suspension, the membrane pressed particle side down onto it and when dry the membrane dissolved away with acetone. Experience however showed it to be very difficult to satisfactorily remove the membrane without detaching the colloidal silver from the foil.

An alternative technique tried was to remove the particles from the oil by centrifuging, wash in hexane using a centrifuge, disperse ultrasonically, pour a drop of the suspension onto the silver foil, mount, coat and examine. Figs.72 - 76 were prepared by this technique. It has the slight disadvantage over the Millipore technique in that examination by optical microscopy is not so easy.
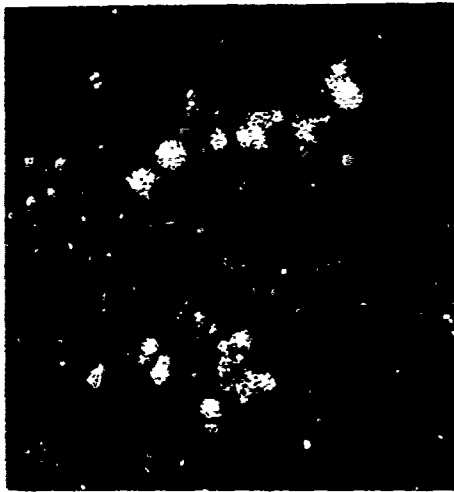
198.

10μ

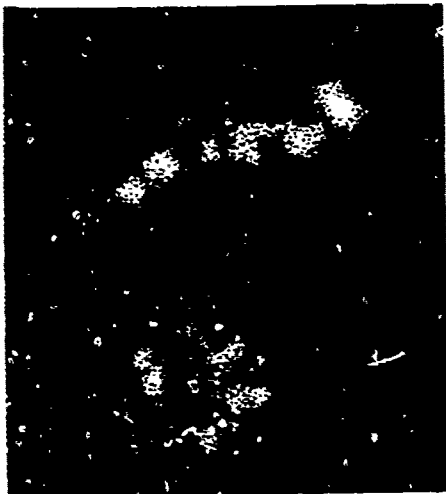Fig.72 TOPOGRAPHY

Fig.73   Fe

Fig.75   Al

Fig.74   Cr

Fig.76   Si

199.

7.2 Techniques for measuring particle and fluid behaviour in a flowing suspension

7.2.1 Summary

A technique has been developed whereby all the important parameters in suspension flow can be measured for each phase separately without any disturbance of the flow. The fluid velocity profile is measured with a technique using a photochromic substance dissolved in the fluid. The particle velocity is measured by filming the motion of coloured particles introduced into the bulk of glass particles, which have the same refractive index as the liquid and thus cannot be seen. The concentration profile is measured by a standard x-ray attenuation technique.

7.2.2 Introduction

Existing methods of measuring the motion of the two phases in a flowing suspension have two major disadvantages. Firstly they involve disturbing the flow in one way or another and secondly, and more important, it is often not possible to measure the behaviour of the two phases separately. Attempts to measure the fluid velocity with a pitot tube for example have tended to give too high values caused by the deceleration of the particles in the stagnation region just in front of the probe. In the case of the pitot tube there is also the problem of particles clogging the probe which will inhibit its use, particularly for measurements of fine suspensions. The hot wire anemometer is another example where the presence of the solids largely affects the measurements. A different class of techniques has involved colouring the liquid by injection of dye, but this again disturbs the flow and the particles may obstruct the coloured liquid.

To overcome these difficulties we have developed a new method whereby all the important parameters in suspension flow can be measured for each phase separately without any disturbance of the flow.

A number of aromatic compounds are known to be photochromic, i.e. they change colour when irradiated with light of certain wave lengths. The change of colour being instantaneous enables one to dye certain well defined parts of a liquid in motion without disturbing it. The coloured liquid can subsequently be traced photographically or by inspection.

Using a suspension of transparent particles in a liquid of the same refractive index, the irradiating beam will go through the suspension without deviating, leaving all fluid elements coloured along the path and leaving the

200.

particles unchanged. The matching of refractive indices and using some coloured particles enables one to follow the translation and rotation of particles irrespective of their position in the cross section. The concentration of particles can be measured by x-ray attenuation. The attenuation is a function of the total mass transversed by the x-ray.

7.2.3 Photochromic Technique

The object was to find a photochromic substance giving rise to an intense colour persisting long enough for our purposes in a liquid which not only was suitable from this point of view but also had the same refractive index as some suitable transparent solid. Literature studies indicated that DNBP* would be a suitable compound. It is colourless in the stable form (except in solutions with high pH values), and the unstable isomer is intensely blue. There is some uncertainty as to the reaction that actually takes place. The following two proposals have been made:
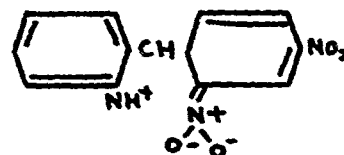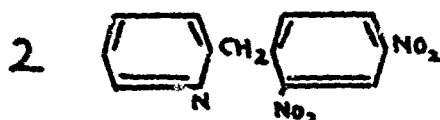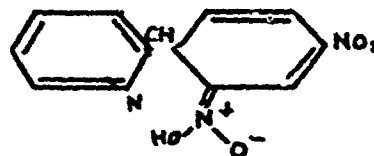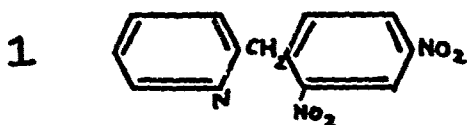
(2,4 dinitrobenzyl) 2 - (2,4 dinitrobenzyl) pyridine

201.

Whichever reaction that actually takes place the coloured form is going to be easily oxidized, and therefore the solutions used may be expected to deteriorate when exposed to both light and oxygen. This has in fact proven true in our experiments.

The rate of the fading reaction has been investigated previously by others. It is a first order reaction with the reaction constant k. Since the reaction involves the transfer of a proton it follows that the pH value should be of importance in a water solution. Higher pH values slow down the reaction (2). Too high pH values will transform the compound into its anionic dark green form however, in which case no change in colour will take place. The importance of the nature of the solvent and the temperature is shown in the following table XX.

Ethyl alcohol	$k = 0,122$ sec.$^{-1}$	at room temp.
" "	$k = 0,01$ "	at -40°C
Isobutyl alcohol	$k = 0,277$ "	at room temp.
Sec-Butyl alcohol	$k = 1,42$ "	" " "
t-Butyl alcohol	$k = 0,153$ "	" " "
Ether	$k = 0,197$ "	" " "
Benzone	$k = 15,2$ "	" " "
Iso-octane	$k = 1,62.10^{3}$"	" " "

TABLE XX   Solvent conditions for photochromic dyes

The absorption spectrum of the stable form shows a peak in the region from 3000 Å slightly into the visible region. There are other peaks at smaller wavelengths but the energy involved is then so high that it may decompose the compound. Thus the light must be filtered so as not to transmit any large amounts below 3000 Å.

The visible absorption spectrum of the unstable blue form is quoted in literature. There is a peak around 5500 Å, hence the blue colour. There is also an indication of a peak in the same region as that of the stable form, i.e. 3000-4000 Å. This indicates that the penetration of a UV- beam into the liquid may be rather limited and that there will be an optimum concentration of DNBP depending on the required depth of penetration and the intensity of the light source.

As described below we decided to use pyrex and a toluene-ethanol mixture. The concentration was chosen with guidance from literature to 0,1% by weight.

202.

Penetration and persistance experiments were made in room temperature with slurry and pure liquid in a pyrex tube of dimensions to be used in later experiments. The internal diameter was 40 mm and the wall thickness was 2.5 mm. The light sources were different flash tubes emitting 200-400 joules in ca 1 millisecond. The wavelength of the light varied over a wide range from far down in the UV-region up in the infra-red. The percentage in the desired region (3000-4000$\overset{o}{A}$)is not known.

The blue colour penetrated into the middle of the tube being less intense the further away from the light source. It penetrated approximately the same length with or without solids present. A large piece of pyrex glass inserted between the light source and the tube had no measureable effect. The results seem somewhat contradicting but the accuracy of measurement was probably not good enough. Photographic recording of the results will be made which will improve the accuracy and also enable measurements to be made very shortly after irradiation. The colour persisted from one to several seconds depending on the initial colour intensity.

Attempts are being made to collect the UV-light by the use of reflectors. Since UV is absorbed in ordinary glass lenses one is limited to the use of MgF_2- coated reflectors or quartz lenses.

Preferably the light should be collected in the form of one intense beam so as to enable one to draw a pencil line through the fluid under investigation. Alternatively one can use a cylindrical reflector in conjunction with a line scurce which will produce line image in the fluid.

A pulse laser would solve the problem of collecting the light. However, the required energy per pulse is larger than that which the common lasers provide. The laser in the department gives pulses of about 1 joule. The frequency would have to be doubled for the   purposes which would decrease the energy to about 0,05 joule per pulse.

7.2.4   Matching of Refractive Indices

The solid must be chosen so as to have the same refractive index as a suitable liquid and at the same time transmit light of 3000 $\overset{o}{A}$ - 4000 $\overset{o}{A}$. A transmission spectrum was made for pyrex. The absorption is approximately constant through the visible region down to 3200 $\overset{o}{A}$ where it increases rapidly. Practically nothing below 3000 $\overset{o}{A}$ is transmitted. Using pyrex glassware will thus serve as a filter for the non wanted lower wavelengths.

Glass spheres are available as load glass (ballatini) or as soda glass. The ballatini spheres could not be made to vanish due to the refractive index not being constant throughout the beads. Etching with hydrofluoric acid did not increase the transparency. Sodium glass beads are only available in a very poor quality and would be even harder to make vanish. Both the lead and the soda glass would in addition absorb large amounts of UV light and would be unsuitable in high concentrations for that reason. Pyrex glass was broken into particles and vanished sufficiently as particles between 200μ and 300μ (by sieving) in a 40 mm tube at a concentration of about 50% by volume.

Since the photochromic technique works well with ethanol ($n = 1,3624$) the aim was to find a liquid with the refractive index higher than that of the glass ($n = 1,4700$) so that a fair amount of ethanol could be added to adjust the refractive index. Benzene and its derivatives are the only solvents with high enough refractive index with the exception of some rather toxic and unpleasant bromocompound. They have refractive indices around 1.5. Mixtures containing either benzene, toluene, xylene or benzyle alcohol were tested for the photochromic reaction. They were equally good and as good as pure ethanol with the exception of the last one which did not work at all. From the point of view of safety we chose to use toluene. The proportions of the slurry:

15,5% by volume of ethanol)
84,5% "   "   " toluene) $n = 1,470$

pyrex $n = 1,470$

7.2.5 Concentration measurement by x-ray attenuation

Concentration measurement by x-ray attenuation is not a new technique and therefore it will only be mentioned briefly here.

The x-ray source is chosen so that as large a change in counts per minute as possible is obtained for a certain percentage change in concentration of solid. The attenuation follows the Lambert- Beer law and therefore this occurs for the value of $Jo/J = e$. The fact that the glass walls also cause attenuation complicates matters somewhat. Since both pathlength and concentration will vary in these experiments anyway, one can disregard the effect of the wall if it is comparatively thin and one does not transverse the tube too far from the centre.

204.
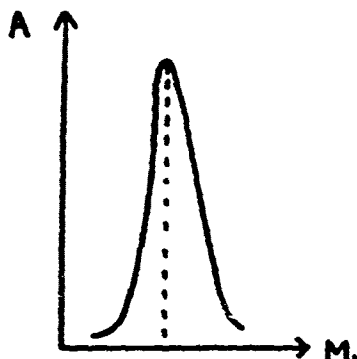
A = sensitivity = $\left(\dfrac{dJ}{Jo}\right)$ $\left(\dfrac{dm}{m}\right)$

Jo = number of counts per unit time with no attenuation

J = number of counts per k unit time

m = mass in the path of the beam

The figure illustrates how the sensitivity changes with the mass. If the attenuation follows the equation

$$J = Jo\, e^{-km}$$

one can deduce the following equation for the sensitivity

$$A = K\, m\, e^{-km}$$

In the present case we have chosen Americium 241 which is a fairly low energy emitter. The path through the centre of the pipe will contain a mass varying with the concentration in a way whereby we will operate on both sides of and on the peak. The recommended equivalent length of Aluminium is 20-30 mm and the actual equivalent length is 20-35 mm if the concentration varies between 0 and 50% by volume. If shorter pathlengths are chosen the sensibility will be high only if the concentration is high. In the actual experiment with horizontal pipes one can expect concentration to be low in the upper parts of the pipe where the path length is short which is a less favourable situation. In the middle and lower parts of the pipe the sensitivity will be around its peak however.

7.2.6   Particle translation and rotation

Individual particles may be traced by introduction of coloured particles and photographing them with a higher speed film camera. Segregation in size fractions etc. may also be detected.

References

(1)   Soush J., Weinstein J., J. of Org. Chem. 1962 p.3155

(2)   Wettermark G., J.A.C.S. 1962 p.3658

Chapter 8

Summary & Conclusions

8.   Summary and Conclusions

This report begins with an analysis of the present state of the art with respect to particulate contamination of hydraulic flight control sub-systems. This analysis is then used to propose an overall strategem within which work should proceed. Because of the complexity of both particle properties and hydraulic systems, progress in this direction will inevitably be slow but this is the only long term method likely to lead to a priori predictions of behaviour. This approach does not invalidate the continued use of more empirical forms of study which enable specific problems to be solved, but the latter technique is in the long term wasteful of effort.

Until the necessary techniques for describing of particles with respect to their bulk behaviour can be established, the methods of analysing system behaviour or studying component behaviour must be capable of application to any future description of particle properties.

This point is exemplified in Chapter 3, Mathematical Modelling of Hydraulic Systems, where a stepwise model is established and in which both the contaminant concentrations within the system and the characteristics of the components are expressed in a general matrix form which is applicable to any method of particle size analysis. This modelling technique, given sufficient information about the components in the system, enables the point at which any position in the system reaches a critical contamination level to be calculated.

In order to study experimentally both operational and laboratory systems it is necessary to be able to remove a representative sample of fluid and analyse that sample. Chapter 2 states the requirements of a sampling device and describes techniques for both the theoretical and experimental study of sampling devices. As far as can be established none of the sampling devices currently used meet all of these requirements, but the magnitude of the errors involved are not known.

Chapters 4 and 5 discuss the meaning of particle size, propose a new description of particle size and give accounts of the study of three well known (e.g., the Coulter Counter, the HIAC Counter, and ARP 598) and one more specialised technique of particle size analysis. Specifically, the assumption of equal distribution of particles on the membrane in an ARP 598 analysis is confirmed to be valid for one size of particle (and would not be expected to differ for other sizes